Journal of Arrhythmia WILEY

2019 APHRS expert consensus statement on three-dimensional mapping systems for tachycardia developed in collaboration with HRS, EHRA, and LAHRS

Young-Hoon Kim[1] | Shih-Ann Chen[2] | Sabine Ernst[3] | Carlos E. Guzman[4] | Seongwook Han[5] | Zbigniew Kalarus[6] | Carlos Labadet[7] | Yenn-Jian Lin[2] | Li-Wei Lo[2] | Akihiko Nogami[8] | Eduardo B. Saad[9] | John Sapp[10] | Christian Sticherling[11] | Roland Tilz[12] | Roderick Tung[13] | Yun Gi Kim[1] (iD) | Martin K. Stiles[14]

[1]Department of Internal Medicine, Arrhythmia Center, Korea University Medicine Anam Hospital, Seoul, Republic of Korea

[2]Division of Cardiology, Department of Medicine, Taipei Veterans General Hospital, Taipei, ROC

[3]Department of Cardiology, Royal Brompton and Harefield Hospital, Imperial College London, London, UK

[4]Hospital Christus Muguerza Alta Especialidad, Monterrey, Mexico

[5]Division of Cardiology, Department of Internal Medicine, Keimyung University School of Medicine, Daegu, Republic of Korea

[6]Department of Cardiology, Medical University of Silesia, Katowice, Poland

[7]Cardiology Department, Arrhythmias and Electrophysiology Service, Hospital Argerich- CEMIC, Buenos Aires, Argentina

[8]Department of Cardiology, Faculty of Medicine, University of Tsukuba, Tsukuba, Japan

[9]Center for Atrial Fibrillation, Hospital Pro-Cardiaco, Rio de Janeiro, Brazil

[10]Division of Cardiology, Department of Medicine, QEII Health Sciences Centre, Dalhousie University, Halifax, NS, Canada

[11]Cardiology, University Hospital Basel, Basel, Switzerland

[12]Medical Clinic II (Department of Cardiology, Angiology and Intensive Care Medicine), University Hospital Schleswig-Holstein (UKSH) – Campus Luebeck, Luebeck, Germany

[13]Center for Arrhythmia Care, Pritzker School of Medicine, University of Chicago Medicine, Chicago, IL, USA

[14]Department of Cardiology, Waikato Hospital, Hamilton, New Zealand

Correspondence:
Young-Hoon Kim, Arrhythmia Center, Korea University Medicine Anam Hospital, 73, Inchon-ro, Seongbuk-gu, Seoul 02841, Republic of Korea.
Email: yhkmd@korea.ac.kr

[Correction added on 13 March 2020, after first online publication:Affiliation 7 was corrected.]

PREAMBLE

This document describes the use of three-dimensional mapping systems and includes recommendations regarding their application in clinical practice based on scientific evidence. Nevertheless, it should be kept in mind that these systems are associated with increased costs. Consequently, their availability as well as reimbursement practice varies widely across different countries largely depending on the economic situation. The societies involved in the development of this document recognize the existence of these factors and the significant barriers that these may pose in everyday practice and on the decision to use or not use a three-dimensional mapping system in a given patient. Thus, in cases where these useful systems are not available or cannot be used in a wide scale due to financial constraints, electrophysiology procedures should certainly be offered to the patients based on established indications. Profound knowledge and experience may compensate lack of advanced technical equipment and prove in the majority of cases sufficient for successful conduction even of complex ablation procedures.

1 | CHAPTER 1: INTRODUCTION

Catheter mapping and ablation are widely performed for various complex tachyarrhythmias that need a better understanding of fundamental technologies of mapping to identify triggers or substrate of arrhythmias. The mapping of arrhythmias used to be performed using multipolar electrode catheters, fluoroscopy to localize the anatomic catheter position within the cardiac chamber, and interpretation of recorded intracardiac electrograms to localize the origin of a focal arrhythmia or critical parts of a tachycardia circuit. The general principles, rationale, and working of the various mapping systems have been well described before.[1-3] The introduction of the three-dimensional (3D) electroanatomical mapping systems greatly facilitated ablation procedures. Three-dimensional mapping systems are categorized as magnetic-based vs. impedance-based according to the catheter location technology, and are also classified as contact based vs. noncontact based according to the data collection technology. During mapping, the electrogram obtained at a certain site is stored and the activation time is defined as compared with a selected electric signal reference. By projecting the activation time compared with a signal reference on the 3D geometry point-by-point, the system allows intuitive review of the activation mode of the whole chamber through the various isochrones in a 3D fashion. In addition to the activation map, 3D mapping displays the voltage of the recorded electrograms, low voltage or scar region defined by voltage map is known to be correlated with the arrhythmogenic substrate. The 3D map can be integrated with imaging modalities such as magnetic resonance imaging (MRI), computed tomography (CT), and intracardiac echocardiography (ICE) for more accurate and vivid anatomic descriptions.

The 3D mapping system does not always accurately represent the mechanism of the tachycardia. The interpretation of the map could lead to a false diagnosis, which may in turn result in an unsuccessful outcome. Good catheter contact, correct interpretation of the colors in the map, appropriate choice of reference electrogram, complete mapping of the correct chamber of interest, and strategies to address catheter tip migration with respiration or change in cardiac rhythm and annotation of complex intracardiac signals are all necessary prerequisites for the success of ablation.[4-7]

The purpose of this expert consensus statement is to provide a state-of-the-art review of currently available 3D mapping systems in the field of cardiac tachyarrhythmias. Representatives nominated by the Heart Rhythm Society (HRS), European Heart Rhythm Association (EHRA), Asian Pacific Heart Rhythm Society (APHRS), and the Latin American Heart Rhythm Society (LAHRS) participated in the project definition, literature review, recommendation development, writing of the document, and its approval. The classification of the recommendations and the level of evidence follow the recently updated ACC/AHA standard. Class I is a strong recommendation, denoting a benefit greatly exceeding risk. Class IIa is a somewhat weaker recommendation, with a benefit probably exceeding risk, and Class IIb denotes a benefit equivalent to or possibly exceeding risk. Class III is a recommendation against a specific treatment because either there is no net benefit or there is net harm. Level of evidence A denotes the highest level of evidence from more than one high-quality randomized clinical trial (RCT), a meta-analysis of high-quality RCTs, or RCTs corroborated by high-quality registry studies. Level of evidence B indicates moderate-quality evidence from either RCTs with a meta-analysis (B-R) or well-executed nonrandomized trials with a meta-analysis (B-NR). Level of evidence C indicates randomized or nonrandomized observational or registry studies with limited data (C-LD) or from expert opinions (C-EO) based on clinical experience in the absence of credible published evidence. Each society officially reviewed, commented, edited, and endorsed the final document and recommendations.

2 | CHAPTER 2: PRINCIPLES OF 3D MAPPING

Cardiac mapping is the registration of the spatial distribution of cardiac functional characteristics, typically of localized electrical potentials. The development and availability of accurate 3D localization technology has made this an important part of routine clinical cardiac electrophysiologic care, most frequently by permitting the visualization and ready comprehension of intracardiac activation sequences and contact electrogram characteristics. Electrodes in contact with functioning cardiac tissue can accurately identify local activation and its timing relative to a reference.[8] This concept was exploited initially for surgical therapy for Wolff-Parkinson-White syndrome[9] and subsequently for endocardial mapping using catheters and fluoroscopy.[10] The development of nonfluoroscopic catheter localization technology with computerized graphic representation of electrophysiologic phenomena in a spatially accurate geometry[11] led to the advent of catheter mapping and ablation of complex arrhythmias.

2.1 | Activation mapping

Activation of cardiac tissue in contact with a unipolar electrode generates the steepest negative slope of the associated electrogram (intrinsic deflection), while for bipolar electrodes local activation is mostly estimated to be at the time of the first sharp peak.[12] Activation mapping can be achieved by combining the known location of a roving mapping catheter with the activation time of tissue with which it is in contact. In a stable cardiac rhythm, this permits the point-by-point construction of a 3D map of propagation of activation across a cardiac surface. This is typically graphically represented as a static color-coded map of local activation time, or as a video portrayal of a moving wavefront of activation (Figure 2-1). A detailed activation map gives useful information that can clarify the mechanism of arrhythmia. Focal arrhythmias will demonstrate centrifugal spread from a site of earliest activation from which the arrhythmia arises.[13,14] Macroreentrant arrhythmias are characterized by propagation around anatomic barriers or scar, with demonstration of the full cycle length within the circuit.[15,16] The addition of functional mapping maneuvers such as entrainment may help distinguish focal arrhythmias from microreentrant circuits or from circuits with unmappable portions (eg, deep/epicardial), each of which might result in centrifugal spread along the endocardial surface.

2.2 | Potential pitfalls of activation mapping

Careful attention is required to construct an accurate contact map of cardiac activation. Two assumptions are made during point-by-point activation 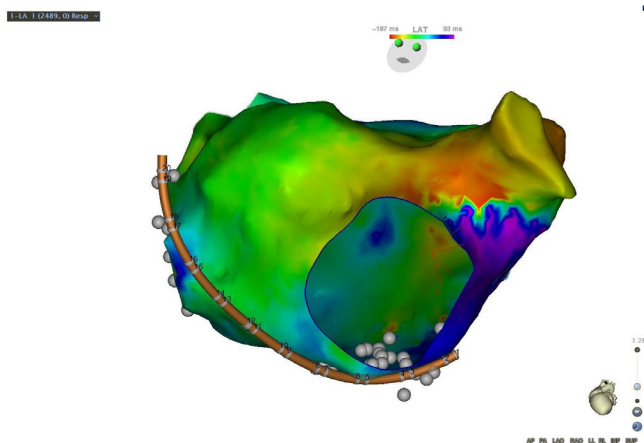mapping, namely: (a) Local activation time can be accurately assessed; (b) Location of the mapping electrode is known. Further assumptions are typically made in order to interpret the map: (a) Activation on the cardiac surface also reflects the electrophysiological property of underlying tissue; (b) The entire cardiac surface/chamber is comprehensively mapped; (c) Activation propagates predictably and homogeneously; (d) The mapped rhythm is stable and repetitive; (e) Cycle length matches activation time of a given chamber. Each of these assumptions may be incorrect and may impact map interpretation (Table 2-1).

2.2.1 | Assessment of local activation time

Bipolar recordings reflect differential electrical potential between two closely spaced electrodes, and will thus be minimally impacted by far-field signals, which would typically result in similar influences on both electrodes, and thus would fail to contribute to the potential difference between them. Local activation has been variously defined for bipolar electrograms, since electrode orientation and wavefront direction influence signal morphology, but perhaps most commonly as the first maximum or minimum signal.[17] Smaller and more closely spaced electrodes will have lesser far-field contributions, and can be combined in multielectrode arrays to rapidly and accurately map activation. The contribution of known interelectrode spacing may also reduce the potential for mapping errors due to insufficient spatial localization accuracy, and can permit very high-density rapid activation mapping with the addition of automated determination of activation time.[18-20] Nonetheless, even ultrahigh-density mapping may encounter challenges with accurately annotating activation time (eg, when a very long-fragmented electrogram is observed in a very small area) and distinguishing reentry from passive activation around conduction barriers or even noise.[21]

2.2.2 | Localization of recording site

Modern 3D mapping systems achieve high localization accuracy, in most cases using a combination of magnetic field sensors and impedance ranging.[22] These measures may be augmented by additional sensors which attempt to confirm tissue contact.[23,24] Furthermore, utilization of catheters with known fixed interelectrode distances may improve the assessment of local activation sequence.

2.3 | Other challenges to map interpretation

Tissue heterogeneity may pose additional challenges to interpretation of 3D contact maps. Detailed correlative studies between cardiac MRI and electrogram characteristics have demonstrated that the myocardium may have 11%-63% scar transmurality beneath an endocardial rim of 2 mm of viable tissue and yet have a bipolar signal amplitude which exceeds 1.5 mV.[25] Assessment of deeper tissue characteristics may be enhanced with the addition of unipolar signal

FIGURE 2-1 A patient with a prior surgical ablation to isolate the pulmonary veins developed recurrent atypical atrial flutter. The mechanism was determined to be counterclockwise perimitral flutter by a combination of activation and entrainment mapping. Activation propagated superiorly up the lateral left atrium, activating the left atrial appendage and superior left atrium, before propagating down the interatrial septum and floor of the left atrium. The atrial cycle length was 290 milliseconds and the timing reference was in the coronary sinus. The cycle length window was arbitrarily set, resulting in an "early meets late" zone at the base of the left atrial appendage

TABLE 2-1 Pitfalls in 3D activation mapping

Pitfall	Consequence	Resolution
Inaccurate Reference Timing	Inaccurate assessment of activation time	Ensure timing reference is from a stable location, that rhythm is stable, and that activation time is accurately and consistently annotated
Inaccurate localization	Inaccurate assignment of location to electrogram	Monitor stability of mapping localization, utilize respiratory gating features
Inaccurate automated timing assessment	Erroneous timing assessment	Manually over-read and edit automated timing assessment
Complex electrogram morphology	Erroneous timing assessment	Complex electrograms must be analyzed in the context of surrounding electrogram characteristics
Far-field signals	Erroneous timing assessment	Complex signals may have components which reflect adjacent tissue (eg, right superior pulmonary venous activity might be recorded in the posteromedial superior right atrium). Pacing the target site or adjacent tissue may alter activation sequence and can help to determine which portion of the nonpaced signal is local. Smaller electrodes with narrow spacing may reduce far-field signals intrusion
Incomplete Map	Erroneous characterization of arrhythmia	Deep or epicardial circuits or focal sources may appear to have radial spread from an endocardial source. A broad area of early activation with similar timing may indicate a deeper source. Pacing/entrainment may clarify the mechanism
Ectopy	Alteration in activation sequence due to catheter-induced or spontaneous ectopy	Monitor for consistency of heart rate and activation sequence
Complex anatomy	Inaccurate matching of activation time to location	Careful attention to map geometry, possibly with comparison to radiographic imaging, to avoid "webbing" anatomic maps across physical barriers, or possibly with use of intracardiac echocardiography to identify important anatomic structural relationships such as papillary muscles
Poor resolution map	Failure to identify critical components	Ensure adequate point density to fully map reentrant circuit; ensure absence of large timing "gaps." Larger tip electrodes may fail to record high-frequency, low-amplitude signals. Use of smaller electrodes with close spacing may permit their recording and reduce the influence of far-field signals

Abbreviation: 3D, three-dimensional.

amplitude.[26] Epicardial,[27] intramyocardial,[28] and ECG imaging[29] recordings have demonstrated the potential 3D complexity of reentry circuits, which may pass deep to endocardial contact catheters.

In most cases, cardiac arrhythmias are mapped with the goal of designing an ablation strategy. For focal arrhythmias, this typically requires only focal activation mapping surrounding the site of earliest activation, while for reentrant arrhythmias the strategy must be individualized to the culprit anatomic/functional substrate. Complex atrial arrhythmias may require a comprehensive map in order to fully understand the reentrant circuit and to design an effective strategy to interrupt it with ablation, or identify a common vulnerable isthmus.[30] Interpretation of the map requires careful identification of activation sequence, and when complex electrograms are observed, careful annotation of fragmented signals (usually indicative of slow conduction) and of double potentials (usually indicative of activation of closely apposed tissues on either side of a line of block) are required.[6,31,32] When double potentials are observed, one useful strategy to accurately create an activation map is to annotate their presence on the map, interpreting it as a site of block, and to assign activation times on either side of the site of double potentials to the potential which has timing contiguous with surrounding tissue timing farther away from the line. Activation mapping can be usefully augmented with the use of functional testing, such as entrainment mapping to distinguish portions of activation which are passive and those which are critical to a reentrant circuit,[33] or the use of pacing to identify the presence of unexcitable scar.[34]

2.4 | Types of 3D maps

3D mapping systems have the potential to portray any value on an anatomic map. There are several useful variations of the most frequently used activation and signal amplitude (voltage) maps. Usual activation maps utilize a continuous scale color gradient; it may be helpful to display the colors as a series of isochrones. Although this is a simplified display of the same information, crowding of isochrones can make zones of slowed conduction more obvious.[35] The same information can alternatively be displayed in video format as a propagation map to aid comprehension of the activation sequence in the patient-specific anatomy and arrhythmic substrate.[19]

Entrainment mapping can be used to provide additional information to an activation map of a cardiac arrhythmia, including ventricular[36] and atrial arrhythmias.[37] The response to entrainment can establish the proximity of the pacing site to the critical elements of a reentrant circuit. This maneuver is typically used to supplement

activation mapping and other mapping strategies rather than to supply values to color code on a 3D map.[38]

The utility of ablation of sites with complex fractionated atrial electrograms for the treatment of atrial fibrillation has remained a topic of active research.[39,40] Electroanatomic maps may be used to portray tachycardia cycle length, dominant frequency or phase mapping or other indices of fractionation to serve as targets for ablation, although the optimal clinical place of these approaches remains uncertain.[41–43]

Ablation of sites with abnormal electrograms within the ventricle has been advanced as a useful strategy for the ablation of scar-related ventricular tachycardia.[44] Automated identification of arrhythmogenic substrate has included mapping of signal amplitude[45] and manual inspection of maps to identify sites of latest ventricular activation,[35] or of myocardial bundles surrounded by denser scar based on signal amplitude[46] or response to pacing.[34,47–50] A newer technique, known as ripple mapping, retains the complexity of recorded signals and graphically portrays local signal amplitude over time in animated images.[51] Rather than simplifying signals into a single activation time, or peak amplitude, this method permits visual analysis of the entire signal and can display conducting channels displayed within scars.[52]

Pace-mapping has been used for decades as a method to map sources of ventricular activation. The similarity of surface electrocardiography between paced beat and spontaneous ventricular ectopy suggest that catheter tip is near the origin of ventricular ectopy. Quantitative comparison of paced beat and spontaneous ventricular ectopy can assist catheter ablation.[53,54]

3 | CHAPTER 3: TECHNOLOGY— COMPARISON OF SYSTEMS

The investigation and localization of complex arrhythmias with fluoroscopy is inaccurate, burdensome, and associated with a high-radiation exposure for the patient and operator. The 3D mapping systems have been introduced into clinical electrophysiology over the decades. On top of the anatomical information, they can non-fluoroscopically provide the precise geometry of any chamber of the heart, movement and position of the catheters, and electrical activation sequences and voltage of tissues. The 3D mapping system helps to interpret the mechanism of complex arrhythmias and targets the ablation site in an effective and safe manner. The commonly used 3D mapping systems are the CARTO 3 (Biosense Webster) and EnSite Precision (Abbott). The Rhythmia system (Boston Scientific) has recently been launched and has played an important role in initiating high-density mapping of complex arrhythmias. The fundamental principle of the three systems will be compared in detail.

3.1 | CARTO 3

The system consists of a location pad with three separate low-level magnetic field emitting coils (5×10^{-6} to 5×10^{-5} tesla) arranged as a triangle under the patient and six electrode patches positioned on the patient's back and chest (Figure 3-1). The latest version is based on a hybrid of magnetic and current-based localization technologies with an accuracy of less than 1mm. Three magnetic field emitters generate three different low-intensity magnetic fields. The magnetic field strength from each coil is detected by a location sensor embedded at the tip of a specialized mapping catheter. The strength of each coil's magnetic field measured by the location sensor is inversely proportional to the distance between the sensor and coil. Hence, by integrating each coil's field strength and converting this measurement into a distance, the location of the catheter tip can be displayed in a 3D geometry of the heart chamber.[55,56] Additionally, the CARTO system sends a small current across the catheter electrode and collects the current-based information, which is used for an adjustment with the magnetic-based data. Each electrode emits current at its own frequency. A current ratio is created by the measurement of the current strength at each patch and stored by the system. The current data from the six electrode patches make the various catheter
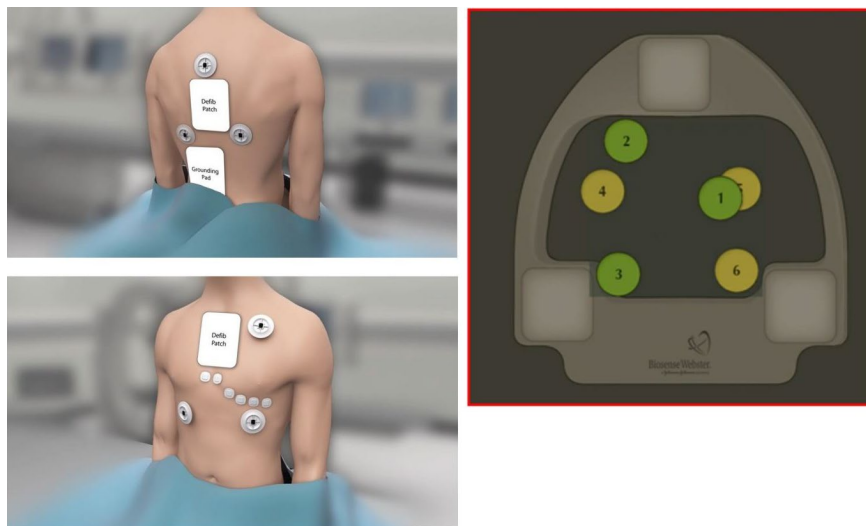

FIGURE 3-1 The patch placement of the principle of the CARTO 3 system. The six patches should be placed inside the mapping zone

electrodes visible in the system.[22,57] Visualization of the catheters is confined to a 3D virtual area called the "matrix," which can be built only by a mapping catheter with a magnetic sensor.[58] The catheter position can be affected by the artifact caused by respirations, patient movement, cardiac contractions, and system movement. Three back patches are used along with the location pad for an anatomical reference, which allows the system to measure the catheter location relative to this anatomical reference for the compensation of patient and system movements. The six patches have magnetic sensors for the localization of the catheters, and the impedance changes detected by the back and chest patches are mainly used for compensation of the respiratory motion. The AccuRESP module supports the compensation of the respiratory artifact by monitoring the respiratory movement of the sensor-based catheter and interpatch currents. For the artifact from cardiac contractions, the system uses an electrical reference to match the catheter location with the time in a cardiac cycle. There are two different modes to show the mapping catheter: stable mode and gated mode. The gated mode locates the mapping catheter at the end of diastole of the electrical reference chamber. The stable mode locates the mapping catheter at the average location of 60 samples per one second; hence, the motion of the mapping catheter is smooth and stable. The stable mode is used in the most recent module and software including the Fast Anatomical Mapping (FAM), Visitag, Time force integral, ablation index, etc

3.2 | EnSite

The EnSite system consists of a set of three pairs of skin patches and a system reference patch. This system is based on impedance-based localization and tracking technologies. The six patches are placed on the skin of the patient to create electrical fields along three orthogonal axes. The patches are placed on both sides of the patient (x-axis), the chest and back of the patient (y-axis), and the back of the neck and inner left thigh (z-axis). The three-paired patches are used to send low-power currents of 350 mA at a frequency of 8 kHz to form a 3D electrical field with the heart at the center. The electrical current transmitted between the patches through the thorax will cause a drop in the voltage across the heart. Intracardiac catheters are equipped with sensing electrodes. The electrodes on the catheters read the relative voltages with respect to a reference electrode. The position of the electrode is identified upon an analysis of the voltages.[59] The 3D localization of the catheters is calculated based on an impedance gradient in relation to a reference electrode. However, the catheter locations are often distorted by a nonlinear impedance of the human body. A process called "field-scaling" may correct that to some extent and adjusts for the nonlinearity of the geometry by considering the measured interelectrode spacing for all the locations within the geometry. The EnSite system uses either the system reference patch on the patient's body or an intracardiac electrode for the anatomical reference and it can improve the compensation for cardiac and respiratory motion artifact. The EnSite system collects the impedance data over a period of 12 seconds from the patches

and intracardiac catheters. It can identify respirations by the breading-dependent changes of the transthoracic impedance. The system provides an algorithm for the compensation of the catheter shift due to the respiratory motion, which makes all catheters look static. It is recommended to use an intracardiac catheter for the anatomical reference that is not used for pacing because the EnSite system does not use an electrical reference for the compensation of the cardiac motion artifact. Hence, the dislocation of the reference catheter may lead to uncorrectable map shifts. The main advantage of the EnSite system is the visualization of multiple catheters from different manufacturers. All displayed catheters in the 3D electrical field can be used for generating the geometry of the cardiac chambers. The electrophysiologic data from the catheter can be integrated into the geometry to form the 3D map.[60]

The EnSite Precision cardiac mapping system is the latest version, which uses the advantages of the hybrid impedance and magnetic field technologies. It allows for a much higher precision and accuracy compared to the prior version of the EnSite system. The Precision system requires an additional source of a magnetic field (EnSite Precision field frame) and two additional sensors on the patient (one on the back and the other on the chest; Figure 3-2). The EnSite Precision field frame is attached under the patient's table and it generates a weak magnetic field like the location pad of the CARTO system. The magnetic field technology works with the new sensor-enabled technology. Sensor-enabled catheters, which interact in the magnetic field, can be used to refine the impedance-based location, especially in the peripheral areas. The magnetic field data help preserve the localization accuracy in case of gradual changes in the impedance field such as lengthy procedures for atrial fibrillation or ventricular arrhythmia ablation. This hybrid technology leads to a navigation accuracy of < 1 mm. For the creation of the left atrial geometry, the Advisor FL circular mapping catheter and Advisor HD grid catheter can be used. For ablation, both the FlexAbility catheter (without contact force) and TactiCath Quartz (with contact force) are available.

3.3 | Rhythmia

This system has been available in the field of electrophysiology since several years ago. The Rhythmia mapping system uses a hybrid tracking technology utilizing both magnetic and impedance-based localization features for the map creation. For magnetic tracking, the system needs one sensor coil embedded back patch and magnetic field generator underneath the patient's table. For an impedance-based localization, the impedance field is generated by applying current to the back patch, patches for the electrocardiographic limb leads, and the V_1, V_3, and V_6 chest leads. The Rhythmia system is the first 3D mapping system to allow for automated high-density mapping with a dedicated steerable 64-electrode mini-basket catheter.[18,61,62] Both point-by-point and continuous mapping can be performed with this system. Continuous mapping can be performed by a rapid and automated annotation based on a

FIGURE 3-2 Surface electrodes placed with three transthoracic pairs and two patient reference sensors, along with the other surface electrodes for the EnSite Precision system.
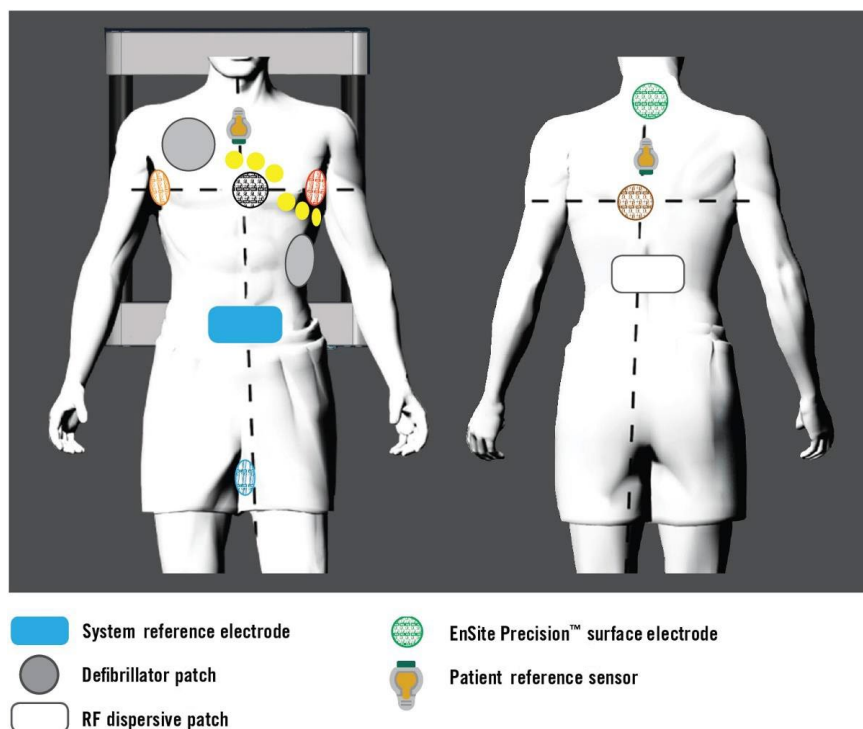
FIGURE 3-3 Magnetic field emitter and reference patch on the back of the patient of the Rhythmia system. The lower panel shows the changes in the shape of the IntellaMap Orion catheter

set of user predefined beat acceptance criteria. The system is optimally designed to work with the IntellaMap Orion high-resolution mapping catheter (Figure 3-3). The IntellaMap Orion Catheter is a sensor embedded, 8.5 Fr bidirectional deflectable 64-pole basket array. The catheter has a variable diameter of 3-22 mm that can be adjusted based upon the anatomic needs. It is made up of eight splines, each having eight equispaced flat, printed electrodes at 2.5 mm apart. The iridium oxide-coated flat electrode (0.4 mm^2) without sensing from the back side of the splines helps avoid far-field signals and records very low local potentials, resulting in a 0.01 mV noise floor. Magnetically tracked catheters are coupled with impedance mapping, such that the system tracks the impedance measurements at each location during the creation and validation of the magnetic-based map. The surface geometry is continuously obtained by the outer most electrode locations associated with acceptable beats. The electrogram of the accepted beat is included in the 3D mapping only when the electrode is within 2 mm of the geometry for a new map. The Rhythmia system

has been shown to collect 25 times more data points per map on average compared to manual mapping.[63] The high density of the points reduces the amount of interpolation between annotated points, which allows for a more accurate and visible propagation pattern and identifies small gaps more precisely. During acquisition of the activations and voltages, the software can display the specified surface and intracardiac electrograms of each beat. A magnetic sensor-embedded open-irrigated ablation catheter is available, but a contact-force catheter has not yet been launched.

3.4 | High-density mapping

High-density mapping is the process of simultaneous acquisition and annotation of multiple electrograms by the automated algorithm, including activation and voltage information. For the fast acquisition of data and better signal quality with a lesser noise to far-field ratio, multiple electrodes with a smaller electrode size have been developed. Each 3D mapping system has developed its own multiple electrode catheters. The Rhythmia system uses the IntellaMap Orion catheter, which has 64 small-printed electrodes. The PentaRay, which is used with the CARTO 3 system, is a magnetic-sensor based catheter with 20 poles arranged in five soft-radiating splines (1 mm electrodes separated by 4-4–4 or 2-6–2 spacing) laid out flat to cover an area with a diameter of 3.5 cm. The EnSite Precision system can use the Advisor HD Grid Mapping Catheter, Sensor Enabled, which has four splines with four electrodes on each spline (1 mm electrodes with 3-3–3 equidistant spacing) in a spade of a grid. The size of the grid is 1.3×1.3 cm^2.

The continuous acquisition of data points is based on a set of user predefined beat acceptance criteria. All three 3D mapping systems have similar categories of the beat acceptance. The criteria include the cycle length stability and/or range, position/distance stability, QRS morphology/electrocardiogram stability, respiratory phase, speed of the catheter motion, etc. These criteria help the system to discern a particular tachycardia or morphology in the presence of multiple arrhythmias or complex ectopy, which allows the system to quickly create an individual 3D map. The Turbo map of the EnSite system provides the ability to map the coexisting arrhythmia using the same recording segments. The Rhythmia system has a unique propagation reference for the atrial arrhythmias, which is used as a secondary reference to confirm the current beat is from the same tachycardia. The time interval between the reference and propagation reference is monitored, and the beat will be accepted if the difference is within a 5 milliseconds range.

The automated annotation methods differ among the systems. In order to find the appropriate target for an effective ablation, the operator should understand the mechanism of the automated algorithm. The activation map is greatly influenced by how precisely each beat is annotated. For the timing of the activation at each point, it is generally accepted to annotate the first peak of the near-field bipolar electrogram or rapid downstroke of the unipolar signal.[64] The CARTO system uses the CONFIDENSE™ module for the auto-annotation. It uses the maximum negative slope of the distal unipolar signal to set the timing of the annotation, and the annotation is displayed on the corresponding bipolar signal. The AutoMap module of the EnSite system allows the user to select which parameter will be used for the annotation including the peak positive/negative voltage, negative/positive slope, absolute slope (steepest slope, either +/−), and absolute voltage (largest voltage, either +/−). The grid mapping catheter with the EnSite system uses a duplicate algorithm. It uses the bipolar electrogram in both directions, along the splines and across the splines. The voltage of the bipolar electrogram can be affected by the direction of the wavefront. The duplicate algorithm displays the largest bipolar voltage at the positive electrode. The Rhythmia system annotates the greatest peak-to-peak voltage of the bipolar signals with the help of the unipolar signals to reduce the far-field signals. The detailed mechanism of the automated annotation algorithm is not open yet, but the efficacy of the algorithm has been proven by clinical experience.[62] The systems provide their own algorithms for special mapping of CFAEs, late potentials, fragmented potentials, etc, based on their fundamental principles. Color-coded activation maps with thousands of electrograms can be created within minutes. Postprocessing is not necessary and is impossible in most cases with thousands of electrograms.

3.5 | Noninvasive panoramic mapping

Noninvasive panoramic mapping combines a noncontrast CT scan to acquire the anatomical information with a 256-electrode vest to obtain the cardiac surface potentials to project them on the epicardial surface of a 3D shell. It offers a comprehensive assessment of the mechanisms and localization of cardiac arrhythmias and it has the proportionated important information to characterize drivers of AF.[41,65] Noninvasive panoramic mapping has been recently used in refractory VT to delineate the substrate and guide stereotactic radiotherapy, making a catheter-free ablation plausible through noninvasive 3D mapping.[66]

4 | CHAPTER 4: CATHETERS FOR 3D MAPPING—MULTI VS SINGLE ELECTRODE, INFLUENCE OF SIZE AND CONFIGURATION

Three-dimensional mapping systems were initially validated using point-by-point technique with the first validation of left ventricular scar detection in a porcine infarct model with a magnetic localization system (CARTO; Biosense Webster) by Callans et al.[67] With an accurate 3D chamber geometry, region of low voltage could be visually stratified by color coding, where a threshold of <1.5m V was shown to be well correlated with pathologic scar. The first animal and human usage of 3D mapping using an ablation catheter was first shown by Shpun et al and Pappone et al in 1997 and 1999, respectively. The most common mapping catheter

configuration used for mapping was an ablation catheter (Navistar, Biosense Webster), which featured a 3.5 mm tip with 1-6-2 spacing from the proximal pair. For nearly a decade, clinical use of 3D mapping systems was performed with the ablation catheter as a single-point mapping catheter to create chamber geometry with voltage sampling. These magnetically based 3D mapping systems require a magnetic sensor embedded into the ablation catheter for real-time localization and acquisition.

Impedance-based electrofield mapping systems (NavX, St. Jude Medical) provide a more open platform, allowing visualization of any electrode catheter connected to the system. In this context, any multielectrode diagnostic catheter could be used to create geometry and record voltage and timing from all electrodes. Rapid creation of chamber geometry as an initial step and subsequent remapping was required to separately acquire and incorporate electrogram data (NaVX Classic, St. Jude Medical). The first published human experience (2008) using a multielectrode catheter to map geometry and characterize atrial arrhythmias in the left atrium utilized a five-spline catheter (PentaRay, Biosense Webster) with the EnSite system.[68] By using a multispline, multielectrode catheter, geometry and mapping information from multiple electrode pairs were achieved expeditiously with high diagnostic accuracy.

In 2009, the accuracy of multielectrode mapping of ventricular scar using an impedance-based system (EnSite, NavX, St Jude Medical) with a linear duodecapolar catheter (2-2-2 Livewire, St. Jude) was validated in comparison with single point mapping in a porcine infarct model.[69] The advantage of a linear catheter is the ability to visualize long conducting channels and to straddle border zone regions with one catheter position. While an initial multielectrode catheter failed to gain clinical popularity (Qwikmap, Biosense Webster), renewed interest in multielectrode acquisition emerged due to the ability to create maps with higher resolution in less time. In 2012, a novel spatiotemporal mapping system (Topera, Abbott Medical) using a 64-electrode basket catheter for biatrial panoramic mapping of AF.[70] In 2014, multielectrode mapping was incorporated in the magnetic sensors placed with a five-spline catheter and decapolar catheter configurations (CARTO MEMS, Biosense Webster). The Rhythmia HDx mapping system (Boston Scientific) became commercially available in 2014 and introduced the first mini-basket 64 electrode configuration with printed mini-electrode technology (0.9 × 0.45 mm) which allowed for noise floor of <0.01 mV (Figure 4-1).

However, a potential disadvantage of multielectrode mapping is that contact force is unlikely to be uniform across all electrode pairs, and in many cases, individual electrodes are intracavitary, completely devoid of contact with the myocardial surface. Basket catheters placed in the endocardium are particularly susceptible to this phenomenon due to the inherent geometric shape, where one hemisphere does not contact the myocardial surface. For this reason, 3D mapping systems have evolved to calculate the relationship of the information obtained with reference to the most outer aspects of the geometric chamber obtained, with the assumption that points that are "internal" to the outer margin samples are not implemented into the working map display. For all multielectrode platforms, the number of points that are utilized are a mere fraction of the total number of points sampled.

Electrogram voltages are inherently dependent on the electrode area (electrode size and spacing) and the relative angle of the incident wavefront to the orientation of the bipole (Figure 4-2).[71] A rigid universal voltage threshold is unlikely to be consistent across the various electrode areas of commercially available catheters (Table 4-1). For this reason, individualized validation is required and comparative studies are needed. In real-world practice, mapping points acquired from a multipolar catheter and single-point catheter are frequently combined on the same map, which is scientifically inaccurate.

Animal studies have highlighted the magnitude of differences in scar delineation between large tip ablation catheters
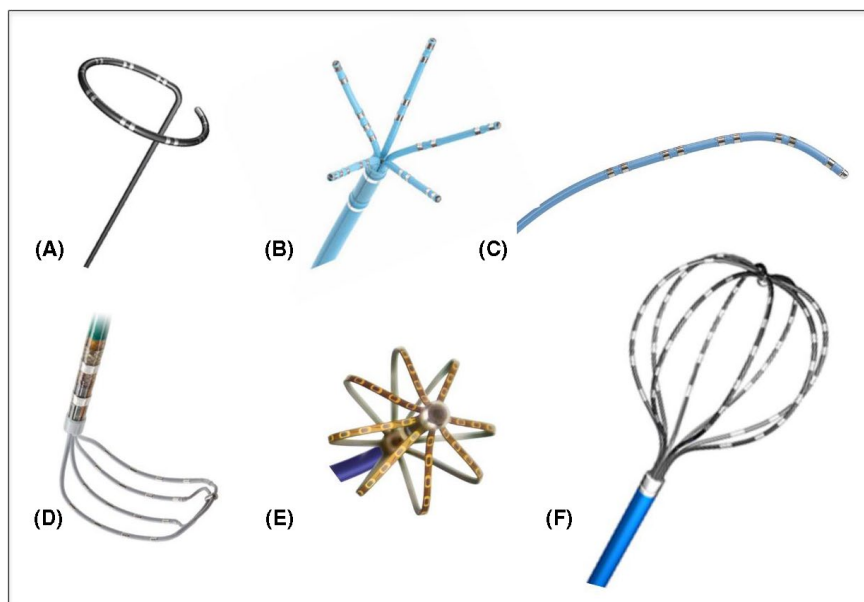

FIGURE 4-1 Commercially available dedicated multielectrode mapping catheters. A, Circular loop catheter; B, Five-splined catheter (PentaRay, Biosense Webster); C, Linear catheter (Decapolar, Biosense Webster); D, Grid catheter (HD Grid, Abbott); E, Mini-basket catheter (Orion, Boston Scientific); F, Basket catheter (Constellation, Boston Scientific)

**Electrode area:
Size and spacing**

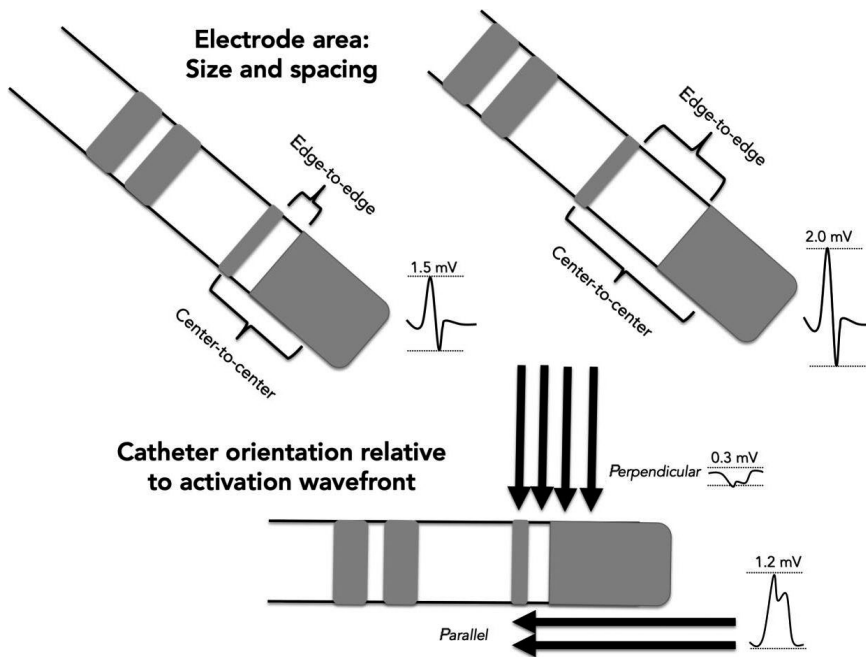**Catheter orientation relative
to activation wavefront**

FIGURE 4-2 Determinants of bipolar amplitude: Electrode area and catheter orientation relative to activation wavefront. Larger interelectrode spacing increases the field of sensing and results in higher bipolar amplitude compared to smaller distance between bipoles. A perpendicular wavefront may result in cancellation of forces and reduced bipolar electrogram amplitude where as a wavefront that runs parallel activates a bipolar pair in sequence and results in a higher amplitude

TABLE 4-1 Summary of various electrode configurations, sizes, and relative spacing with commonly used catheters

Model	Manufacturer	Electrodes	Tip electrode size	Ring electrode size	Spacing (edge-to-edge)	Spacing recorded (center-to-center)
Ablation catheters						
ThermoCool ST	Biosense Webster	4	3.5 mm	1 mm	1 6 2	3.25
ThermoCool/ SF	Biosense Webster	4	3.5 mm	1 mm	2 5 2	4.25
Navistar	Biosense Webster	4	4 mm/8 mm	1 mm	1 7 4	3.50
CoolFlex	St. Jude Medical	4	4 mm	1 mm	0.5 5 2	2.75
Safire/Cool Path	St. Jude Medical	4	4 mm	2 mm	2 5 2	5.00
FlexAbility	St. Jude Medical	4	4 mm	1 mm	1 4 1	3.50
Tacticath	St. Jude Medical	4	3.5 mm	1 mm	2 5 2	4.25
Blazer II/OI	Boston Scientific	4	4 mm	2 mm	2.5 2.5 2.5	4.50
MiFi	Boston Scientific	4	—	1 mm	1.5 mm	2.50
Multielectrode mapping catheters						
PentaRay	Biosense Webster	20	—	1 mm	2 6 2	3.00
Decapolar	Biosense Webster	10	2.4 mm	1 mm	2 8 2	3.00
Lasso	Biosense Webster	20	—	1 mm	2 6 2	3.00
Duodecapolar (Livewire)	St. Jude Medical	20	2	1 mm	2 2 2	3.00
IntellaMap Orion	Boston Scientific	64	—	0.9 mm × 0.45 mm	1.6 mm	2.50
Constellation (60mm)	Boston-Scientific	64	—	—	5	—
Inquiry Optima	St. Jude Medical	24	—	1mm	1 4.5 1	—
Inquiry AFocus II	St. Jude Medical	20	—	1mm	4	—

and dedicated multielectrode mapping catheters. Tschabrunn and Anter et al[72] demonstrated that scar areas were 22% smaller when mapped with a multielectrode catheter with 1mm electrode size (PentaRay) compared to a standard ablation catheter at a fixed threshold of <1.5 mV. On the contrary, Berte and colleagues found that scar areas were larger with multiple spline small electrodes (PentaRay) compared to a Navistar catheter (4 mm tip, 3.5 center-to-center).[73] With over four times the mapping density achieved with smaller electrodes using a multielectrode catheter, the authors speculated this difference as a result of less far-field sensing. Tung et al demonstrated a linear relationship between bipolar voltages and increasing interelectrode spacing, which resulted in smaller

low voltage area detected at a fixed threshold.[74] Differences in scar area have been demonstrated in the left atrium when data were acquired with large-tip single point catheter compared to multielectrode acquisition.[75]

The widespread use of electroanatomic mapping for both simple and complex arrhythmias has become a mainstay in clinical practice. Single and multielectrode acquisition techniques have been shown to be clinically effective, where a trend toward multielectrode use has been observed in mapping of complex arrhythmias, such as left atrial flutter and scar-related VT. As the toolbox of diagnostic and ablation catheters continues to expand, the recognition of the influence of electrode size and configuration on electrogram recordings is an important fundamental concept to 3D mapping.

# 5 | CHAPTER 5. USE OF 3D MAPPING IN SUPRAVENTRICULAR TACHYCARDIA

The term of supraventricular tachycardia (SVT) includes inappropriate sinus tachycardia, atrial tachycardia (AT), macroreentrant AT (including typical atrial flutter), junctional tachycardia, atrioventricular nodal reentrant tachycardia (AVNRT), and atrioventricular reentrant tachycardia (AVRT).[76] The term SVT does not generally include AF.[76] This section will focus on the use of 3D mapping system for the treatment of AVNRT and AVRT. Catheter ablation cures AVNRT and AVRT in most patients with a low risk of complications and can therefore be offered as a first-line therapy to symptomatic patients and to those who cannot tolerate or do not wish to take anti-arrhythmic agents.[76]

An invasive electrophysiological study and catheter ablation of AVNRT and AVRT can be performed under the guidance of fluoroscopy. Currently, advanced mapping systems should be available in the electrophysiology (EP) laboratory for complex ablation procedures.[77] Since the complex ablation procedures such as atrial

fibrillation (AF), AT, and ventricular tachycardia ablation procedures are increasingly performed, the use of 3D mapping has become more widely available and has been used in the cases of SVT ablation procedures as well (Tables 5-1 and 5-2).

In patients undergoing SVT ablation, there are several reasons favoring the use of 3D mapping systems. First, as conventional fluoroscopy-guided catheter ablation is curative in SVTs, currently keeping the radiation dose as low as can be achieved (ALARA) principle is recommended. Previous studies have demonstrated that the use of 3D mapping systems is useful to reduce procedure time, fluoroscopy duration, as well as fluoroscopy dose, in patients undergoing SVT ablation.[78–81] The relation between radiation dose from medical imaging and the attributable lifetime risk of cancer[82] and genetic anomaly[83] stresses the pivotal importance of minimization of x-ray exposure in cardiac EP practice for both the patient and the operator. As patients with SVTs are expected to be younger and have longer lifelong period after index ablation, it may be more critical to reduce radiation exposure in these group of patients, especially in pediatric patients. In pregnant patients with SVTs, if urgent ablation is needed, the use of a 3D mapping system is recommended to minimize or even eliminate radiation exposure.[84] Second, success rates of catheter ablation for AVRT depends on accessory pathway (AP) localization. The success rate for left free wall AP ablation is the highest among all APs, whereas right free wall AP has the lowest success rate. 3D activation map of the area close to the pathway insertion is useful in addition to conventional mapping to precisely localize and tag the atrial and ventricular AP insertion site. This can be particularly useful in redo procedures or cases with impaired catheter stability (eg, right-sided free-wall pathways), after catheter dislodgement during ablation (eg, due to tachycardia termination) or when consecutive mapping from different anatomical sites (eg, atrium, ventricles, coronary sinus, or aortic root) or approaches (eg, transseptal vs. retrograde) is performed. Standard fluoroscopy, CT, MRI, and intracardiac

FIGURE 5-1 AVNRT ablation using CARTO Univu. RAO 30° and LAO 40° projection. Yellow dots represent His EGM. Green: real-time CS. Brown: shadow CS allowing detection of catheter dislodgement. Abl, Ablation catheter; AVNRT, atrioventricular nodal reentrant tachycardia; Cs, coronary sinus catheter; EGM, electrogram; His, His catheter; LAO, left anterior oblique; RAO, right anterior oblique
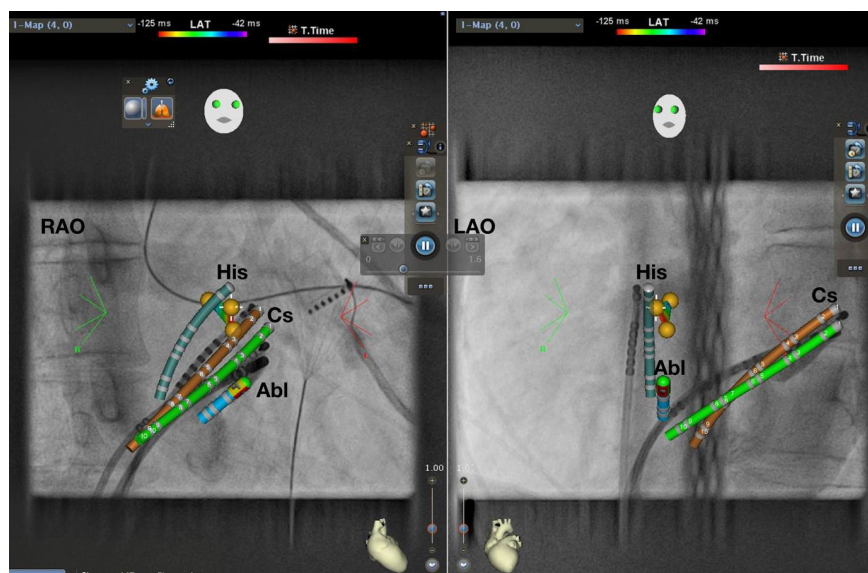
ultrasound images can be integrated with electroanatomic mapping systems to link electrogram information with anatomical structures. This allows nonfluoroscopic catheter localization, reducing radiation exposure during catheter ablation procedures.[85] Third, 3D mapping systems allow continuous visualization of the ablation catheter and has therefore the potential to improve the safety of the procedure. For instance, during ablation of targets close to the normal conducting system (eg, AVNRT or parahisian/midseptal APs), catheter visualization may reduce the risk

of complete AV block. Fourth, in many SVT procedures such as complex AVRT ablation, a stable intracardiac reference (typically the coronary sinus catheter) is mandatory. Catheter dislodgement can be detected not only by intracardiac signals but also by visualization of the intracardiac reference catheter. Most mapping systems allow real-time visualization of the intracardiac reference catheter thereby allowing early detection and reposition in case of catheter dislodgement. Additionally, successful SVT ablation does not only depend on the precise location of the ablation
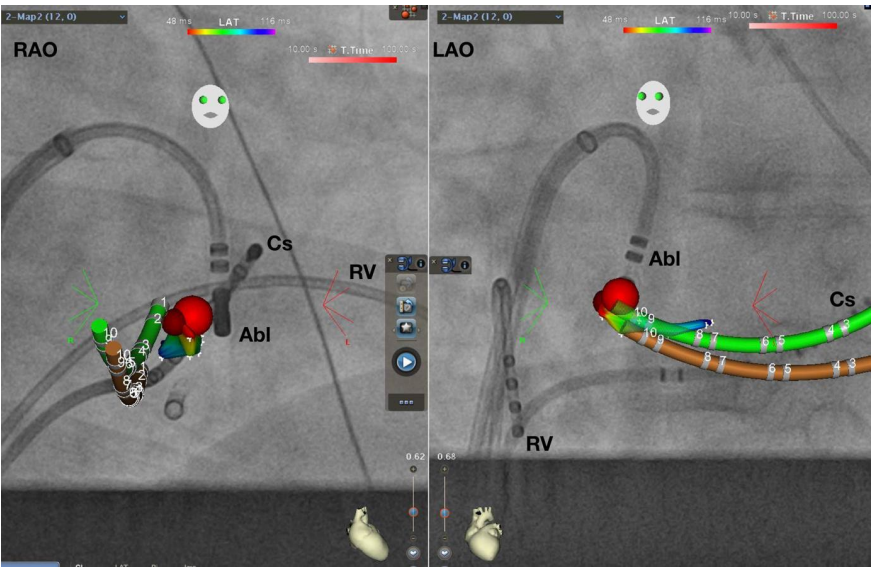

FIGURE 5-2 AVRT ablation using CARTO Univu. RAO 30° and LAO 40° projection. Coronary sinus activation map shows earliest ventricular signal during preexcitation in red color. Red dot represents successful ablation site. Green: real-time CS. Brown: shadow CS allowing detection of catheter dislodgement. Abl, Ablation catheter; AVRT, atrioventricular reentrant tachycardia; Cs, coronary sinus catheter; LAO, left anterior oblique; RAO, right anterior oblique

TABLE 5-1 Consensus recommendations

Use of 3D mapping in supraventricular tachycardias			
Recommendation	**Class**	**LOE**	**References**
In pediatric patients or pregnant patients undergoing SVT ablation, the use of a 3D mapping system is recommended to reduce radiation exposure to a minimum and to reduce the risk of complications such as total AV block.	I	C-LD	84,89–91
In patients with midseptal or parahisian pathways undergoing SVT ablation, the use of a 3D mapping system is recommended to reduce radiation exposure and to reduce the risk of complications such as total AV block.	I	C-LD	87
The use of a 3D mapping system is reasonable for redo ablation procedures or cases with impaired catheter stability (eg, right-sided free-wall pathways), after catheter dislodgement during ablation (eg, due to tachycardia termination) or when consecutive mapping from different anatomical sites (eg, atrium, ventricles, coronary sinus, aortic root) is performed to facilitate the ablation procedure, to better understand the anatomy to reduce procedure duration and radiation exposure for both the patient and the operator.	IIa	C-LD	81,92–95
For localizations of APs with lower success and higher recurrence rates, such as right-sided APs, it is reasonable to use a 3D mapping system to reduce procedure and fluoroscopy time.	IIa	B-R	78

Abbreviations: 3D, three-dimensional; AV, atrioventricular; AP, accessory pathway; LOE, level of evidence; SVT, supraventricular tachycardia.

TABLE 5-2 Data from the literature on the use of 3D mapping in supraventricular tachycardias

Paper	Number of patients	Mean Age	Technology	Diagnosis
Papagiannis 2006[96]	40	12	NavX	AVRT, AVNRT
Drago et al 2012[97]	21	11	CARTO	Right-sided AP
Smith et al 2007[89]	30	13	NavX	AVNRT, AP
Tuzcu et al 2007[90]	28	13	NavX	AVNRT, AP, Right AT
Nagaraju et al 2016[91]	63	13	CARTO	AVNRT, WPW, Concealed AP
Earley et al 2006[81]	49	48	CARTO NavX	AVNRT, AP, Typical atrial Flutter
Alvarez et al 2009[93]	50	50	NavX	AVNRT
Casella et al 2011[92]	50	34	NavX	AVNRT, AP, Typical atrial flutter, Right-sided AP
Fernández-Gómez JM et al 2014[94]	328	55	NavX	Typical atrial flutter, AVNRT, AVRT, Atypical atrial flutter, AT
Ma Y et al 2015[78]	64	33	NavX	Right-sided AP
Giaccardi et al 2016[95]	297	58	NavX	AVNRT, Atrial flutter, AP, AT, His ablation, VT
Sporton et al 2004[79]	102		CARTO	Paroxysmal SVT, WPW
Kesek et al 2006[80]	365		LocaLisa	AVNRT, WPW, Atrial Flutter

Abbreviations: 3D, three-dimensional; AP, accessory pathway; AT, atrial tachycardia; AVNRT, atrioventricular nodal reentrant tachycardia; AVRT, atrioventricular reentrant tachycardia; VT, ventricular tachycardia; WPW, Wolff-Parkinson-White.

target but also on adequate lesion formation. Radiofrequency (RF) lesions size is determined by several parameters including contact force, time, and power. Novel software modules allow for automated ablation lesion tagging within the 3D mapping system based on different algorithms such as the force-time integral or the lesion size index. Target ablation sites are mostly located endocardially and do not require transmural lesion formation.[86] It is critical to balance the optimal ablation lesion size as very large and transmural lesions may harm coronary arteries or the AV nodal conduction and inadequate small lesions may result in arrhythmia recurrence.[87] Furthermore, particularly in patients with complex anatomy (eg, congenital heart disease, twin AV node, post cardiac surgery, etc), the 3D mapping systems allow a better understanding of the anatomy and the pathophysiology of the arrhythmia. In these complex patients, the combination of the 3D mapping system with image integration and remote magnetic navigation have been shown to be useful to facilitate ablation with very low fluoroscopy exposure.[88] Last but not least, 3D mapping systems facilitate the training of young electrophysiologists. Integration of the fluoroscopy into the mapping system (CARTO Univu, Mediguide) allows better understanding of the anatomy and might be associated with a faster learning curve and a better safety profile due to continuous catheter visualization during ablation thereby potentially avoiding complications such as an AV block during slow pathway ablation (Figures 5-1 and 5-2). The disadvantages of 3D mapping system for SVT ablation include higher cost, as well as additional training, support, and procedure preparation time.

6 | CHAPTER 6: USE OF 3D MAPPING IN ARRHYTHMIAS IN CONGENITAL HEART DISEASES AND POSTSURGICAL CORRECTION

Arrhythmias are frequently encountered in patients with congenital heart disease (CHD; with or without corrective surgery) and respond poorly to pharmacologic therapies.[98–100] Catheter ablation is a valuable treatment option but must respond to many challenges with regard to the anatomical variances, type of arrhythmia substrate, and access to the target chamber.[88,101–104] In all these patients, a careful review of the entire hemodynamic and arrhythmia situation needs to be performed prior to the procedure and, if available, operation notes need to be reviewed. Besides identifying potential substrates for arrhythmias such as surgical patches or incision (eg, from atriotomy or cardio-pulmonary bypass connections), chamber dilatation due to volume or pressure overload can lead to extensive fibrosis which can typically give rise to multiple different arrhythmias in a single individual.[100,105] Progression from sustained AT to AF is frequent and may change the hemodynamic conditions for clot formation substantially, such that catheter ablation may not be feasible in the end.[106–108]

The advent of the sequential mapping systems allowed a first major improvement in the mapping during ongoing AT.[109] Due to recent available technologies it is now very feasible to address all types of ablation procedures even in patients with the most complex arrhythmias and CHD conditions (eg, Bethesda class 3; Figure 6-1).[88,100,110] The choice of 3D mapping systems is focused mostly on sequential (eg, electroanatomical mapping)[110] or high-density mapping systems,[111] but both require direct access to the target chamber (Table 6-1). More recently, simultaneous mapping combining body surface mapping with noncontrast CT imaging has been used to noninvasively map arrhythmias in CHD patients.[112] The advantage of this global mapping attempt is helpful when arrhythmias are only transient and/or multiple arrhythmias (eg, ectopy) need to be addressed.

6.1 | 3D image integration options

The use of 3D roadmaps to understand the underlying anatomy is a tool available to essentially every 3D mapping system.[113,114] Source data for these 3D virtual heart models can be quickly and reproducibly obtained from contrast CT scans or noncontrast cardiac MRI (Table 6-1). Dedicated 3D software can be used as stand-alone or as part of the 3D mapping software package (eg, Polaris, CARTO, Biosense Webster). Direct complex image merge is particularly important with good registration results to facilitate the navigation process across heart valves or artificial patches. Best anatomical registration is achieved using the aorta as the reference chamber since the tubular structure is easily mapped and the 3D shape including the aortic arch is usually well depicted in 3D scans.[115] ICE is an
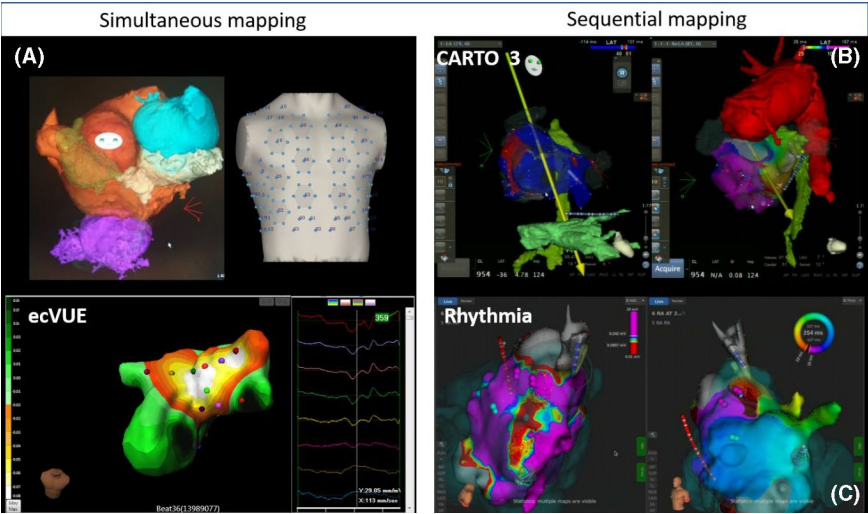

FIGURE 6-1 Options of 3D mapping systems. 3D, three-dimensional

TABLE 6-1 Options of 3D image integration

Type of imaging	Advantage	Disadvantage
Contrast CT	Quick scanning time Widely available Easy 3D reconstruction on all software packages	Contrast exposure and transit times may be long due to the reduced cardiac output resulting in high-radiation burden
Noncontrast CMR	Nonstandard sequence in many laboratories Unlimited field of view (allows to scan from neck to groins to assess access options) No radiation burden	More difficult and time-consuming to 3D reconstruct on the available 3D software packages No resolution within stents or close to metallic objects Implantable devices (even when conditional) may cause artefacts
ICE	Excellent 3D reconstructions of any given 3D anatomy	Requires intracardiac access Expertise may be difficult to obtain in CHD
3D TTE or TEE	Increasingly available Popular tool in interventional procedures	Stand-alone 3D reconstructions not directly integrated in 3D mapping TEE requires general anesthesia and intubation if performed throughout the entire procedure

3D, three-dimensional; CHD, congenital heart disease; CMR, cardiac magnetic resonance; CT, computed tomography; ICE, intracardiac echocardiography; TEE, transesophageal echocardiography; TTE, transthoracic echocardiography.

alternative modality to aid 3D reconstruction of complex anatomy in CHD,[116] but lacks the pre-procedural planning phase. Especially in patients with limited vascular access, there might not be enough room to advance an ICE probe, which also requires a large lumen sheath.

6.2 | Additional advanced technologies

Remote magnetic navigation has been established a valuable tool for ablation in very complex CHD patients as it allows to reach "hidden" or difficult to access target chambers and essentially avoids doing any transbaffle punctures.[88,115,117,118] An additional advantage is that the workstation allows picture-in-picture display of all catheters (including nearby diagnostic catheters) in 3D, which greatly increases operator's orientation and results in very low fluoroscopy exposure (Figure 6-2).

6.3 | Types of arrhythmia in CHD

Various groups have reported on their results using 3D mapping in CHD patients (Table 6-2). Sustained atrial arrhythmias have been mostly reported with good follow-up results.[88,101,110,118] However, AF ablation in CHD is still in its infancy and results are still quite sobering and fall far below the success rates in non-CHD patients, even for paroxysmal AF.[119-121] In VT ablation, the most important identification of a "surgically" created isthmus (eg, around the outflow tract patch in patients after surgical repair of Tetralogy of Fallot) was made a decade ago, which led to a well-established
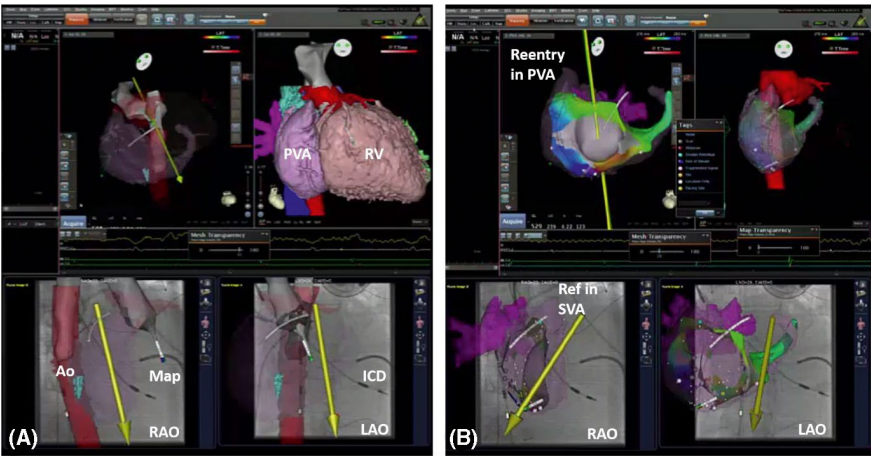

FIGURE 6-2 Example of picture-in-picture 3D imaging + 3D mapping. Examples of 3D image integration from 3D DICOM files (CT) in a patient with transposition of the great arteries (TGA) and Mustard repair plus ICD implantation. A, The merging of the 3D fast anatomical map (FAM) of the aorta during retrograde remote-controlled mapping to allow best registration. Please note that the magnetic catheter has just crossed the aortic valve and is aligned in parallel to the magnetic field vector (yellow arrow). B, The 3D local activation time (LAT) map of a peritricuspid reentry in the pulmonary venous atrium (PVA). Please note the timing reference catheter (REF) in the systemic venous atrium (SVA). 3D, three-dimensional

TABLE 6-2 Consensus recommendations

Use of 3D mapping in arrhythmias in congenital heart diseases and postsurgical correction			
Recommendation	**Class**	**LOE**	**References**
In AT patients with CHD or postsurgical correction, use of 3D mapping is recommended.	I	B-NR	109–112
In AF patients with CHD or postsurgical correction, 3D mapping is recommended.	I	B-NR	119,120
In patients with VT and underlying CHD or postsurgical correction, 3D mapping is recommended.	I	B-NR	122
In patients with AT or VT underlying CHD or postsurgical correction, 3D mapping is recommended, to lower duration of fluoroscopic exposure.	I	B-NR	88,117,118

Abbreviations: 3D, three-dimensional; ASD, atrial septal defect; AT, atrial tachycardia; CHD, congenital heart disease; VT, ventricular tachycardia.

ablation procedure that is recently a standard of care for these patients.[122]

7 | CHAPTER 7: THREE-DIMENSIONAL MAPPING-GUIDED CATHETER ABLATION OF ATRIAL FIBRILLATION

Catheter ablation of AF, introduced nearly 20 years ago, is currently a well-accepted therapeutic strategy for AF.[123,124] Percutaneous catheter ablation is now widely used as an interventional tool for nonpharmacological AF rhythm control, especially in patients who are refractory to anti-arrhythmic medications.[125] Studies have demonstrated that the myocardium around the pulmonary veins (PV) play an important role in the initiation and maintenance of AF.[126–128] This important finding led to the development of PV ablation.[123,124] In order to facilitate this task with less radiation than plain fluoroscopy, electroanatomical mapping have been developed, enabling the tracking of intracardiac electrodes in 3D maps and the navigation of catheter ablation. In the late 1990s, 3D localization systems were first introduced to invasive electrophysiology as complementary to real-time x-ray[11] and to the systematic study of 3D-guided AF ablation in the early 2000.[129] In 2001, Pappone et al applied 3D mapping to guide circumferential ablation and target the remaining electrograms after the first round of isolation.[130] Acquisition, processing, and spatial projection of mapping points into a 3D mesh facilitate identification of the anatomy/substrate for arrhythmia, track sites of ablation, and generate the geometry for pure anatomically based ablations such as PV isolation (PVI). The most common 3D mapping systems for AF ablation are the Carto (Biosense Webster) and the EnSite NavX system (Abbott Medical). Advanced mapping systems emerged from the need to better understand and ablate complex AF substrate, by improving the acquisition and illustration of electrophysiological information.

7.1 | Ablation strategy of pulmonary vein isolation

PVI is one of the common end points of all AF ablation procedures and is most often validated using a preshaped circular catheter. In the last decades, PVI has evolved from an electrophysiologically guided segmental ostial approach to a more anatomically guided circumferential PV ablation approach, generally using a 3D mapping system. Segmental PVI at the ostium is associated with an increased risk of PV stenosis and this complication led to the wider use of wide antral circumferential PV ablation to achieve entrance and exit block as end point of PVI.[131] The innovation of 3D mapping systems used for anatomy reconstruction and as guide for the delivery of ablation lesions avoids the use of multiple transseptal punctures and multiple catheters in the left atrium. Segmental PVI with the combined use of 3D mapping and a circular catheter facilitate electrical isolation of the PVs compared with conventional fluoroscopy-guided segmental ablation with the use of a circular

catheter.[39] However, the AF-free outcomes of segmental PV ablation and wide antral circumferential ablation were found to be equivalent according to a worldwide survey. Newer technologies allow for simultaneous integration of the multipolar catheter with automatic annotation and high-density mapping to facilitate identification of gaps at the PVs.[111,132–134] In order to avoid complications (PV stenosis, perforation, phrenic nerve, or esophageal injury), and achieve electrically continuous and transmural lesions, a reliable 3D navigation was required. This also facilitates this task with less radiation than plain fluoroscopy.[135] With the advantages of current 3D mapping techniques, 3D map-based anatomic ablation is replacing traditional electrophysiology (fluoroscopy and electrogram)-guided AF ablation.

7.1.1 | Application of image tool in pulmonary vein isolation

The accuracy of 3D mapping systems has been established prior to their clinical adoption. Currently, 3D precision, accuracy, and innovation of software and hardware facilitates and standardizes AF ablation procedures. The amount of comparative clinical trials on 3D mapping with the preexisting conventional x-ray based procedure is rather limited. Comparing the conventional fluoroscopy-guided ablation and 3D mapping-guided ablation, some studies evaluated the use of CT-merged 3D for PV ablation (Figure 7-1). In order to enhance recognition of anatomical variations, integration of pre-procedural CT/MRI data or intraprocedural ICE (CartoSound®, Biosense Webster) is possible through merging of the 3D models.[136] CT can provide highly detailed information of complex anatomic structures and validate the acquired anatomy at the time of ablation (Figure 7-2). These trials showed reductions in fluoroscopy time, comparable safety end point, and improved ablation outcomes. However, the use of CT scan acquisition leads to additional x-ray exposure and radiation safety remains a major concern in current practice. Recently, the CARTO SOUND module available in the CARTO system allows for real-time integration of acquired anatomical information via intracardiac ultrasound with the 3D maps (Figure 7-3).[136]

7.1.2 | Obtaining durable PVI

It is well recognized that a major determinant of lesion size during RF application is the electrode tissue contact force.[137] In the meta-analysis by Shurrab et al,[138] contact-force sensing technology was found to be associated with a lower rate of AF recurrence, less ablation and procedure time, and fluoroscopic time as compared with conventional ablation catheters.[138] In the EFFICAS I, a minimum force-time integral (FTI) <400 gs had a greater chance of PV reconnection at 3 months follow-up.[139] The 3D mapping systems with automatic lesion index integration of contact-force feedback help to visualize and evaluate the efficiency and stability of lesions along the ablation
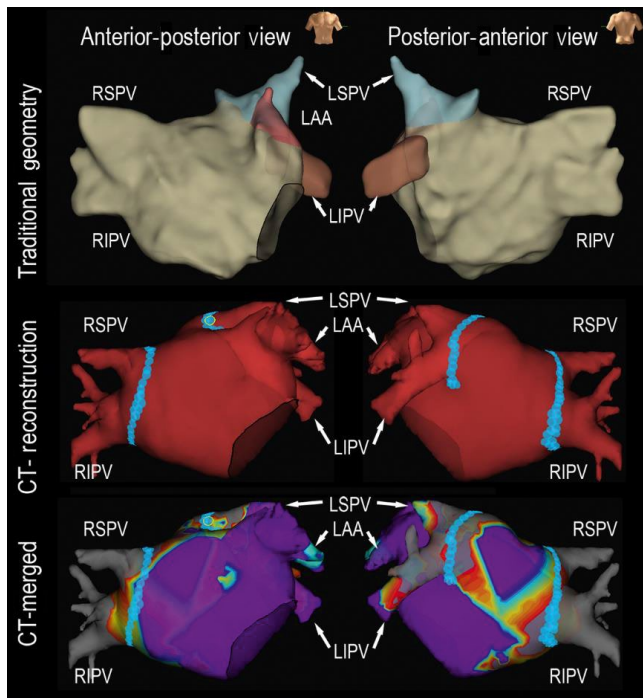
FIGURE 7-1 A representative case using CT reconstruction for paroxysmal atrial fibrillation catheter ablation. Upper panel: 3D geometry created by traditional circular catheter; Middle panel: Merged CT reconstruction geometry during catheter ablation; Lower panel: Merged CT reconstruction with 3D bipolar voltage mapping using a circular mapping catheter. 3D, three-dimensional; CT, computed tomography; LAA, left atrial appendage; LIPV, left inferior pulmonary vein; LSPV, left superior pulmonary vein; RIPV, right inferior pulmonary vein; RSPV, right superior pulmonary vein

line.[24,140,141] Additionally, AF ablation with contact-force technology and strict criteria of stability was reported as a safe procedure and is associated with an improvement in efficiency and a reduction in AF recurrence.[142,143]

7.2 | Ablation strategy of AF outside of the PV

There is no consensus on the optimal strategy beyond PVI among patients with persistent AF. Ablation of persistent AF is more challenging and is associated with less favorable outcomes.[144,145] Despite technical advances and growing experience in performing catheter ablation using RF ablation or cryotherapy, the long-term procedural success rates for persistent AF have not paralleled those of paroxysmal AF. Therefore, effort has been directed toward identifying additional strategies to improve the outcomes of persistent AF. Recently, substrate modification techniques, including linear ablation,[146,147] complex fractionated atrial electrogram (CFAE) ablation,[148,149] rotor ablation,[146,150] and scar homogenization,[151,152] have been studied in patients with persistent AF in addition to PVI as alternative approaches. Although the results from STAR AF II revealed no difference in the rate of recurrent AF when either linear ablation or ablation of CFAE was performed in addition to PVI,[39]
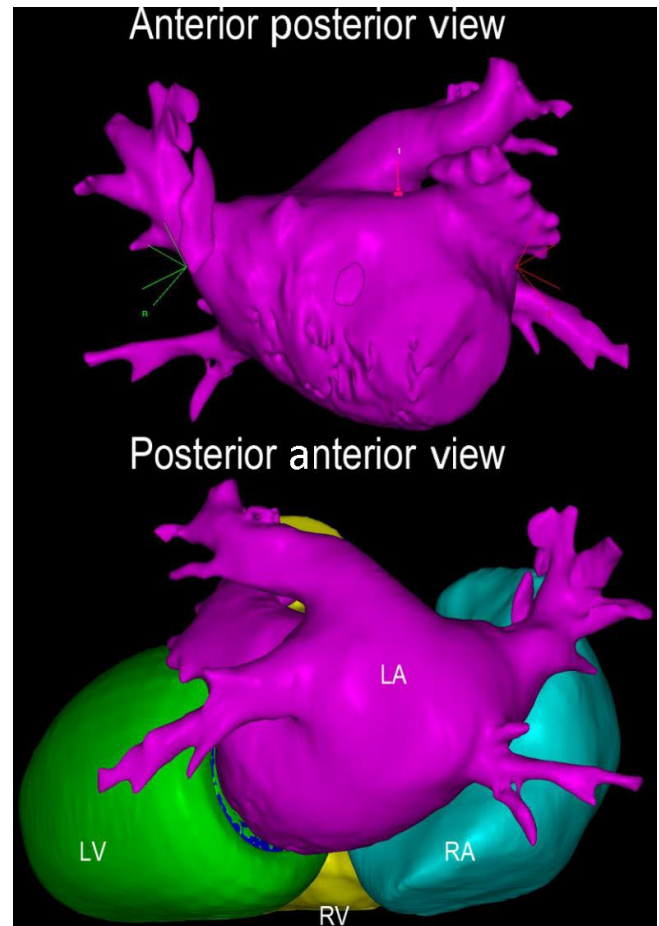

FIGURE 7-2 Contrast-enhanced CT with three-dimensional reconstruction. Contrast-enhanced CT images were uploaded to CARTOSEG CT Segmentation Module software (Biosense Webster, Inc). Structures of the left and right atria and ventricles were created without any prior manual input. CT, computed tomography; LA, left atrium; LV, left ventricle; RA, right atrium; RV, right ventricle

most laboratories still perform additional substrate modification in patients with nonparoxysmal AF. Table 7-1 shows the summary of ablation strategies beyond PVI and their characteristics. Searching for non-PV triggers is recommended after restoration of sinus rhythm by AF procedural termination or electrical cardioversion. Activation mapping is recommended at any step if AF transformed to an organized AT. Conventional mapping catheters are limited by their inability to identify complex reentrant circuits and small conducting gaps. In contrast, high-density mapping based on 3D electroanatomic systems is able to identify PV gaps and macroreentrant circuits.[111,132]

7.2.1 | Linear ablation

The linear ablation technique has been reported as a substrate modification strategy in addition to PVI from a prospective randomized study conducted by Willems and colleagues.[147] The most commonly targeted linear lesion sets are the left atrial roof and mitral isthmus.
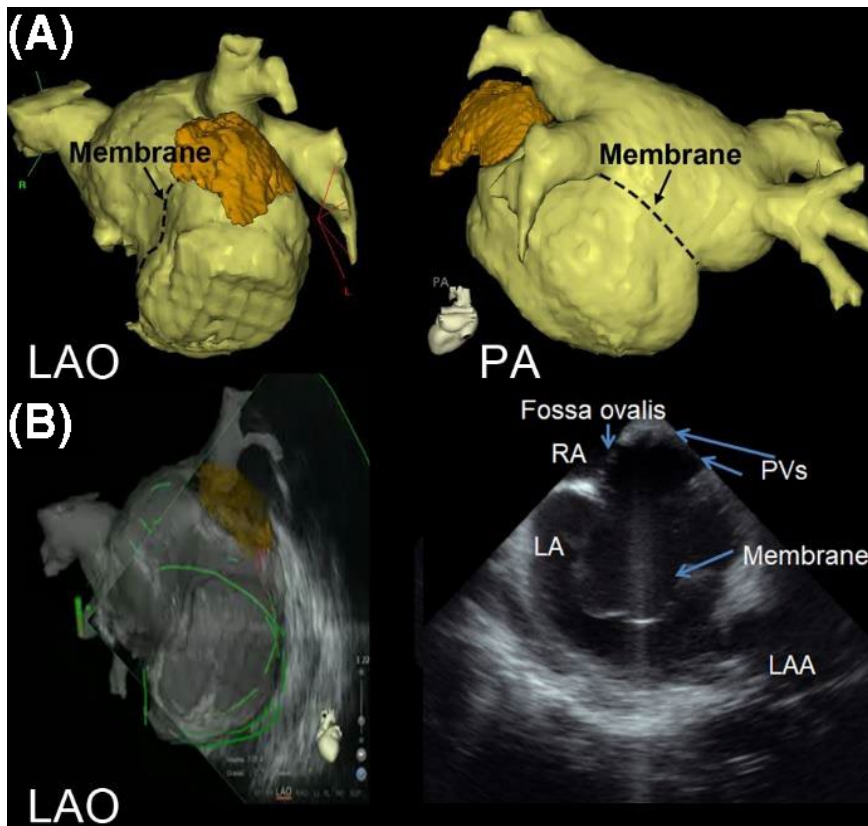
FIGURE 7-3 A representative case using intracardiac echocardiography and CT reconstruction for atrial fibrillation catheter ablation in a patient with cor triatriatum. A, 3D reconstruction of the LA image by computed tomography (CT) is shown in LAO view and PA view. The location of the membrane is marked with dotted lines. B, LA geometry is created by real-time intracardiac echocardiography under the guidance of reconstructed CT. The PVs are identified above the membrane by intracardiac echocardiography and the sound geometry is created. 3D, three-dimensional; LA, left atrium; CT, computed tomography; LAO, left anterior oblique; PA, posterior anterior; PV, pulmonary vein

TABLE 7-1 Summary of ablation strategies beyond PVI and its characteristics

Ablation Strategy	Arrhythmia Type	How to Identify Critical Sites	Ablation Lesion Locations
Linear ablation	Organized AT Persistent AF	– Activation mapping of 3D mapping system – Entrainment mapping	– Roof line – Mitral and tricuspid isthmus line – Connecting two anatomical obstacles
CFAE ablation	Persistent AF	– Visually identified fractionated electrograms – Automatic algorithm of 3D mapping system	– Left atrium and right atrium
Non-PV trigger ablation	Paroxysmal AF Persistent AF	– EKG – Multiple mapping catheters – 3D mapping system	– Left atrial anterior, posterior wall, appendage, ligament of Marshall, septum, other Non-PV triggers identified in the right or left atrium – Superior vena cava – Coronary sinus
Rotor ablation	Persistent AF	– Nonlinear analysis and phase mapping	– Rotor or focal source identified in the right or left atrium by mapping system
Substrate-guided ablation	Persistent AF	– 3D mapping system – MRI	– Low-voltage zones identified in the right or left atrium by mapping system

Abbreviations: 3D, three-dimensional; AF, atrial fibrillation, CFAE, complex fractionated atrial electrogram; EKG, electrocardiogram; PV, pulmonary vein.

Iesaka et al reported that PVI followed by biatrial predetermined linear ablations for substrate modification is feasible and AF termination happened in 51% of patients with an AF-free rate of 74% after 1.7 procedures and 1.5-years of follow-up.[153,154] Pak and Kim proposed that linear ablation at left atrial anterior wall resulted in a better clinical outcome among persistent AF patients.[155]

Currently, additional linear lesions failed to show benefits among patients with paroxysmal AF. An updated meta-analysis of randomized controlled trials published that additional linear ablation did not exhibit any benefits in terms of sinus rhythm maintenance following a single procedure, but increased the mean procedural, fluoroscopy, and radiofrequency application times.[156] Even among patients with persistent AF, the outcome of linear ablation is still controversial.[157,158] A recent prospective randomized study also showed no significant difference in the 1 year freedom from atrial tachyarrhythmias between the stand-alone PVI and a stepwise approach of PVI plus CFAE and linear ablation for persistent AF.[159] Therefore, linear ablation itself may only be helpful in eliminating AF sources during the index procedure; however, the lack of durable and incomplete lesions on follow-up procedures can be proarrhythmic and even complete lines have been shown to promote reentry. Assessment of line completeness shall be considered using 3D mapping, and the presence of bidirectional conduction block of lines shall be confirmed as the end point of the linear ablation. However, 3D mapping is not necessary for confirmation of CTI line block.

7.2.2 | Non-PV sources of AF

Localization of AF triggers is an important electrophysiologic strategy for catheter ablation of AF. Previous studies also described that 6% to 65% of patients have non-PV AF initiators.[160] The majority of non-PV triggers initiating AF have a specific anatomical distribution in the left atrium (LA) (26.3%), superior vena cava (SVC) (22.6%), coronary sinus (CS) (17.6%), right atrium (RA) including the crista terminalis (16.9%), interatrial septum (7.4%), and followed by the ligament of Marshall (LOM; 4.4%).

Localization of AF triggers is an important electrophysiologic strategy for the catheter ablation of AF. Previous publications have demonstrated algorithms for localization of trigger sites of origin using endocardial activation timing from the high RA, His bundle, and distal/proximal portion of the CS to predict non-PV ectopy.[160-163]

For unmappable infrequent beats originating from uncommon areas, the activation mapping by fixed multipolar catheters may not be efficient for localizing the AF triggers. Therefore, the development of a novel single-beat analysis by invasive or noninvasive high-density mapping systems is needed. Advancements in mapping and alternative energy modalities with 3D navigation are likely to play an important role in non-PV ectopy ablation. The noncontact mapping (NCM) system (EnSite Array, Abbott, St. Paul, MN) and the body surface 252-electrode vest[164-166] (CardioInsight Mapping Vest, Medtronic, Inc) have the specific advantage of their ability to map extrapulmonary vein ectopy and macroreentrant circuits that can initiate and maintain AF, because of their high-resolution capability and the feasibility of analyzing a single beat. These tools are useful for the identification of non-PV ectopies using only a single beat for analysis.

7.2.3 | Specific AF source ablation of rotors

Rotors are defined as stable and sustained spiral activation around a center of rotation, whereas focal impulses are defined by centrifugal activation from a source. Because of the advancement of signal processing systems, mapping systems, and mapping catheters, several recent studies were able to demonstrate successful rotor identification during AF ablation. Lin et al, Haissaguerre et al, and Narayan et al used phase mapping-based strategy to identify rotors during procedures,[70,146,167] while Atienza et al, Jadidi et al, and Seitz et al used activation-based strategy to identify rotors (Table 7-2).[168-170] Pooled data on the efficacy of rotor-guided AF ablation suggest increased freedom from AF/AT relative to conventional strategies.[171] Rotor-guided ablation has emerged as a potential therapeutic target for persistent AF ablation. Robust data from randomized trials with a standardized rotor-mapping protocol are still needed.

7.3 | Scar homogenization using MRI or voltage mapping

There is growing evidence that atrial fibrosis plays a key role in the maintenance of AF. Left atrial scarring can be identified by contact 3D mapping and some centers target the atrial substrate using sinus rhythm voltage for substrate modification. There is also growing evidence of the association between the progression of AF and atrial fibrosis identified by delayed enhancement MRI (DE-MRI); however, the quality and resolution of images of atrial fibrosis remains technically challenging.[151,172] MRI may be performed before catheter ablation of AF to identify atrial fibrosis or after ablation to visualize RF ablation lesions (Figure 7-4).[173,174]

TABLE 7-2 One year outcome of rotor-guided ablation vs. conventional strategy

First author (year)	Study type	Mapping materials	ORs [95%CI]
Atienza_PAF (2014)[168]	RCT	Activation mapping	0.88 [0.42, 1.86]
Atienza_PerAF (2014)[168]	RCT	Activation mapping	0.76 [0.37, 1.57]
Lin (2016)[146]	RCT	Phase mapping	0.38 [0.14, 1.01]
Narayan (2012)[70]	Non-RCT	Phase mapping	0.27 [0.11, 0.65]
Haïssaguerre (2014)[167]	Matched	Phase mapping	0.42 [0.19, 0.94]
Jadidi (2016)[169]	Matched	Activation mapping	0.22 [0.11, 0.45]
Seitz (2017)[170]	Matched	Activation mapping	0.46 [0.23, 0.93]

CI, confidence interval; ORs, odds ratios; PAF, paroxysmal atrial fibrillation; PerAF, persistent atrial fibrillation; RCT, randomized control trial.
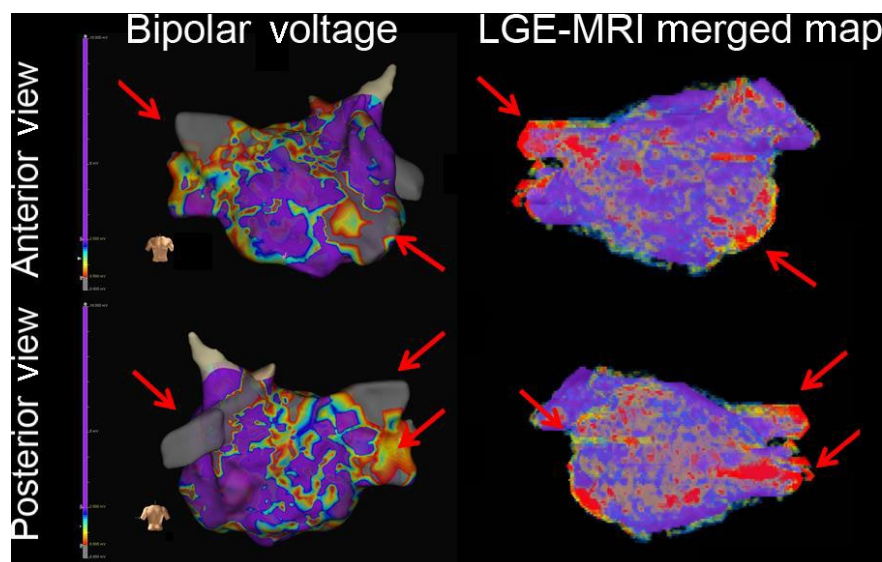
FIGURE 7-4 A representative case using LGE-MRI reconstruction for persistent atrial fibrillation catheter ablation. 3D mapping (left panel) with bipolar voltage mapping is shown in anterior view (upper panel) and posterior view (lower panel). The LGE-MRI reconstruction (right panel) showed compatible fibrosis areas in the mitral area, RSPV, RIPV, and LIPV. MRI was merged with 3D electroanatomic mapping during the procedure. 3D, three-dimensional; LA, left atrium; LGE-MRI, late gadolinium enhancement-magnetic resonance imaging; LIPV, left inferior pulmonary vein; RIPV, right inferior pulmonary vein; RSPV, right superior pulmonary vein

TABLE 7-3 Consensus recommendations

Use of 3D mapping: Three-dimensional mapping-guided catheter ablation of atrial fibrillation			
Recommendation	**Class**	**LOE**	**References**
Careful identification of the PV ostia and left atrial geometry using a 3D mapping system is recommended to avoid ablation within the PVs, and obtain durable PV ablation.	I	B-NR	39,111,131–135
If linear ablation lesions are applied, 3D mapping and pacing maneuvers is recommended to assess for line completeness.[a]	I	C-LD	39,125,147,153–155
If non-PV triggers initiating AF are identified, using a 3D mapping system to locate the potential origin of extrapulmonary sources of AF can be useful.	IIa	C-LD	125,161
Use of a 3D mapping system to delineate the substrate, identify the low-voltage zone, and identify the rotational activity or focal sources of AF is reasonable.	IIa	B-NR	125,146,151,160–163
For patients with persistent or long-standing persistent AF, 3D mapping-guided linear ablation as an initial or repeat ablation strategy is not well established.	IIb	B-R	39,125,147,153–155
For patients with persistent or long-standing persistent AF, 3D mapping-guided ablation of rotational activity or reentrant sources is not well established.	IIb	B-NR	125,146,167–170
For patients with persistent or long-standing persistent AF, the usefulness of 3D mapping and ablation of areas of abnormal myocardial tissue identified with voltage mapping or MRI as an initial or repeat ablation strategy is not well established.	IIb	B-R	125,151,172–174
For patients with persistent or long-standing persistent AF, the usefulness of 3D mapping and ablation of complex fractionated atrial electrograms as an initial or repeat ablation strategy is not well established.	IIb	B-R	39,125,149

Abbreviations: 3D, three-dimensional; AF, atrial fibrillation; PV, pulmonary vein; MRI, magnetic resonance imaging.

[a]3D mapping is not necessary for confirmation of CTI line block.

However, high-resolution MRI for identification of atrial fibrosis or postablation lesions still remains technically challenging with limited reproducibility.[175] In the multicenter prospective DECAAF trial, AF recurrence 325 days after ablation was independently associated with the extent of atrial fibrosis.[151] In the 2017 expert consensus document,[125] the strategy of mapping and ablation of areas of abnormal myocardial tissue identified by voltage mapping or MRI as an initial or repeat ablation strategy for persistent or longstanding persistent AF was given a class IIb recommendation. Voltage- and MRI-guided substrate ablation in addition to PVI has been performed successfully; however, supporting data are mostly based on nonrandomized observation studies with a possible increased risk of complication from extensive ablation.

Among patients with persistent and long-lasting AF, the role of substrate-guided AF ablation remains promising. Current mapping technologies offer additional tools (improved automatic algorithm for annotation, multiple electrode mapping, high-density mapping, and application of different processing techniques) to identify the putative mechanism underlying AF.

Contemporary 3D mapping facilitates AF ablation with reduction in radiation and improvement in safety and efficacy. Electrically continuous and transmural lesions are important for complete electric isolation of PV and block from linear ablation, which all benefit from reliable 3D navigation. Image integration, contact-force feedback and integration tools facilitate durable PV ablation lesion. Innovative mapping approaches overcome spatio-temporal organization of AF and identify the different AF sources. The improved electrical signals recorded by narrow-spaced catheters and automatically annotated high-density maps as well as the DE of MRI provide value for scar-based ablation. The writing group recommendations for use of 3D mapping for ablation of AF are in Table 7-3.

8 | CHAPTER 8: VENTRICULAR TACHYCARDIA—SCAR-RELATED ISCHEMIC AND NONISCHEMIC ETIOLOGIES

8.1 | History and validation

Prior to the advent of 3D mapping systems, ablation of VT was guided solely by local abnormal electrograms during sinus rhythm and VT, with a heavy reliance on fluoroscopy to direct the catheter toward desired anatomic locations. The validation of 3D mapping and implementation into clinical usage is perhaps the greatest technological advancement to the field of complex ablation of scar-related VT in early 2000s (Table 8-1). In nonfocal arrhythmias, where more extensive substrates are often present, the ability to reconstruct chamber geometry without fluoroscopy, localize low-voltage regions in real-time, and reproducibly navigate to annotated mapped locations has allowed for the development of "substrate-based ablation" strategies that more extensively target anatomic scar.

Validation of the accuracy of 3D mapping for detecting and characterizing scar as low-voltage regions with single-point contact mapping was first demonstrated in porcine infarct models. Callans et al demonstrated excellent correlation between infarct size by pathology and low-voltage areas that consisted of bipolar electrograms <1.0 mV using CARTO (Biosense Webster).[67] The authors noted that border zone electrograms were intermediate in amplitude relative to a fixed cutoff. This work was instrumental in the development of anatomically based ablation approaches, whereby short linear lesions aimed to connect dense scar regions (<0.5 mV) to normal tissue or anatomic boundaries was first shown to be effective in reducing recurrent VT in a seminal human cohort reported by Marchlinski et al[45] The authors used control data from six normal patients without structural heart disease to define a statistical cutoff, whereby

TABLE 8-1 Consensus recommendations

Use of 3D mapping in ventricular tachycardia: Scar-related ischemic and nonischemic etiologies			
Recommendation	Class	LOE	References
The use of a 3D mapping system is recommended for mapping of scar-related VT to define the low-voltage substrate and annotate abnormal electrograms to reduce procedure duration and radiation exposure for both the patient and the operator.	I	B-NR	44,45,184,207,208
The use of a 3D mapping system is recommended for ablation of scar-related VT to guide, track, and record ablation applications and lesion locations to reduce procedure duration and radiation exposure for both the patient and the operator.	I	C-LD	44,45,184,207,208
In cases of percutaneous epicardial mapping and ablation, the use of 3D mapping system is recommended to reduce radiation exposure during substrate characterization and annotate ablation.	I	C-LD	188,198,209,210
The use of multielectrode catheters when using a 3D mapping system for high-density delineation of the substrate to reduce mapping duration and improve resolution can be beneficial.	IIa	B-NR	73,206,211–213

95% of electrograms recorded exceeded a bipolar voltage of 1.5 mV. Using this cutoff in 16 patients (ischemic cardiomyopathy [ICM] = 9, nonischemic cardiomyopathy [NICM] = 7) ablation within low-voltage regions (median of 4 lines, 55 lesions) resulted in an 8-month freedom from VT of 75%. In 2003, the accuracy of combined epicardial-endocardial mapping with the CARTO system was shown by Reddy et al in a porcine infarct model. Wrobleski et al also demonstrated that electrogram duration (>50 milliseconds) was comparable to bipolar electrogram amplitude for distinguishing normal from scar tissue.[176] As a result of the aforementioned seminal work, the fixed bipolar voltage threshold of <1.5 mV to define low-voltage scar and <0.5 mV indicating dense scar has been universally implemented for the past two decades with 3D mapping for scar-related VT.

8.2 | Evolution of mapping system platforms

Aside from magnetic localization technology, the use of impedance-based electrofield localization (NavX, St. Jude Medical) provides advantages that include the ability to compensate for patient motion and localization of any diagnostic catheter connected to the system. Validation of multielectrode catheter delineation of ventricular substrate was first demonstrated using the EnSite NavX system in the human right ventricle by Casella et al (2009) in the left ventricle with combined epicardial-endocardial mapping a porcine infarct model with a linear duodecapolar catheter (Livewire, 2-2-2) by Tung et al (2011).[69,177] These studies demonstrated significantly higher density delineation of low-voltage scar in one-third of the mapping of single-point mapping technique, with comparable accuracy (Figure 8-1). The evolution of the NavX platform has eliminated the need to create chamber geometry and electrogram information separately (NavX Classic to Velocity). NavX Precision system enables an automated mapping algorithm with inclusion of magnetic sensor information to improve localization and chamber geometry accuracy. In 2014, multielectrode mapping was incorporated in the magnetically based mapping system (CARTO MEMS, Biosense Webster) with the ability to acquire data with automated annotation

(CONFIDENSE™, Biosense Webster). Commonly employed dedicated mapping catheters with the CARTO system include a five-splined catheter (PentaRay) and linear decapolar catheter (DecaNav). Impedance-based systems are limited by changes in thoracic impedance (additional catheter and wires placed, procedural fluid shifts, or cardioversion). 3D Mapping systems have evolved to employ the strengths of both magnetic and impedance localization technology.

In 2013, a fully automated high-resolution mapping system (Rhythmia, Boston Scientific) with acquisition from 64 mini-electrodes on a small basket catheter (Orion) was introduced, featuring the highest mapping density (>5000 points) and a noise level of <0.01 mV. In theory, improved signal to noise ratio allows for the optimal identification of abnormal bipolar electrogram components within dense scar. The accuracy of the system to detect and characterize scar was demonstrated in preclinical models with high-resolution delineation of infarct architecture by Tanaka et al and Tschabrunn et al[178,179]

8.3 | Ablation strategies with voltage-based electroanatomic scar

With accurate delineation of the low-voltage regions that defines myocardial scar, various ablation lesion strategies have been shown to be clinically effective. As an emulation of encircling ventriculotomy,[180] circumferential ablation around the border zone may be performed. With a paradigm that VT exits the circuit at border zones, extension into dense scar (<0.5 mV) may increase the likelihood of transecting an isthmus region.[181] Limited ablation at a border zone that exhibits a pace-mapping match with extension into a dense scar (T-shaped lesion) were employed in SMASH VT,[182] while more extensive linear lesions transecting the entire scar were proven effective in EURO VT (Figure 8-2).[183] More recently, extensive homogenization aimed to target all abnormal electrograms with low voltage has been shown to be more effective when compared to limited ablation strategies.[184–186] Extensive ablation strategies of scar during sinus rhythm are highly reliant on the accuracy
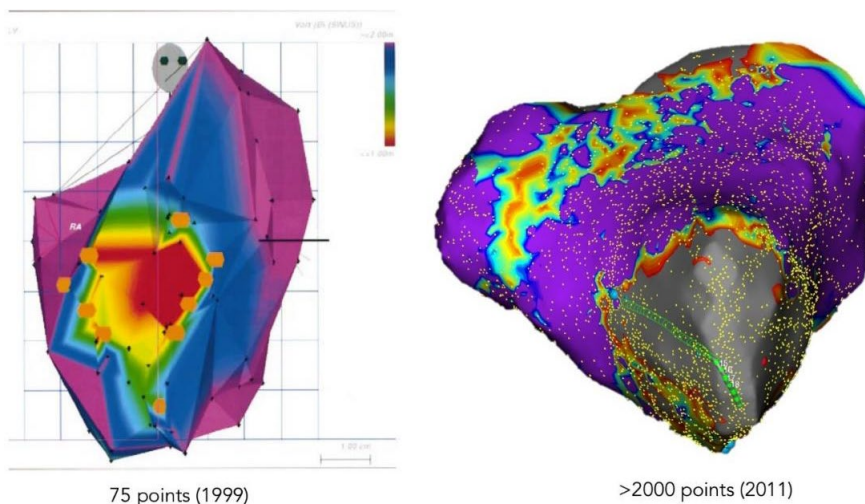

75 points (1999)   >2000 points (2011)

FIGURE 8-1 Evolution of mapping systems with depiction of anteroapical scar from porcine validation of single-point mapping systems (CARTO) to higher resolution mapping with multielectrode acquisition in human (NavX)

FIGURE 8-2 Anatomically based substrate ablation strategies during sinus rhythm. A, Border zone modification with T-shaped lesions; B, Linear transection; C, Extensive homogenization; D, Dechanneling
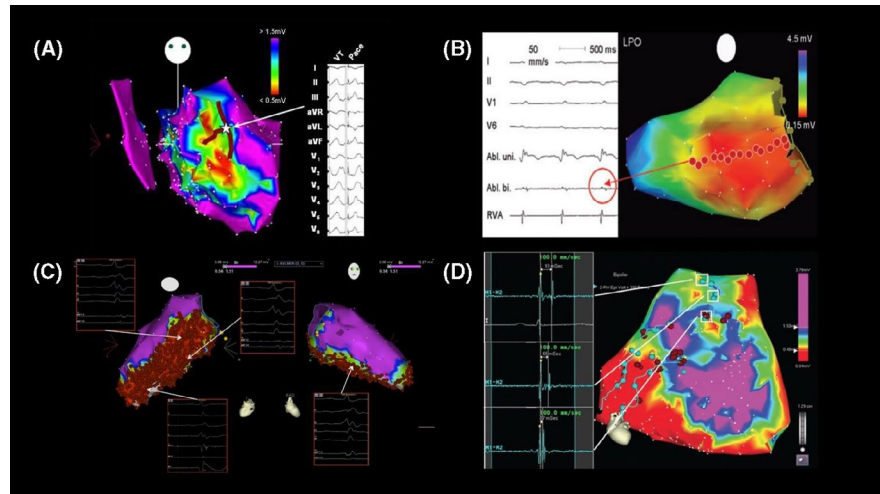
of low-voltage regions mapped, although electrogram signatures such as split high-frequency components and late potentials may be useful when differentiating scar from poor contact. Complete elimination of local abnormal ventricular activity (LAVA) may require pacing endocardial maneuvers to reveal the local electrogram component, that are otherwise superimposed during the baseline activation wavefront.[44] Bipolar electrogram amplitudes may be variable depending on electrode area and orientation relative to the activation wavefront.[71,187]

8.4 | Epicardial mapping and ablation in NICM

Strategies implemented for ICM have been extrapolated and broadly applied to NICM, which fundamentally assumes that the reentrant circuit and mechanisms across etiologies are similar. The technique for percutaneous mapping via subxiphoid puncture was first introduced by Sosa et al using the CARTO system to characterize and target epicardial scar in patients with Chagas disease and ischemic cardiomyopathy refractory to endocardial approach.[188,189] Low-voltage regions identified during epicardial mapping may represent epicardial fat (>4 mm) and electrogram characteristics may be useful to differentiate insulated myocardium from scar.[190] With impedance-based systems, the pericardial space does not have a uniform impedance consistent with the blood pool, and the spatial relationship between epicardium and endocardium is subject to distortion.

Successful epicardial mapping and ablation-guided by 3D mapping has been shown across various NICM etiologies, as well as arrhythmogenic right ventricular cardiomyopathy (ARVC), where low-voltage regions with abnormal electrograms are often more extensive than endocardial scar.[191-194] A unipolar display of endocardial voltage maps, in the absence of bipolar voltage abnormalities, has been shown to be correlated with the presence of epicardial bipolar voltage abnormalities by Hutchinson et al and Polin et al in NICM and ARVC substrates using the CARTO system at a threshold of < 5.5 mV in the RV and < 8.3 mV in the left ventricle (LV), respectively.[26,195]

8.5 | Newer mapping system functions based on electrograms and activation

Late potentials or widely split local electrograms have been shown to have high sensitivity for critical sites for reentry.[196] Mapping windows may be adjusted to highlight regions of ventricular activation that are most delayed in the post-QRS portion of the total activation. Elimination of all delayed activation has been demonstrated to be effective to prevent recurrent VT.[197] Targeted ablation of the entrance sites upstream from the most delayed late potentials may be a more physiologic method to eliminate critical conducting channels, by a dechanneling technique that requires fewer ablation lesions when compared to homogenization.[47,198] These techniques are not reliant on the voltage display of the mapping system, but rather the timing of local electrograms. Isochronal maps of the baseline rhythm may be useful to obtain a global activation display of scar and expose regions of isochronal crowding, or zones of deceleration, which have been shown to be correlated with critical sites.[35] Automated mapping features to annotate the latest component of individual electrograms may be useful to generate activation maps (Precision [Abbott] and LumiPoint [Rhythmia]). A major limitation to current mapping systems is a singular annotation for each electrogram, which may not be accurate in the event of long duration fractionated or split electrograms. A dynamic unique ripple mapping feature (CARTO) allows for continuous display of activation for the entirety of a local electrogram with voltage projection of local electrogram amplitude during a video playback mode.[199] This feature circumvents the issues of single annotation and has been shown to be useful to identify low-voltage conducting channels within scar.

8.6 | 3D mapping of the reentrant circuit

Sites with matched pace-mapping may be annotated in real-time in all 3D mapping. Pace-maps with long Q-QRS (>30 milliseconds) are typically seen when pacing within low-voltage regions and when matched for VT, are reasonable surrogates for isthmus sites.[200] Abrupt shifts in pace-map morphology have been shown to be correlated with isthmus
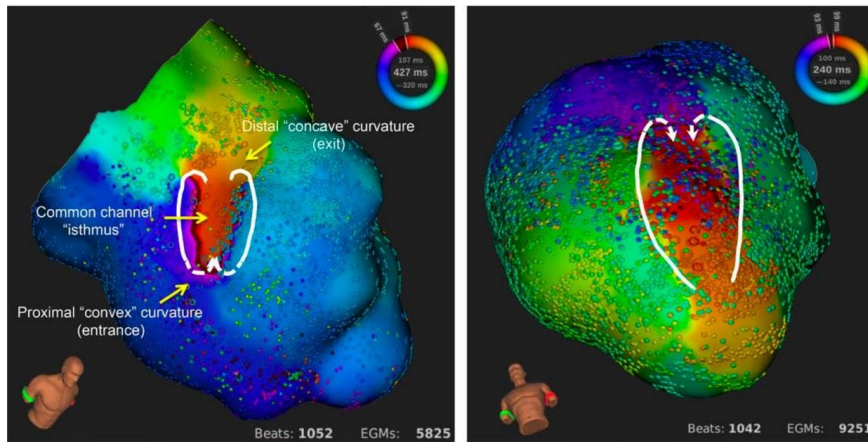
FIGURE 8-3 High-resolution mapping of complete endocardial reentrant circuit with mini-basket automated system (Rhythmia)

sites with access to multiple exits.[201] Pace-mapping with an automated percentage of concordance (CARTO, PaSO) to the targeted morphology has been demonstrated to have strong correlation with the reentrant circuit during VT by de Chillou et al[50] Responses to entrainment mapping can be annotated on the electroanatomic map to construct the putative circuit based on entrance, exit, isthmus, and bystander sites responses, when activation mapping of the entire circuit cannot be achieved.[181,202]

Limited clinical studies that successfully delineate the reentrant circuit have been achieved in humans.[203] Activation mapping has not been shown to be superior to substrate-based approaches during sinus rhythm with regard to intermediate-term freedom from VT.[204] High-resolution mapping of the complete reentrant circuit with the Rhythmia system has been demonstrated in a porcine model (Figure 8-3) and human experience which shows accurate automated annotation of figure-of-eight patterns and complex activation and regions of high curvature at entrance and exit sites.[205,206] Studies that correlate the reentrant circuit with sinus rhythm electrograms may further refine identification of surrogates during substrate-based ablation.

Significant advances in scar-related VT ablation have been achieved due to the introduction and evolution of 3D mapping systems. Preclinical animal studies have been performed with all clinically available mapping systems that demonstrate accuracy with pathologic scar. With accurate delineation of scar by low-voltage regions, higher resolution substrate has been achieved with evolving technology by automated annotation and multielectrode catheters with clinical validation on both endocardium and epicardial surfaces across the spectrum of ICM and NICM etiologies. 3D mapping allows for voltage-based strategies, electrogram activation displays during sinus rhythm, and activation mapping during reentry.

9 | CHAPTER 9: VENTRICULAR TACHYCARDIA—FASCICULAR-PURKINJE VT AND BUNDLE BRANCH REENTRY VT

9.1 | Purkinje-related monomorphic VTs

In Purkinje-related monomorphic VTs, there are four distinct groups: (a) verapamil-sensitive left fascicular-Purkinje VT, (b) Purkinje

fiber-mediated VT post infarction, (c) non-reentrant fascicular-Purkinje VT, and (d) bundle branch reentry (BBR) and interfascicular reentry VTs (Table 9-1).[214–216] The mechanism of these VTs except non-reentrant fascicular VT is macroreentry, and the mechanism of non-reentrant fascicular VT is abnormal automaticity from the distal Purkinje system. These VTs usually occur in specific locations and have specific QRS morphologies, whereas VTs associated with structural heart disease and not associated with the Purkinje system have a QRS morphology that tends to indicate the location of the scar.

9.2 | Reentrant fascicular-Purkinje VT

9.2.1 | Pathophysiology and classification

Verapamil-sensitive fascicular-Purkinje VT is the most common form of idiopathic left VT. It was first recognized as an electrocardiographic entity in 1979 by Zipes et al,[217] who identified the following characteristic diagnostic triad: (a) induction with atrial pacing, (b) right bundle branch block (RBBB) and left-axis configuration, and (c) manifestation in patients without structural heart disease. In 1981, Belhassen et al[218] were the first to demonstrate the verapamil sensitivity of the tachycardia, a fourth identifying feature. Ohe et al[219]

TABLE 9-1 Purkinje-related Monomorphic VTs

I. Verapamil-sensitive left fascicular-Purkinje VT
1. Left posterior type
i. Left posterior septal fascicular-Purkinje VT
ii. Left posterior papillary muscle fascicular-Purkinje VT
2. Left anterior type
i. Left anterior septal fascicular-Purkinje VT
ii. Left anterior papillary muscle fascicular-Purkinje VT
3. Upper septal type
II. Purkinje fiber-mediated VT post infarction
III. Non-reentrant fascicular-Purkinje VT
IV. Bundle branch reentry VT and Interfascicular reentry VT

Abbreviation: VT, ventricular tachycardia.

reported another type of this tachycardia, with RBBB and a right-axis configuration, in 1988. Later, Nogami et al[214] and Talib et al[215] reported the upper septal fascicular tachycardia. According to the QRS morphology, verapamil-sensitive left fascicular-Purkinje VT can be divided into three subgroups, namely[214] (a) left posterior fascicular-Purkinje VT, in which the QRS morphology exhibits an RBBB configuration and a superior axis; (b) left anterior fascicular-Purkinje VT, in which the QRS morphology exhibits an RBBB configuration and inferior axis; and (c) upper septal fascicular VT, in which the QRS morphology exhibits a narrow QRS configuration and normal or right-axis deviation.[214,215,220] Left posterior type is common, left anterior type is uncommon, and left upper septal fascicular VT is very rare. Upper septal fascicular VT sometimes occurs after a previous catheter ablation of another fascicular-Purkinje VT.

Reentrant circuit of verapamil-sensitive fascicular-Purkinje VT can involve the Purkinje network lying around the papillary muscles.[216] In addition to the current classification with three subtypes, papillary muscle fascicular VT is another identifiable verapamil-sensitive fascicular-Purkinje VT. Finally, verapamil-sensitive left fascicular-Purkinje VT can be classified into five subgroups (Table 9-1; Figure 9-1). Papillary muscle fascicular VT and VT from myocardium of papillary are basically different entities, while there must be some overlap.

9.2.2 | Substrate and anatomy

Some data suggest that the tachycardia may originate from a false tendon or fibromuscular band in the LV.[221–224] Using intracardiac echocardiography and 3D mapping system, successful ablation site appears to be at the connection of false tendon and ventricular wall in some patients. However, this is not always seen at the successful ablation site. The Purkinje networks in these small anatomic structures are important when considering the mechanism of left

fascicular-Purkinje VT. In the papillary muscle fascicular VTs, fibromuscular bands near papillary muscles can be the substrate of the circuit.

9.2.3 | VT circuit diagram

During tachycardia, two distinct potentials are recorded at the midseptum. The mid-diastolic potential (P1) is recorded earlier from the proximal rather than the distal electrodes, the fused presystolic Purkinje potential (P2) is recorded earlier from the distal electrodes. During sinus rhythm, recording at the same site demonstrated P2, which is recorded after the His-bundle potential and before the onset of the QRS complex, suggesting P2 as potentials of left posterior fascicle.

Figure 9-2 shows the hypothesized circuit of fascicular VT and the fascicular or Purkinje potentials during sinus rhythm. In this circuit, P1 represents the activation potential in the distal portion of the specialized Purkinje tissue; it has decremental properties and verapamil sensitivity. P2 represents the activation of the left posterior fascicle or Purkinje fiber near the left posterior fascicle and it is a bystander during VT. P1 represents the anterograde limb of the circuit in VT and left ventricular septal muscle is the retrograde limb.

9.2.4 | Mapping and ablation

Left posterior septal fascicular VT

Conventional left ventricular septal mapping using a multipolar electrode catheter is useful in patients with left posterior septal fascicular-Purkinje VT.[214,215] Two distinct potentials, P1 and P2, can be recorded during the VT from the midseptum. The apical third of the septum is usually targeted, to avoid the creation of left bundle branch block (LBBB) or atrioventricular block (AVB).

FIGURE 9-1 New classification of verapamil-sensitive left fascicular-Purkinje ventricular tachycardia (VT). According to the QRS morphology and site of successful ablation, VT can be classified into five subtypes (From Komatsu Y, Nogami A, Kurosaki K, et al. Non-Reentrant Fascicular Tachycardia: Clinical and Electrophysiological Characteristics of a Distinct Type of Idiopathic Ventricular Tachycardia. *Circ Arrhythm Electrophysiol.* 2017; 10. pii: e004549. With permission.)
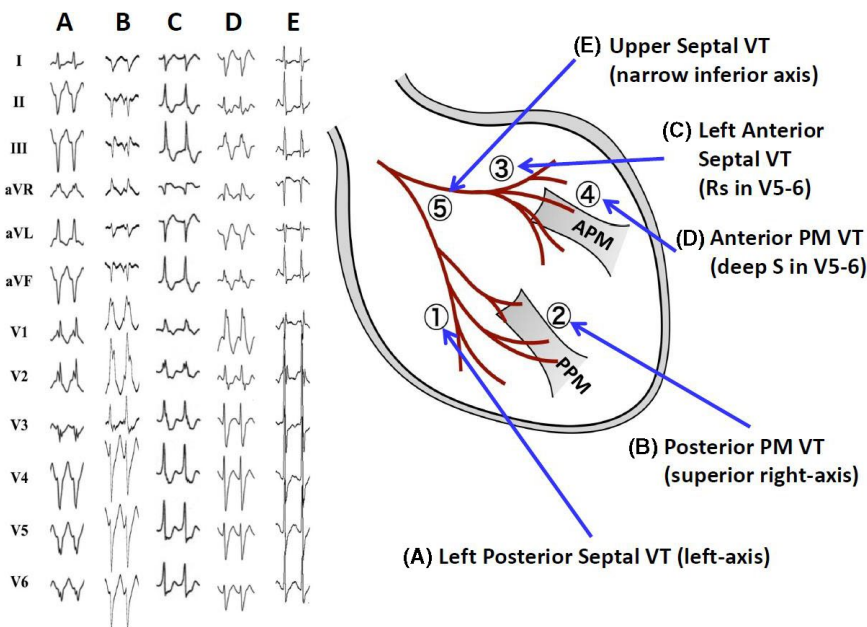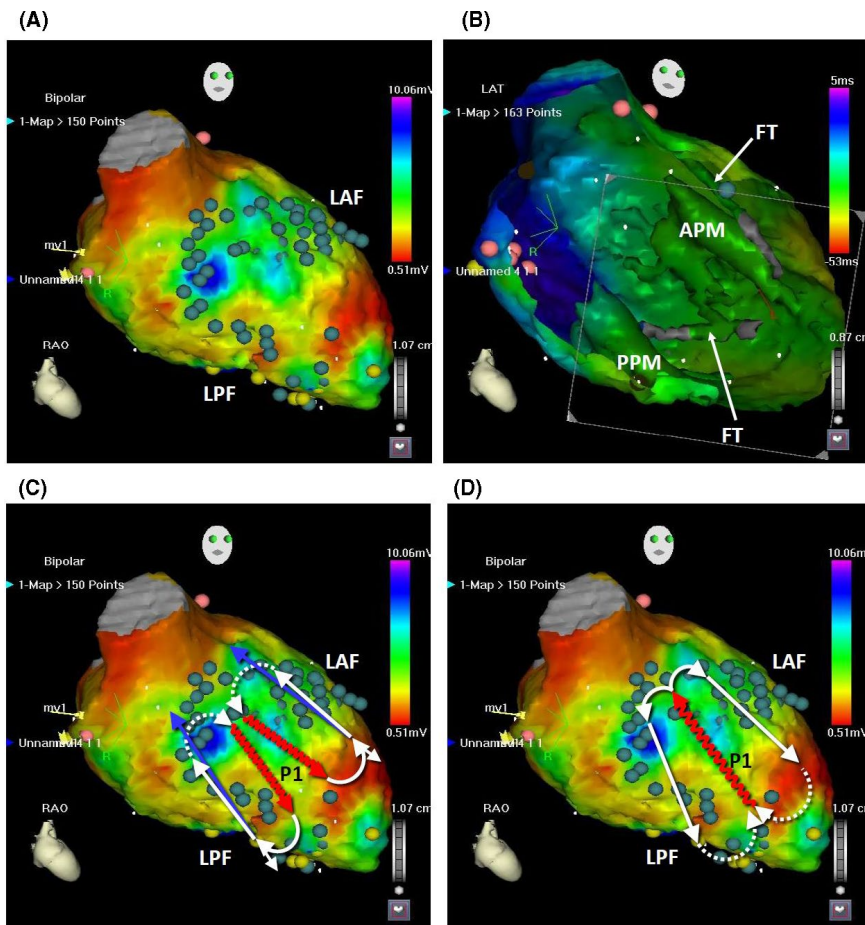
FIGURE 9-2 The position of fascicular VT circuits and the Purkinje potentials during sinus rhythm. A, The tags in the CARTOMERGE image indicate the potentials of the left anterior fascicle (LAF), posterior fascicle (LPF), and distal Purkinje fibers during sinus rhythm. B, In the left ventricular cavity, the anterior papillary muscle (APM), posterior papillary muscle (PPM), and false tendons (FT) are observed (endoscopic view). C, The circuits of the left posterior fascicular VT and left anterior fascicular VT are shown. The dotted lines indicate the ventricular myocardium as the proximal bridge between the diastolic and presystolic Purkinje potentials. The undulating line represents a zone of slow conduction. D, The circuit of the left upper septal fascicular VT is shown

Left posterior papillary muscle VT

Diastolic Purkinje potential (P1) can be recorded near the papillary muscles during VT. Ablation of the diastolic potential is highly effective for suppressing this VT. Figure 9-3 shows an example of RF catheter ablation of a left posterior papillary muscle VT.[216] VT exhibited RBBB configuration and superior right-axis deviation. At the successful ablation site, both P1 and P2 were sequentially recorded during VT. The successful ablation site was located on the posterior papillary muscles, which was confirmed by real-time intracardiac ultrasound image (Supplemental Video 9-1).

Left anterior septal fascicular VT

Figure 9-1C shows the 12-lead ECGs of a verapamil-sensitive left anterior septal fascicular VT which exhibits Rs pattern in V5-6. In those patients, a Purkinje potential is recorded in the diastolic phase during VT at the mid-anterior left ventricular septum.[12,13] Left anterior fascicular VT circuit is shown in Figure 9-2C. Left anterior and posterior fascicular-Purkinje VT circuits are mirror images.

Left anterior papillary muscle fascicular VT

Figure 9-1D shows the 12-lead ECGs of left anterior papillary muscle fascicular VT which exhibits deep S-waves in V5-6. Left ventricular endocardial mapping during left anterior fascicular-Purkinje VT identified the earliest ventricular activation in the anterolateral wall of the left ventricle.[216,225]

Left upper septal fascicular VT

Figure 9-2D shows the schematic diagram of upper septal fascicular VT.[215] P1 represents the activation potential of the specialized Purkinje tissue at left ventricular septum. P2 represents the activation of the left anterior and posterior fascicles. Both left anterior and posterior fascicles are the anterograde limbs of the reentrant VT circuit. This explains why this VT exhibits a narrow QRS configuration and inferior axis (Figure 9-1E). This VT was ablated successfully at the left ventricular midseptum.

9.2.5 | Troubleshooting the difficult case

If no VT, or even some echo beats, can be induced, then the empirical anatomic approach can be an effective strategy for ablation of left posterior septal fascicular-Purkinje VT.[226] First, the VT exit site is sought by pace-mapping during sinus rhythm, and RF energy is delivered to that site. Second, a linear lesion is placed at the midseptum, perpendicular to the long axis of the LV, approximately 10 to 15 mm proximal to the VT exit. This anatomic approach is also useful in patients in whom diastolic Purkinje potentials cannot be recorded during VT. Figure 9-4 (Supplemental Video 9-2) shows activation mapping during VT. Although the earliest myocardial activation site was observed at the inferoapical septum, diastolic potentials could not be recorded. RF energy application to this exit
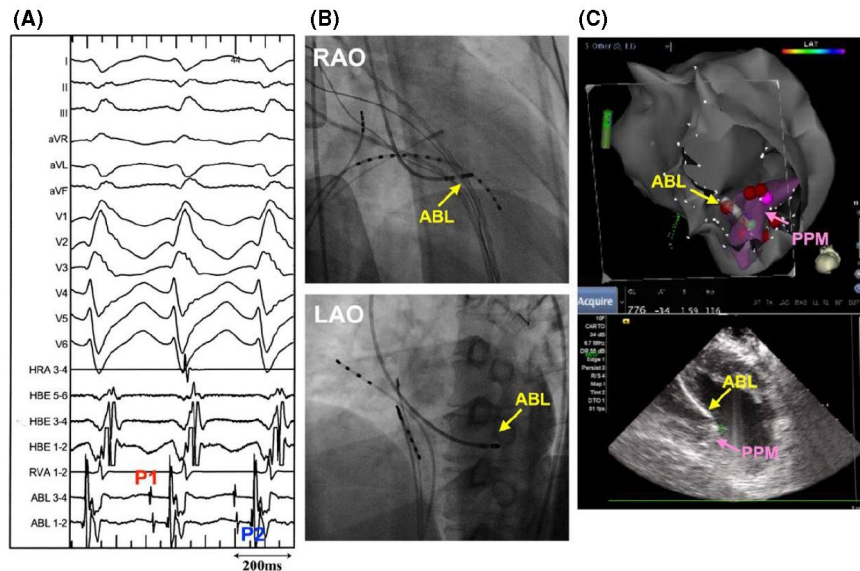
FIGURE 9-3 Catheter ablation of posterior papillary muscle fascicular-Purkinje VT. A and B, VT exhibited RBBB configuration and superior right-axis deviation. At the successful ablation site, both P1 and P2 are recorded during VT. C, The successful ablation site was located on the posterior papillary muscles (PPM), which is confirmed by real-time intracardiac ultrasound image (Supplemental Video 9-1). ABL, ablation catheter; LAO, left oblique projections; and RAO, right oblique projections (From Komatsu Y, Nogami A, Kurosaki K, et al. Non-Reentrant Fascicular Tachycardia: Clinical and Electrophysiological Characteristics of a Distinct Type of Idiopathic Ventricular Tachycardia. *Circ Arrhythm Electrophysiol.* 2017; 10. pii: e004549. With permission.)

FIGURE 9-4 Anatomic approach when diastolic Purkinje potential cannot be recorded during VT. While the earliest myocardial activation site is observed at the inferoapical septum, diastolic potential could not be recorded (Supplemental Video 9-2). RF energy was delivered to the exit site, but that was ineffective. Proximal linear lesion successfully suppressed the VT. LAT, lateral projection; LV, left ventricle; RAO, right anterior oblique projection
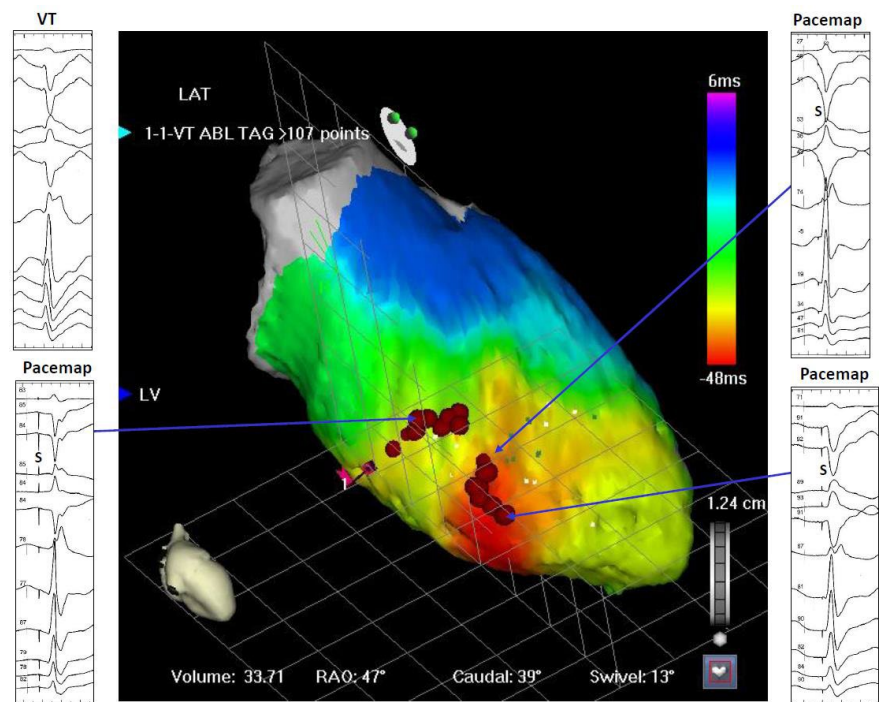
site was ineffective. A linear RF lesion proximal to the VT exit successfully suppressed the VT.

9.3 | Purkinje fiber-mediated VT post infarction

Hayashi et al[227] first reported four postmyocardial infarction patients who presented with left posterior fascicular-Purkinje VT.

Intravenous administration of verapamil terminated VT in one patient; however, verapamil was not administered in the rest of the patients because of a poor left ventricular function. Both diastolic and presystolic Purkinje potentials were sequentially recorded along the left ventricular posterior septum during VT. Bogun et al[228] reported 81 consecutive patients with postinfarction fascicular-Purkinje VT. Morishima et al[229] described a postinfarction left anterior fascicular-Purkinje VT. Those VTs have several characteristic
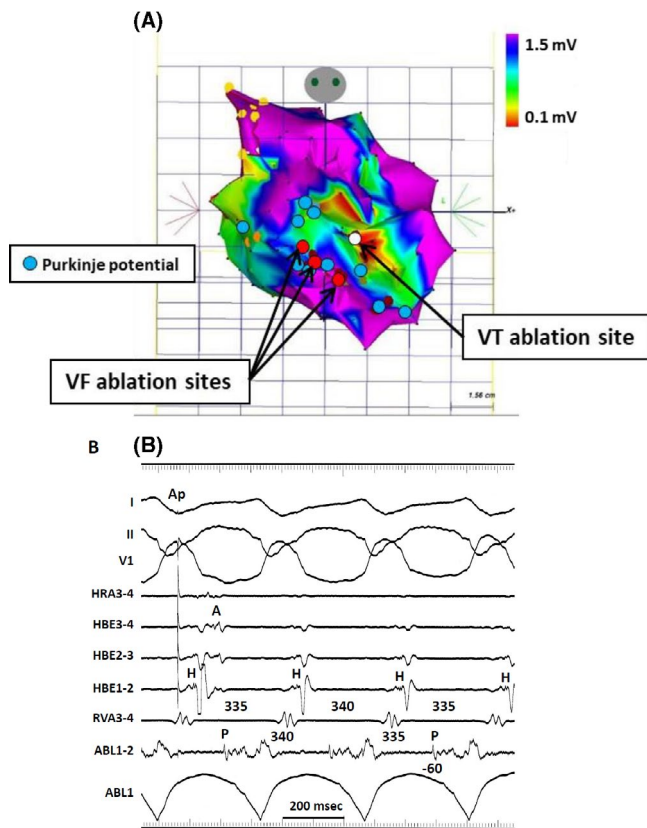
(A)

(B)

FIGURE 9-5 Electroanatomical mapping of postinfarction, Purkinje-fiber mediated VT. A, The electroanatomical map was created during the second session for monomorphic VT. The red tag indicates the ablation site for ventricular fibrillation in the first session, superimposed on the same map. The white tag indicates the successful ablation site for VT in the second session. The blue tags indicate the Purkinje potentials during sinus rhythm. B, Diastolic Purkinje potentials were recorded during VT and the change of P-P intervals preceded the changed of V-V intervals. Single RF energy delivery terminated the VT (From Masuda K, Nogami A, Kuroki K, et al. Conversion to Purkinje-related monomorphic ventricular tachycardia after ablation of ventricular fibrillation in ischemic heart disease. Circ Arrhythm Electrophysiol. 2016; 9. pii: e004224. With permission.)

differences compared to the usual scar-related VT post infarction: (a) a relatively narrow QRS duration during VT, (b) verapamil sensitivity, (c) presystolic or diastolic Purkinje potentials during VT, and (d) VT termination by a single or a few RF energy applications to that site. Monomorphic VT sometimes occurs after successful ablation of ischemic ventricular fibrillation. (Figure 9-5).[230]

9.4 | Non-reentrant fascicular-Purkinje VT

9.4.1 | Clinical and electrophysiologic characteristics

Another type of fascicular-Purkinje VT is non-reentrant tachycardia from the Purkinje system[231] (Table 9-1). This VT is classified as propranolol-sensitive automatic VT.[232] Although this VT is usually observed in patients with ischemic heart disease,[233] it

is also observed in patients with structurally normal hearts.[234,235] This VT can be induced by exercise and catecholamines (eg, isoproterenol and phenylephrine); however, it cannot be induced or terminated by programmed ventricular stimulation. Although this VT is responsive to lidocaine and beta-blockers, it is usually not responsive to verapamil. The clinical and electrophysiologic characteristics of this VT have not been well defined. Gonzalez and colleagues[234] reported the electrophysiologic spectrum of Purkinje-related monomorphic VT in eight patients and showed the mechanism to be consistent with abnormal automaticity or triggered activity in five patients. Talib et al[231] reported 11 patients (2.8%) with idiopathic non-reentrant fascicular VT among 530 idiopathic VT patients without structural heart disease. All patients had monomorphic VT with a relatively narrow QRS (123 ± 12 milliseconds), and they did not respond to verapamil. VT exhibited RBBB and superior-axis configuration in 11 patients (73%), inferior axis in three (20%), and LBBB and superior-axis configuration in one patient (7%).

9.4.2 | Mapping and ablation

The ablation target of non-reentrant fascicular-Purkinje VT is the earliest Purkinje activation during VT, whereas that of verapamil-sensitive reentrant fascicular-Purkinje VT is not necessarily the earliest Purkinje activation. Figure 9-6 (Supplemental Video 9-3) shows the mapping and ablation of non-reentrant fascicular VT from the distal Purkinje system of the left posterior fascicle. Presystolic Purkinje potentials are recorded from various sites in the LV; however, the earliest Purkinje potential is recorded at the basal inferior wall. Pace mapping at this site produced an identical QRS complex, with an S-QRS interval equal to the P-QRS interval during the VT. RF current delivered to this site suppressed the VT.

9.5 | Bundle branch reentry VT and interfascicular VT

Bundle branch reentry (BBR) VT is an unique, fast (200-300 beats/min), monomorphic tachycardia associated with hemodynamic collapse, syncope, and/or cardiac arrest. It is caused by a macro-reentry circuit involving the right and left bundle branches, and septal ventricular muscle. BBR-VT occurs in patients who have dilated cardiomyopathy and in those with coronary artery disease, valvular heart disease, muscular dystrophy, congenital heart disease, left ventricular noncompaction, arrhythmogenic right ventricular cardiomyopathy, or even no heart disease with associated His-Purkinje conduction system disturbances. The incidence is reported to be 3.5% and 6% of VTs in separate series and 20% in a series of patients with nonischemic cardiomyopathy alone undergoing evaluation for ablation.[236-238] Likely, BBR is under-recognized as a clinical problem.

FIGURE 9-6 Ablation of non-reentrant fascicular VT with RBBB configuration and left-axis deviation. A, Electroanatomic mapping during VT (Supplemental Video 9-3). Tags indicate the sites with the presystolic Purkinje potential during VT. The earliest Purkinje potential was recorded at the basal inferior wall, and radiofrequency current delivered to this site suppressed the VT. ABL, Ablation catheter; CS, coronary sinus; HBE, His-bundle electrogram; HRA, high right atrium; LAT, local activation time; RAO, right anterior oblique projection; RVA, right ventricular apex
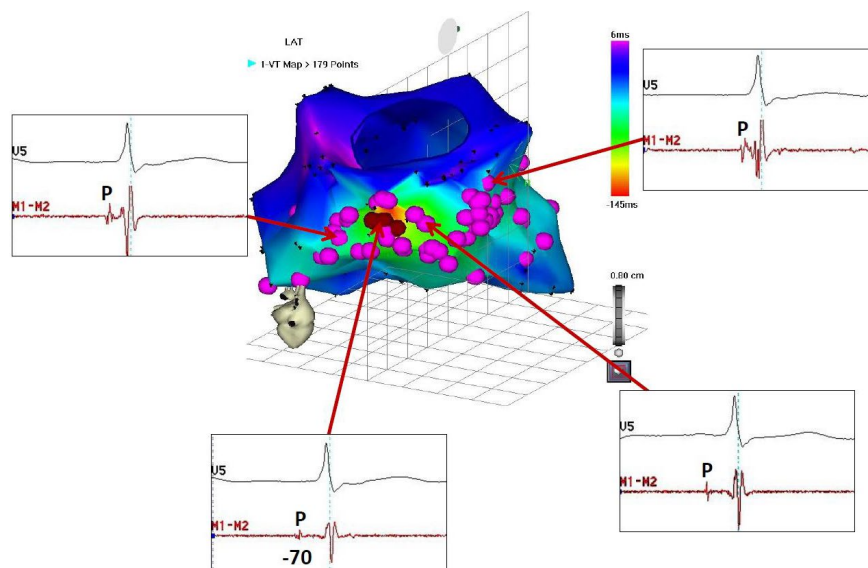
9.5.1 | Classification and pathophysiology

The morphology of the tachycardia can have a typical LBBB pattern or RBBB pattern (Figure 9-7). Some patients have both counterclockwise and clockwise BBR, causing a LBBB and RBBB morphology, respectively. Tchou et al described three categories of BBR-VT (Table 9-2).[239] Type A (Figure 9-7A) and type C (Figure 9-7C) are the classic counterclockwise and clockwise BBR-VT circuits. Type B (Figure 9-7B) is reentry within the left bundle branch (LBB) fascicles (interfascicular reentry). A RBBB and left hemiblock pattern is more consistent with interfascicular tachycardia. The ECG morphology of counterclockwise BBR (type A) is a typical LBBB with an R-wave transition between leads V4 and V5. Type A BBR-VT is the cause of 98% of episodes of BBR-VT.[236]

9.5.2 | Differential diagnosis

It is important to recognize BBR-VT and interfascicular tachycardia because they can be cured with catheter ablation. The differential diagnosis for BBR includes (a) VT due to myocardial reentry, (b) idiopathic left intrafascicular VT, (c) supraventricular mechanism with aberrant conduction in the presence of a 1:1 ventriculo-atrial relationship, and (d) atrio-fascicular reentry.

9.5.3 | Mapping

In type A and C BBR-VTs, the onset of ventricular depolarization is preceded by His bundle, RBB, or LBB potentials with an appropriate sequence of His bundle > RBB>LBB activation. Spontaneous variations in V-V intervals are preceded by similar changes in H-H/RBB-RBB/LBB-LBB intervals. Recording from both sides of the septum may help to identify the BBR mechanism. 3D electroanatomical

mapping is also valuable in demonstrating the entire reentrant circuit (Figure 9-8; Supplemental Video 9-4).[240]

9.5.4 | Catheter ablation

Pharmacologic anti-arrhythmic therapy, empirically or electrophysiologically guided, is usually ineffective. RF catheter ablation of a bundle branch can cure BBR-VTs and is currently regarded as first-line therapy. BBR-VT may be prevented by ablation of the right or left main bundle branch. Even though most patients demonstrate some conduction delay in the LBB, the RBB is typically the target for ablation. This is so because of the technical ease of ablation of the RBB, in contrast to the difficulties involved in ablation of the LBB. In sinus rhythm, complete RBB or LBB develops with successful ablation, although QRS changes may be subtle in patients with preexisting conduction abnormalities. Electrical axis changes may be the only manifestation of fascicular ablation. Elimination of retrograde V-H conduction has been used as a marker of successful ablation. The reported incidence of clinically significant conduction system impairment requiring implantation of a permanent pacemaker varies from 0% to 30%.[241]

For many patients with BBR-VT who have LBBB during sinus rhythm, anterograde slow conduction over the LBB is present[240,242] or exclusive retrograde conduction of LBB is present. In patients with a complete LBBB pattern during sinus rhythm, anterograde ventricular activation occurs solely via the RBB. These patients are at risk of developing complete AVB with RBB ablation. To avoid this potential complication, the retrograde conduction over LBB might be targeted in such patients with LBBB during sinus rhythm.[242]

In interfascicular reentry, RBB ablation will not cure the tachycardia because the RBB is a bystander. Similarly, ablation of the main LBB would not be expected to terminate the tachycardia because the circuit is distal to this point. Catheter ablation of the LAF or the
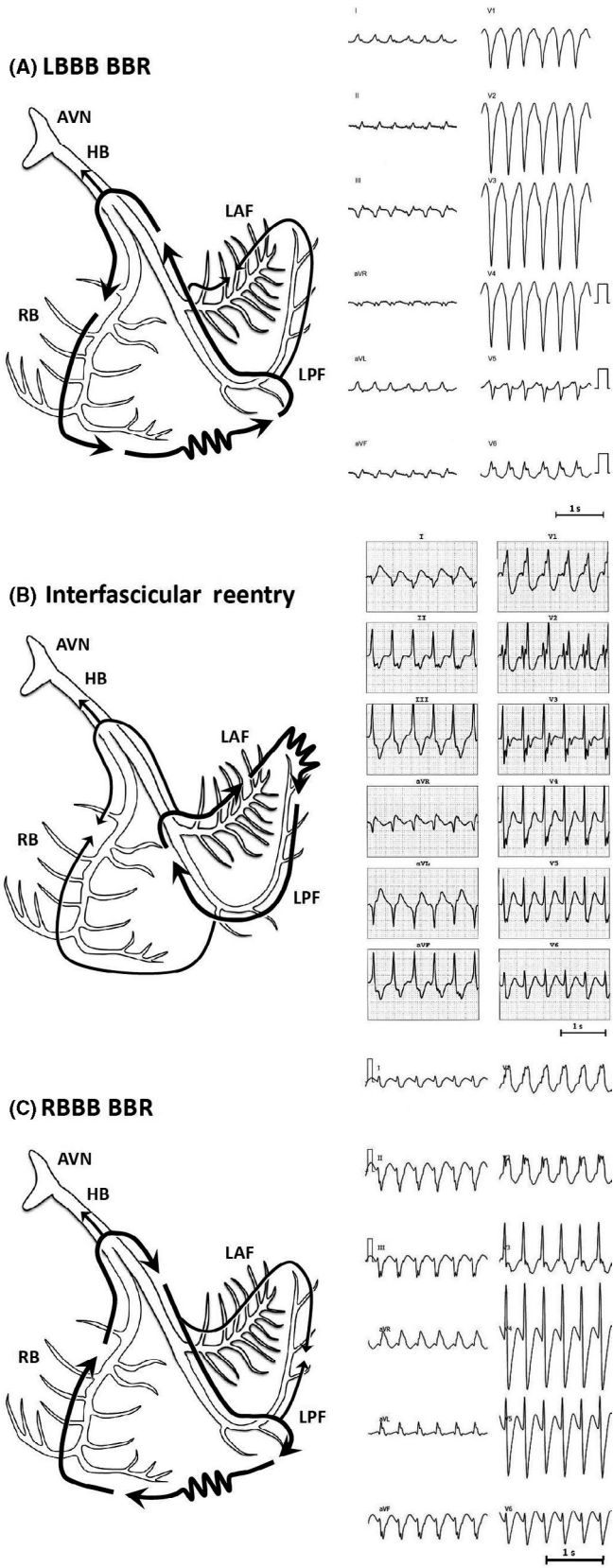
(A) LBBB BBR

(B) Interfascicular reentry

(C) RBBB BBR

FIGURE 9-7 Twelve-lead ECGs and schematic illustrations of reentrant circuits for BBR and interfascicular reentry tachycardias. A, Type A: Typical type of BBR in which retrograde conduction occurs via the left bundle branch (LBB) and anterograde conduction over the right bundle (RBB) branch. B, Type B: Interfascicular reentry with anterograde and retrograde conduction over opposing fascicles of the LBB. C, Type C. Reversal of the circuit depicted in type A *AVN*, Atrioventricular node; *BBR*, bundle branch reentry; *HB*, His bundle; *LAF*, left anterior fascicle; *LPF*, left posterior fascicle; *RBB*, right bundle branch (Modified from Nogami A: Purkinje-related arrhythmias. Part I: Monomorphic ventricular tachycardias. Pacing Clin Electrophysiol 34:624-650, 2011.40)

TABLE 9-2 Types of bundle branch reentry tachycardia

	Type A	Type B (Interfascicular Tachycardia)	Type C
ECG morphology	LBBB pattern	RBBB pattern	RBBB pattern
Anterograde limb	RBB	LAF or LPF	LBB
Retrograde limb	LBB	Contra-left fascicle	RBB

Abbreviations: LAF, left anterior fascicle; LBB, left bundle branch; LBBB, left bundle branch block; LPF, left posterior fascicle; RBB, right bundle branch; RBBB, right bundle branch block.

10 | CHAPTER 10: IDIOPATHIC OUTFLOW TRACT VENTRICULAR TACHYCARDIA

The outflow tract (OT) of the RV and LV, its adjacent structures in the aortic cusps, LV summit, and aortomitral continuity are frequently the source of PVC or nonsustained and sustained VT.[243,244] The vast majority of cases occur in patients without structural heart disease but the OTs may also be involved in patients with cardiomyopathies. The underlying mechanisms are delayed afterdepolarization and triggered activity so that OT-VT may be induced by isoproterenol infusion or burst pacing in the electrophysiology laboratory.[243]

All OT-VT display an inferior axis with LBBB morphology. RVOT-VT, which accounts for 70% of all OT-VT, show a late R/S transition between V3 and V4. Ventricular arrhythmias (VA) from the LVOT have an R/S transition between V2 and V3 or earlier. Knowledge of these simple ECG hallmarks suffices to consent a patient and plan the procedure. There are more sophisticated ECG algorithms to further localize the focus of the lateral or septal RVOT,[245] pulmonary valve, different cusps of the aortic valve, or LV-summit.[246]

The OT constitutes a complex anatomical structure and it is critical to understand the anatomy of the OT and its adjacent structures to successfully ablate arrhythmias originating from these structures (Figure 10-1). The 3D mapping systems lend themselves nicely to precisely determine the anatomical location and correlate these with electrophysiological measurements.[247] This is particularly important since operators may need to change the position of the catheter in cardiac chambers repeatedly during the procedure. Most parts of

LPF will result in termination of the tachycardia. Recommendations for 3D mapping of fascicular-purkinje VT and bundle branch reentry VT are described in Table 9-3.

TABLE 9-3 Consensus recommendations

Use of 3D mapping in ventricular tachycardia: Fascicular-Purkinje VT and bundle branch reentry VT			
Recommendation	Class	LOE	References
In patients with healed myocardial infarction undergoing ablation of fascicular-Purkinje VT, the use of a 3D mapping system is recommended.	I	C-LD	227–230
The use of a 3D mapping system is recommended for ablation for fascicular-Purkinje VT to better understand the anatomy (eg, left ventricular septum, papillary muscles, fascicules, Purkinje fiber) to reduce procedure duration and radiation exposure for both the patient and the operator.	I	C-LD	216,231
For bundle branch reentry VT or interfascicular VT, the use of 3D mapping system is reasonable to detect the optimal ablation target and to reduce the potential risk of atrioventricular block.	IIa	C-LD	240,242
The 3D mapping system may be considered for the anatomical ablation for fascicular-Purkinje VT if tachycardia is noninducible or nonsustained.	IIb	C-LD	226

the RVOT are usually easy to reach.[248] In symptomatic RVOT PVC or VT, RFCA has a much higher success rate than medical therapy and has been classified as a class I, level B indication in recent guidelines[249,250] with excellent success rates exceeding 90% with < 1% major complication rates.

The use of 3D mapping systems not only allow correct understanding of the anatomical relationship when one is approaching the ablation target from different sites but also significantly reduce fluoroscopy time. In fact, many of these procedures can be performed completely without the use of fluoroscopy.[251] In a fluoroscopic view it may be difficult to determine where the pulmonary valve is located exactly. Using 3D mapping systems it could be shown that a voltage cutoff value of 1.9 mV accurately delineates the level of the pulmonary valve.[252] If the earliest activation is more than 1 cm below the pulmonary valve a RVOT origin can be excluded. If it is within 1 cm below the valve it could still originate from the aortic cusps but very unlikely from another left-sided structure.[252]

Recent data indicate that around 90% of RVOT PVC actually arise from the pulmonary valve cusps into which muscular sleeves extend.[253] This can be readily tested with activation mapping in cases with frequent PVC. At successful ablation sites, earliest activation on the bipolar local electrogram usually precedes the earliest QRS onset by 15-45 milliseconds during the PVC.[254] One of the big obstacles of OT-PVC ablation is that often times the patient only displays very few PVC at the time of the study, a problem that is compounded in patients undergoing this procedure under conscious sedation or general anesthesia, for example in children or adolescents.[53] Frequency of PVC
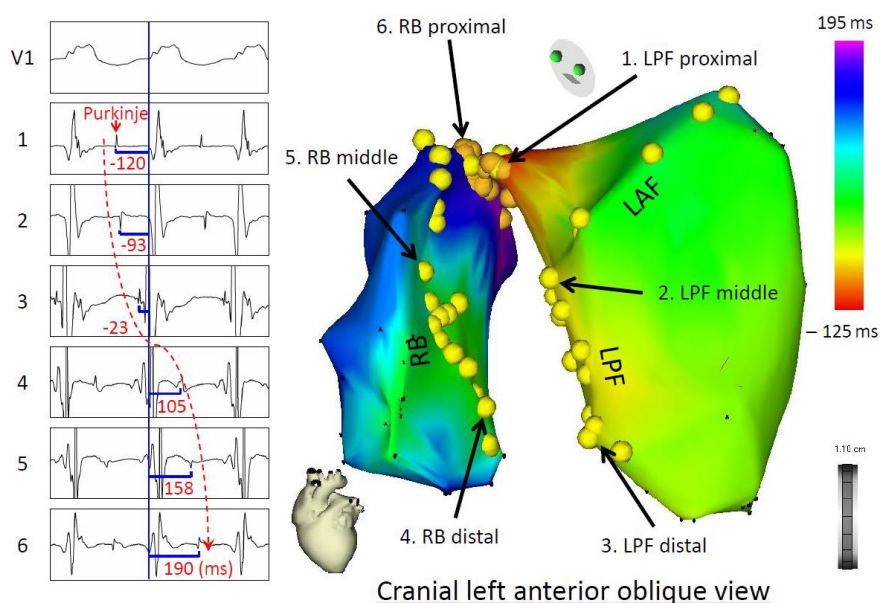
FIGURE 9-8 A 3D activation map (right panel) of BBR-VT descending the left posterior fascicle (LPF) and ascending the right bundle branch (RBB), with the earliest activation displayed in red (LPF proximal) and the latest in violet (RBB proximal). The yellow dots and the numbered sites with arrows indicate fascicular potentials and local activations of the His-Purkinje system (left panel), respectively. Sequential activations of the local His-Purkinje system accounted for the entire tachycardia cycle length. The propagation map of BBR-VT also demonstrated that anterograde activation through the left anterior fascicle and LPF resulted in a collision at the middle portion of the left anterior fascicle—a bystander of the reentrant circuit (Supplemental Video 9-4). From Machino T, et al: Three-dimensional visualization of the entire reentrant circuit. Heart Rhythm 10:459-460, 2013. With permission
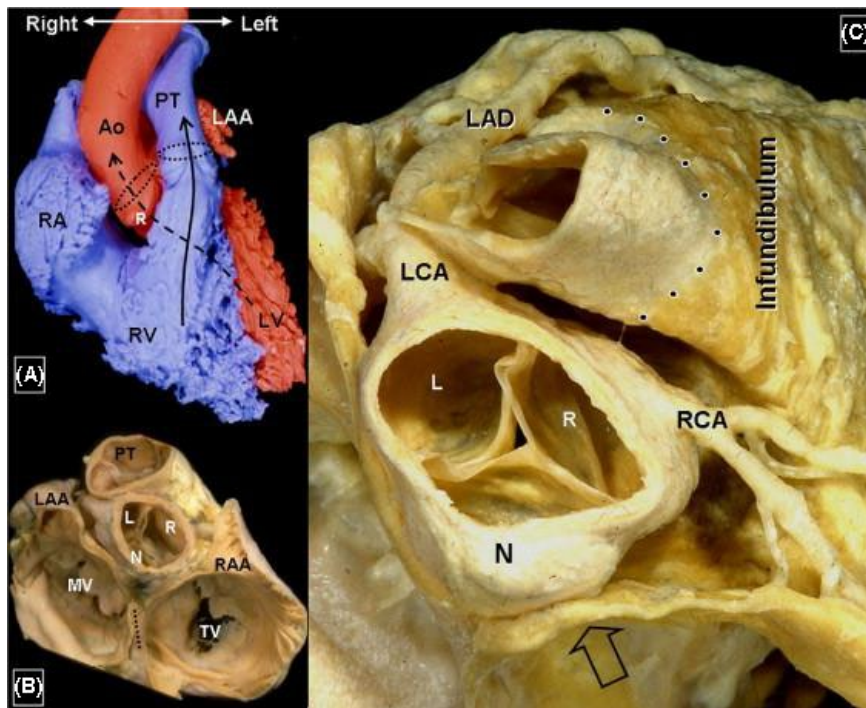
FIGURE 10-1 Anatomical specimen of the ventricular outflow tract (from: Ho SY. Anatomic insights for catheter ablation of ventricular tachycardia. Heart Rhythm 2009;6:S77-80). Ao: aorta; L: left coronary cusp; LAA: left atrial appendage; LAD: left anterior decending artery; LCA: left circumflex artery; LV: left ventricle; MV: mitral valve; N: noncoronary cusp; PT: pulmonary trunk; R: right coronary cusp; RAA: right atrial appendage; RCA: right coronary artery; RV: right ventricle; TV: tricuspid valve
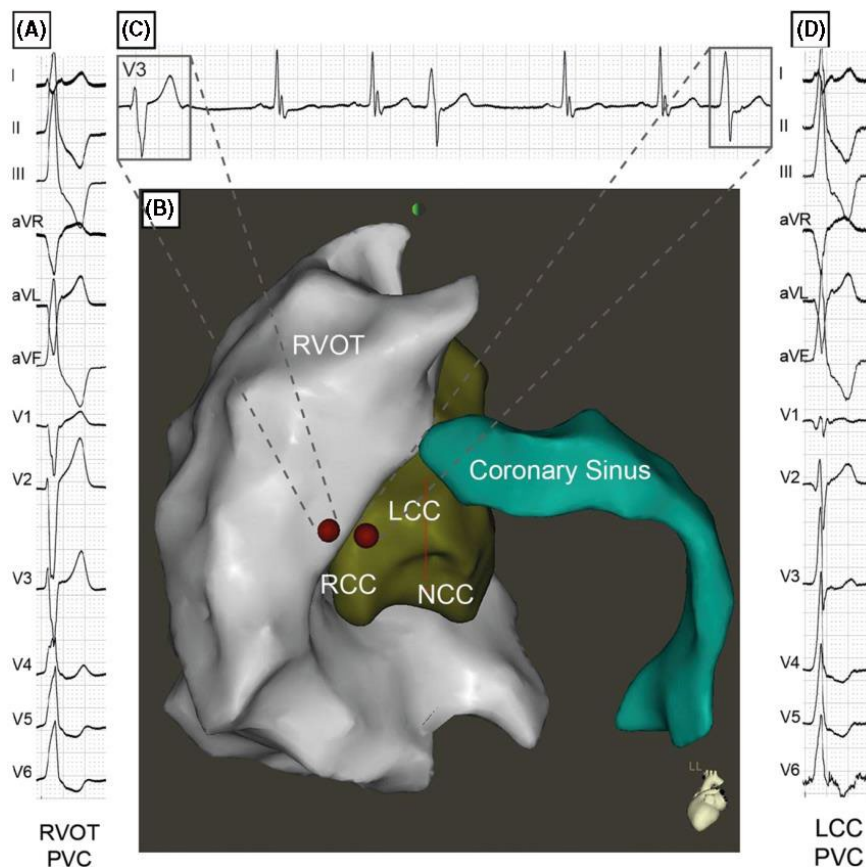
FIGURE 10-2 3D map (B) and electrograms showing the changing exit site from a PVC initially ablated from the RVOT (A). The subtle change in QRS morphology in V3 (C) indicates a changing exit to the left coronary cusp (D) where it was successfully ablated (Pavlovic N, Knecht S, Kuhne M, Sticherling C. Changing exits in ventricular outflow tract tachycardia. Heart Rhythm 2014;11:1495-6). RVOT: right ventricular outflow tract; LCC: left coronary cusp; NCC: noncoronary cusp; PVC: premature ventricular contraction; RCC: right coronary cusp; RVOT: right ventricular outflow tract

less than 1 PVC/min is associated with a significantly lower success rate.[255] In such case, pace-mapping remains the only option to localize the origin of the arrhythmia. One needs to be aware, though, that pace-mapping is less accurate than activation mapping, particularly when performed with high-stimulation outputs which are virtually always required around the pulmonary or aortic valves. However, clinically this method has been proven to be accurate enough to successfully ablate the majority of these foci. During pace-mapping, resulting 12-lead QRS complexes can be compared to spontaneous PVC. Using automated pace-map algorithms integrated in an 3D mapping system

(PaSO software, Biosense Webster) is very helpful and precise in this context, leading to an ablation success close to the one achieved by pure activation mapping.[255] Using all these methods, the success rate for ablation in the RVOT exceeds 95%.

Left-sided OT-VT arising from the aortic cusps, aortomitral continuity, or LVOT can also be ablated with a high success rate but it mandates a retrograde aortic or sometimes transseptal or epicardial approach and are therefore a class IIa, level B indication for catheter ablation.[256–259] Ablation procedure should be performed in experienced centers.[249] Since target foci may be ablated from the RVOT, LVOT, aortic cusps, left ventricle, or epicardially through the coronary sinus or even after a pericardial puncture, precise knowledge of the anatomy is paramount and 3D mapping plays their full potential. It may be necessary to target a focus from more than one ablation site since a) only insufficient energy can be delivered from one site to the target area in some cases, or b) the exit site may change after ablation. Integration of pre-procedure images or angiograms can further help to increase the safety of left-sided ablation, particularly in the aortic root or LV summit[256,257] when knowledge of the distance to the coronary arteries is critical. Figure 10-2 illustrates the close vicinity of the anatomical structures and the usefulness of identifying changing exit sites.[260] Here it is possible to observe the subtle change in the morphology of lead V3 when the exit changes to the left coronary cusp after the exit in the RVOT has been ablated. 3D mapping allows for marking the RVOT ablation site and precise placement of the catheter on the opposing part of the right coronary cusp of the aortic valve.

About 12 to 45% of OT tachycardia arise from outside of the RVOT. The majority of those can be readily ablated from the sinus of Valsalva, mostly from the right, left, or junction of the right and left coronary cusps. The noncoronary cusp is almost never involved. The aortomitral continuity and the LV summit also are frequent sources. Ablation techniques do not differ from right-sided ablation with the exception that one needs to take care of the location of the coronary

artery system and more often must ablate from different anatomical sites to eliminate the focus. The latter has been recently coined "anatomical ablation" and carries a moderate success rate.[258] Up to 9% of idiopathic VA arise from the ventricular epicardium from the vicinity of the coronary sinus system. They are increasingly ablated from within the coronary venous with high success and low complication rates.[259]

In summary, ablation of idiopathic OT-VT or OT-PVC can be ablated with a high success rate. Using 3D mapping systems allows to perform these procedures without fluoroscopy. One should start in a stepwise approach mapping the RVOT first followed by the coronary cusps, cardiac veins, and LVOT through a retrograde aortic access. The 3D mapping then allows to precisely delineate the close anatomical proximity of the different structures of the ventricular OT. Recommendations for 3d mapping of idiotaphic outflow tract ventricular tachycardia VT are described in Table 10-1.

11 | CHAPTER 11: VENTRICULAR TACHYCARDIA, IDIOPATHIC, NON-OT VT AND INTRACAVITARY, PAPILLARY MUSCLE

The 3D mapping plays a crucial role in the treatment of idiopathic ventricular arrhythmias, among whom the papillary muscles (PMs)[261–264] represent a special challenge due to their complex anatomy and independent motion during the cardiac cycle. Catheter ablation in that scenario is thus limited by anatomical, navigation, and stability issues and is associated with a lower success rates when compared to other locations. The PMs have been recently related to ventricular arrhythmias in patients with mitral valve prolapse.[265] Importantly, the PMs have also been described as a source of triggers for ventricular fibrillation (VF) both in normal and diseased hearts.[266,267]

11.1 | Anatomical definitions

In the LV, the anterolateral and posteromedial PMs insert their chordae to the mitral valve and most commonly have a single and two heads, respectively. There are usually two PMs in the RV, also named anterior and posterior PMs. The moderator band (MB), in contrast, is a prominent muscle that connects the RV free wall to the septum, supporting the anterior PM of the tricuspid valve.[268] Histologically, a prominent subendocardial network of Purkinje fibers among the ventricular myocytes is observed, which probably explains the characteristic sensitivity to catecholamines and the focal (triggered activity or automatic) mechanism commonly found during mapping and ablation as well as the frequent "Purkinje potentials" recorded. In post-infarct patients, scar-related reentry can also be provoked during EP study.[269]

11.2 | ECG recognition

Distinct ECG patterns have been described and can be quite helpful in preparing for the ablation procedure.[263,270–272] Ventricular

TABLE 10-1 Consensus recommendations

Use of 3D mapping in ventricular tachycardia: Idiopathic outflow tract tachycardia			
Recommendation	Class	LOE	References
In pediatric or pregnant patients, 3D mapping systems are recommended to avoid or minimize radiation exposure.	I	C-LD	249,251
Due to the complex anatomy of the outflow tract, the primary use of a 3D mapping system is recommended in all OT-VT that do not stem from the RVOT.	I	C-LD	256,260
In case of recurrent RVOT-VT the use of a 3D mapping system is reasonable.	IIa	C-EO	

3D, three-dimensional; OT, outflow tract; RVOT, right ventricular outflow tract; VT, ventricular tachycardia.

arrhythmias originating from anterior LV PM present with a RBBB morphology and inferior axis (negative in I and aVL) with a late precordial transition (V3-V5). An interesting characteristic recently described is inferior lead discordance (negative in lead II, positive in lead III),[273] which appears to be associated with this site of origin as well as the parahisian, RV PM, and RV MB regions. Posterior LV PM origin is suggested by a RBBB morphology, late transition but with a superior axis (negative in leads II and III).[261]

Important differential diagnosis includes other LV arrhythmias occurring in normal hearts such as mitral annular and fascicular origin. Fascicular arrhythmias usually have a narrower QRS and rsR pattern in V1, which is not present in LV PM origin.[274] Mitral annular arrhythmias usually present with positive precordial concordance due to its more basal location.[275] Right PM and MB arrhythmias typically present with a LBBB QRS pattern with a characteristic late precordial transition and left superior axis.[272,276]

11.3 | Mapping and ablation

3D mapping (CARTO or NavX) and intracardiac echocardiography ICE are extremely helpful for appropriate anatomical delineation, catheter positioning, and adequate contact.[277] Activation mapping, using either retrograde aortic or transseptal access (Figure 11-1), is the main mapping strategy, complemented by pace-mapping as needed. However, pace-mapping can be limited by discordance between foci origin (deep in the muscle) and exit in the PMs (base vs apex). Multipoint mapping (with a multipolar catheter) can facilitate faster and more reliable mapping due to less catheter-induced PVCs.

The CARTO-Sound platform allows for rapid integration of the anatomical echo-based data in the 3D mapping, even before a mapping catheter is inserted into the ventricles. The contours of the LV PMs and MB can be separately incorporated in the anatomic maps. ICE is a great imaging tool to evaluate catheter-tissue contact in the PMs, which can be quite challenging.[277,278] Clear LV PM view can be easily obtained with the ICE catheter in the RV and this allows for direct visualization of the ablation catheter tip orientation (Figure 11-2).

Ablation can be difficult not only due to the PM anatomy and stability of the catheter but also related to the origin deep in the PM and multiple potential exit sites. Both RF and cryoablation energies can be used for treatment of PM arrhythmias. When using RF, contact force can be helpful not only as a contact guidance but also due to the vector orientation information provided. Standard electrocardiogram characteristics to guide ablation are used, such as activation earlier than −30 milliseconds pre QRS and unipolar QS recording.[279] Use of high power (up to 50 W) is common to compensate for poor stability. Also, long waiting times (>30 minutes) after arrhythmia elimination is recommended. When dealing with deep intramural locations (in case of no significant early activation, only far-field signals observable, and prolonged ablation time required to suppress arrhythmia), long RF (up to 5 minutes)[264,280,281] applications can be used to allow time for deeper penetration. A recently described alternative strategy is to deliver circumferential lesions around the base of the PM, which has been shown to increase the success rates when focal RF ablation at the earlier activation site fails.[282] Usually several RF lesions are required along different segments of the PMs to eliminate all arrhythmias, most likely due to the
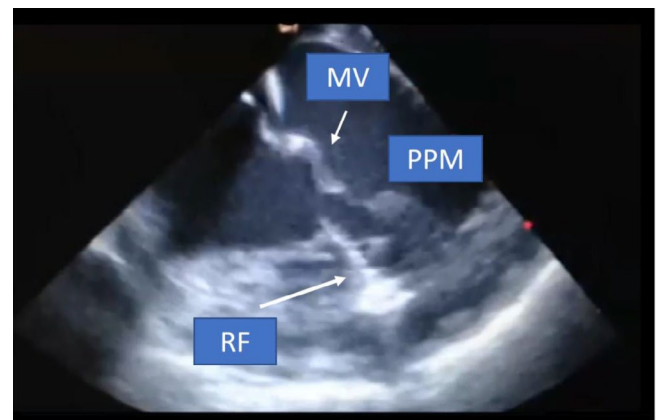
FIGURE 11-2 ICE picture acquired from the RV showing RFCA at the base in one of the posterior PM. Evident tissue edema due to RF application is seen as bright white lesion on ICE (arrow). ICE, intracardiac echocardiography; PM, papillary muscle; RV, right ventricle
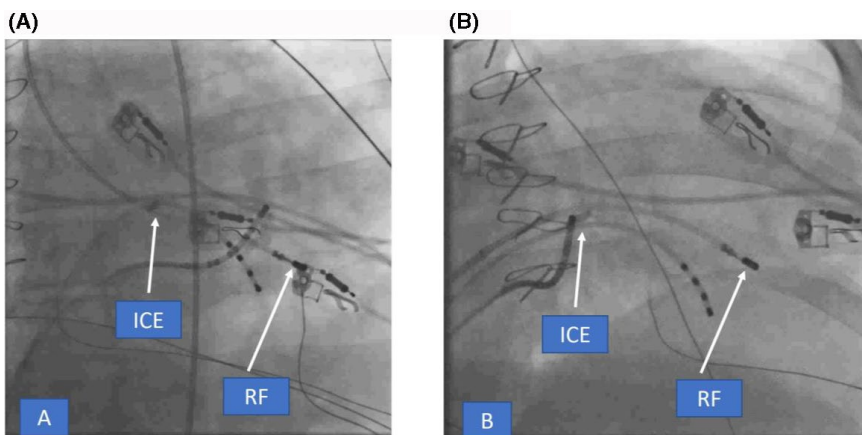
FIGURE 11-1 Fluoro pictures in RAO showing retrograde (A) and transseptal (B) accesses to map the posterior PM in the LV. ICE catheter is depicted in the RV (arrows). ICE, intracardiac echocardiography; LV, left ventricle; PM, papillary muscle; RAO, right anterior oblique; RV, right ventricle
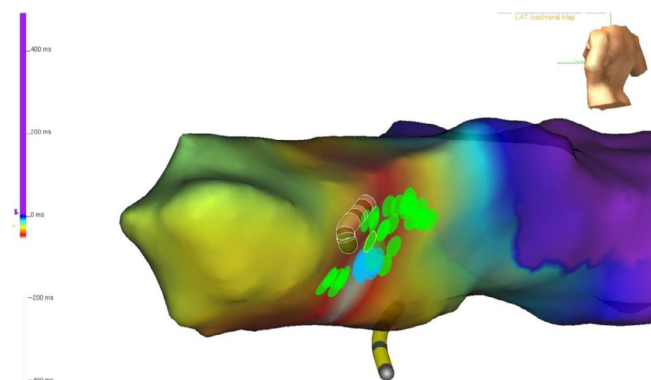
FIGURE 11-3 NavX-guided LV activation map after PVC ablation in the PMs, showing focal pattern of activation and depicting the best RF application sites (blue dots) as well as the extra lesions in different segments of the PM to ensure all exits were targeted (green dots). LV, left ventricle; PM, papillary muscle; PVC, premature ventricular contraction

multiple potential exit sites that a single arrhythmia focus can have. Also, false tendon connections can facilitate this observation. Even subtle QRS morphology changes can be a sign that remapping and ablation at a different site are needed (Figure 11-3). Extra care is needed to avoid catheter entrapment leading to mitral chordae rupture and consequent significant mitral regurgitation. Also PM dysfunction after extensive ablation is one of possible complications.

In the RV MB, insertion sites (free wall or septum) are the usual targets for ablation. RBBB can be created due to the frequent crossing of right bundle fibers at this region. Ablation at the septal RV PM has also been recently described using the same 3D/ICE combination.

11.4 | Role of cryoablation

Focal cryo energy is a suitable alternative to RF, especially when catheter stability is an issue. The natural tissue adherence at the catheter tip limits its mobility and improves contact. Potential drawbacks are the inability to project the catheter tip on the 3D map (which can be overcome by ICE imaging) and reduced lesion depth.

As such, multiple freeze-thaw-freeze cycles around the lesion of interest are recommended. A 6 mm tip catheter may be preferred due to less far-field recording and shorter diameter when compared to the 8 mm tip.

A recent small study including 21 patients undergoing LV PM mapping and ablation with either RF (9 pts) or 8mm cryoablation (12 pts) via a transseptal approach reported higher rates of PVC suppression (78% vs 100%), catheter stability (25% vs 100%), lower incidence of multiple PVC morphology (77% vs zero), and lower 6-month arrhythmia recurrence rate (44% vs zero) favoring cryoablation.[278]

11.5 | VF and PM related PVCs

There is a significant relation between VF and PVC originating from PMs and MB, with clear documentations of triggers originating from the PMs and MB (irrespective of the presence of structural heart disease) inducing VF[267,269] as well as VF induction during energy delivery at these sites in patients without previous spontaneous VF, most likely related to their dense Purkinje network. Excellent rates of freedom from recurrent VF have been reported when the PMs were targeted, with significant reductions in implantable cardioverter defibrillator (ICD) recorded shocks.[266,267]

In summary, mapping and ablation of PMs and MB-related arrhythmias represent a significant challenge due to their anatomical characteristics and catheter stability issues. 3D mapping and ICE are critical in accurate delineation of these structures and in monitoring for adequate tissue contact and energy delivery. Cryoablation is an alternative source that can improve stability and outcomes (Table 11-1).

12 | CHAPTER 12: INHERITED PRIMARY ARRHYTHMIAS SYNDROME

The inherited primary arrhythmias syndrome (IPAS) is composed of different channelopathies and genetic disorders without structural heart disease and is known for causing sudden arrhythmic death at young age. In the last consensus, the IPAS included:

TABLE 11-1 Consensus recommendations

Use of 3D mapping in ventricular tachycardia idiopathic, non-OT VT and intracavitary, papillary muscle			
Recommendation	Class	LOE	References
3D mapping-guided ablation with detailed activation mapping and anatomical delineation is recommended for non-OT VTs.	I	C-LD	277–279
3D mapping-guided pace-mapping annotation and morphology scoring in cases of non-OT VTs is reasonable.	IIa	C-LD	279
3D mapping and ICE-guided catheter placement and anatomical position monitoring is reasonable when ablating in the papillary muscles, near the left main coronary and when bipolar ablation is intended.	IIa	C-LD	277,278

congenital long QT syndrome (LQTS), Brugada Syndrome (BrS), catecholaminergic polymorphic ventricular tachycardia (CPVT), short QT syndrome (SQTS), progressive cardiac conduction disturbance (PCCD), early repolarization syndrome (ER), and idiopathic ventricular fibrillation (IVF).[283] Although ARVC was not included in the mentioned guidelines, it will be analyzed in this section. The diagnosis, risk stratification, and treatment of this very particular population are extremely challenging and are constantly being updated and revised.

The ICD is the most widely accepted therapy for those patients with ion channel mutation who have had sustained VT, usually polymorphic, or VF. However, many patients suffer frequent arrhythmic episodes leading to ICD shocks with consequent deterioration in their quality of life and risk of potentially fatal electrical storm. In the last years, there have been significant advances in mapping and ablation techniques in these patients, with several reports of effective ablation targeting PVCs that trigger VT/VF, or ablating abnormal substrate facilitated by the use of a 3D mapping system.

Essentially, there are no randomized clinical trial or studies with large number of patients with RFCA and follow-up, perhaps due to the lower prevalence of these disorders, when compared with other arrhythmic conditions. Most of communications are case series performed with and without 3D mapping and will be revisited in this document (Table 12-1). A European survey about diagnosis and treatment of IPAS (ARVC not included) revealed that after recurrences of VT/VF, approximately 5%-10% of patients are treated with RFCA. The most frequent channelopathy was BrS (8%), followed by LQTS and CVPT (5%-6%). Unfortunately, there are no data collected about the use of 3D mapping systems.[284]

TABLE 12-1 Cases reports of VT/VF ablation in inherited primary arrhythmia syndrome

Author	n, age, gender	Symptoms	Sites of ablation	3D mapping	Follow-up/outcome
LQTS					
Haissaguerre[310] 2003	4 pts, 38 ± 7, men	Syncope PVT-VF	3 PVC's LV PP 1 PVC's RVOT	NO	24 ± 20 mo. No recurrence
Sanchez[285] 2011	1 pt, 56, female	VF	PVC Posterior RVOT. No PP	Yes	14 mo. No Recurrence
Srivathsan[286] 2012	1 pt, 24, female	VF	PP in mid-posterior septal LV	Yes	6 mo. No Recurrence
Cheng[287] 2012	1 pt, 19, man	PVT/VF	PVC free wall RV	Yes	29 mo. No recurrences
Yap[288] 2013	1 pt, 22, female	VF	Inferoseptal RV	Yes	5 mo. Single recurrence
CPVT					
Kaneshiro[289] 2011	1 pt, 38, female	PVC's, VF	LV inferoseptal with PP Left coronary cusp	Yes	16 mo. No recurrences
Shirai[311] 2017	1 pt, 24, female	PVT Bidirectional VT	LV coronary cusp LV anterior with PP and LV inferoseptal	Yes	24 mo. No recurrence
BrS					
Haissaguerre[310] 2003	3 pts, 39 ± 7, 2 men 1 woman	PVT, VF	RVOT and RV Purkinje system	NO	7 mo. No recurrences
Darmon[312] 2004	1 pt, 18, male	PVT, VF	Posterior RVOT	Yes	9 mo. No recurrences
Nakagawa[292] 2008	1 pt, 41 male	VF	Lateral and posterior RVOT	NO	29 mo. No recurrences
Nademanee[294] 2011	9 pts, 38, males	Resuscitated Cardiac Arrest	Anterior RVOT epicardium	Yes	20 ± 9 mo. One recurrence
Sunsaneewitayakul[295] 2012	10 pts, 38, males	PVT, VF. 4 with storm	RVOT endocardial substrate	Yes	30 mo. Pts with storm, no recurrences
Brugada[296] 2015	14 pts, 39, males	7 PVT or VF. 5 NSVT. 2 Induced VF	Epicardium substrate in RVOT and anterior RV	Yes	No inducibility in all pts. Normalized ECG Br pattern
Pappone[297] 2017	135 pts, 39.9 ± 11.4	G1 = Previous VT/VF G2 = Inducible VT/VF	Epicardium substrate in RVOT	Yes	No inducibility in all pts. Normalized ECG Br pattern

Abbreviations: 3D, three-dimensional; Br, Brugada; G1, Group one; G2, Group two; LV, Left ventricle; NSVT, nonsustained ventricular tachycardia; PP, Purkinje potential; PVC, premature ventricular contraction; RV, right ventricle; RVOT, right ventricular outflow tract; VF, ventricular fibrillation; VT, ventricular tachycardia; PVT, polymorphic ventricular tachycardia.

12.1 | Congenital long QT syndrome

In high-risk patients with LQTS, beta-blockers and ICD are the established therapy for preventing and treating VT/VF. Nevertheless, there have been some reports showing the beneficial effects of RFCA in selected cases (Table 12-1). Mostly, the patients had electrical storm of complex management, high density of PVCs, and documented induction of VT/VF by PVC with identical morphologies. Haissaguerre and his colleagues published three cases of polymorphic VT (PVT). In two cases, the ablation was performed successfully in the peripheral Purkinje arborization in the left ventricle, including the ramification of posterior or anterior fascicles, where a Purkinje potential preceding the triggering ectopy was recorded. In the other patient, the site of ablation was in the RVOT.[3] Interestingly, they did not use 3D mapping system. Sanchez et al described a LQTS case with PVC-induced VF, eliminated with RF ablation in the RVOT, without Purkinje signals using CARTO system.[285] As displayed in Table 12-1, other authors have published similar findings.[286-288] Although this ablation can be performed with traditional mapping, the use of 3D mapping has several advantages: once the shell is created, the sites of interest with Purkinje potential during sinus rhythm and preceding the PVC can be tagged. This is important because the catheter can be repositioned in the tagged points, once it has been moved and in case of the disappearance of PVC due to the bumping of the focus with the catheter. When the triggering ectopy is originated in the RVOT (not Purkinje-related) the local activation map or the pace-mapping with tagging are other advantages of the 3D mapping systems.

12.2 | Catecholaminergic polymorphic ventricular tachycardia

Catecholaminergic PVT is an inherited arrhythmogenic disorder characterized by PVT provoked by physical or emotional stress. This is a frequent cause of sudden death in young patients and an ICD is often placed after the patient has been resuscitated from cardiac arrest. There have been only few case reports of ablated patients with this channelopathy (Table 12-1). Kanesiro et al studied a case with frequent PVCs with identical alternating morphologies triggering VT/VF. The ablation was performed successfully with 3D mapping system, through tagging the areas with Purkinje potential preceding the PVCs.[289] Another case with alternating PVCs was ablated successfully in the left coronary cusp and the left Purkinje network, under fluoroscopic navigation.[290] There are insufficient reported cases with LQTS or CPVT to make a strong recommendation about the use of 3D mapping.[291,292] Although the mapping could be done conventionally in an emergency, we recommend using 3D mapping as a Class I indication with level of evidence C in both syndromes. Some patients suffer VT/VF storms and must be ablated promptly. 3D mapping will be particularly helpful in these cases. Robust evidence is lacking regarding SQTS, PCCD, and ER to make any recommendations. IVF will be analyzed in another section. Recommendations for 3D mapping of IPAS is described in Table 12-3.

12.3 | Brugada syndrome

The BrS is a channelopathy that can cause sudden death at a young age. The ICD is the treatment of choice for patients who have recovered from polymorphic VT/VF or had syncope event with spontaneous type I pattern in the surface ECG. Many patients have frequent ICD discharges for recurrences which recently can be treated with ablation. Table 12-1 displays the experience with ablation in this syndrome.

Haissaguerre published three patients with frequent ICD shocks for VF.[293] There was consistent monomorphic PVCs triggering the tachyarrhythmia. He successfully performed a conventional ablation of the PVCs by mapping the earliest activation in the RVOT endocardium in two patients, and the anterior right ventricular Purkinje network in the third. In subsequent reports with more cases, the procedures were performed with 3D mapping. A hallmark study reported the presence of electrophysiological evidence of an arrhythmogenic substrate localized in the RV epicardium.[294] There were nine patients with BrS with frequent ICD therapies. In this series, epicardial and endocardial 3D mapping was performed, which enabled the creation of maps, based on different parameters such as: late potentials, low voltages, and fractionated electrograms. Interestingly, all these signals were exclusively localized over the anterior aspect of the RVOT epicardium and were tagged as target sites for ablation. In contrast, mapping the opposite area, that is the endocardium, did not identify any abnormal signals. 3D mapping-guided ablation at those sites rendered VF noninducible and resulted in normalization of the Brugada ECG pattern in most cases. Likewise, Brugada et al published their experience of catheter ablation in 14 male patients with Brugada pattern type 1 (spontaneous or induced by flecainide) and history of VT, VF, or ICD implantation.[295,296] High-density detailed endocardial and epicardial maps were performed using 3D mapping system to define areas of low voltage and delayed fragmented electrograms during stable sinus rhythm. After flecainide, the low-voltage epicardial areas expanded and the duration of abnormal electrograms increased in almost all patients, facilitating localization and subsequent ablation of abnormal substrates, which in many patients extended from the RVOT toward the anterior aspect of the RV free wall. In the largest series published so far, Pappone et al also showed similar results using 3D mapping, confirming the importance of epicardial substrate.[297] Furthermore, in his report only two of 27 patients with frequent appropriate ICD discharges had recurrences postablation.

The use of 3D mapping in BrS is extremely useful for the mapping of triggers, which can be localized in the RVOT endocardium and, most importantly, to define zones with low voltage and fractionated, late and long potentials, which seem to predominate in the RVOT epicardium and could be the substrate that underlies the arrhythmogenic substrate in this channelopathy. In BrS, the data clearly

supports the use of 3D mapping to guide ablation and it should be a Class I recommendation with level of evidence C.

12.4 | Arrhythmogenic right ventricular cardiomyopathy

ARVC is an inheritable heart muscle disease characterized by predominant RV endo-epicardial fibrofatty replacement, producing a patchy scar pattern. Unlike the previously mentioned channelopathies, this fibrosis provides a substrate for reentry and VT, often monomorphic, like other scar-related VTs. RFCA has shown different and conflicting results with noninducibility rate at the end of procedure, ranging from 46% to 75% and a VT recurrence rate during 3-5 years of follow-up is reported to be 50%-70% (Table 12-2). These poor results may be caused by the progression of the fibrosis and different approaches or techniques.

In the beginning, the feasibility of VT ablation in ARVC patients was demonstrated using fulguration. Since then, many authors have used techniques of entrainment but, in the last 10 years, most communications report the use of 3D mapping. There is no prospective study comparing both strategies, and few authors compared the results with and without 3D mapping. In a nonrandomized study (n = 87), VT-free survival rate was significantly higher in patients who underwent RF ablation with 3D mapping.[298]

Using conventional endocardial approach with entrainment techniques, Ellison et al rendered 42% noninducible at the end of the procedure but did not inform about follow up results.[299] Nogami et al reported endocardial ablation in 18 patients (only five with 3D mapping), guided by modification of isolated delayed components in sinus rhythm and did not find differences in the recurrence rate of VT between conventional mapping and 3D mapping.[300] Dalal et al did not report differences either, but only 10 out of 48 cases underwent 3D mapping-guided ablation.[301] After publication of these studies, all the procedures have been guided by 3D mapping (Table 12-2).

Although no randomized comparisons are available, in ARVC patients with VT, the incorporation of epicardial mapping and ablation seems to be associated with better outcomes than endocardial ablation alone. Nevertheless, several authors propose an endocardial approach first and if the VT remains inducible or recurrent, an epicardial ablation be performed.[192,302–305]

Marchlinski et al reported favorable outcomes with endocardial substrate-based ablation in areas with low voltages (<1.5 mV) like postinfarction VT.[306] Other added zones with fragmented or isolated delayed potentials located intrascar or in the border zone can be tagged in a separate way or incorporated to the low-voltage map.[305–307] To define if a predominant pericardial substrate is present, a unipolar endocardial voltage map created with 3D mapping can be of great help. A cutoff value of <5.5 mV to predict a more

TABLE 12-2 VT Ablation in ARVC. Approach, use of 3D mapping systems and outcome

Authors	n	Approach	ICD	Use of 3D mapping	F-Up (months)	Outcome reported
Ellison[299] 1998	5	Endo	No	0		Noninducible: 42%
Marchlinski[306] 2004	21	Endo	21	100%	27 ± 22	Freedom of VT: 84%
Verma[307] 2005	22	Endo	18/22	100%	37	Recurrences 1 and 3 yrs: 23% and 47%
Dalal[301] 2007	24	Endo	17/24	25%	32 ± 36	Recurrence-free: 1.5, 5 and, 14 m: 75%, 50%, and 25%
Nogami[300] 2008	18	Endo	2/18	27%	61 ± 38	Recurrences: 33%
Garcia[192] 2009	13	Endo/Epi	12/13	100%	18 ± 13	Freedom VT: 77%
Bai[302] 2011	49	Endo 23/Epi 26	49/49	100%	40 ± 10	Freedom VT: 52% Endo, 84% Epi
Philips[298] 2012	87	Endo/Epi	82/85	69%	88.3 ± 66	To 1, 2, 5 yrs Freedom VT 3D mapping: 50%, 34%, and 24% Freedom VT Conventional: 36%, 16%, and 8%
Santangeli[304] 2015	62	Endo 23/Epi 39	62/62	100%	56 ± 44	Freedom of VT: 71%
Philips[303] 2015	30	Epi	30/30	100%	19.7 ± 11.7	Recurrences: 27%
Müssigbrodt[305] 2016	45	Endo 23/Epi 22	45/45	100%	31 ± 27	Freedom of VT: 57,8%
Berruezo[308] 2016	42	Epi/Endo	42/42	100%	32 ± 21	Recurrences: 26,8%

Abbreviations: 3D, three-dimensional; ARVC, arrhythmogenic cardiomyopathy; Endo, endocardial; Epi, epicardial; VT, ventricular tachycardia.

TABLE 12-3 Consensus recommendations

Use of 3D mapping in inherited ventricular arrhythmias			
Recommendation	Class	LOE	References
BrS: 3D mapping-guided ablation is recommended for endo/epi ablation of substrate and/or triggers.	I	B-NR	293–297
ARVC: 3D mapping-guided ablation is recommended for endo/epi ablation of substrate/triggers and isthmus channels of conduction and for mapping of VT circuit.	I	B-NR	192,298–308
LQTS: 3D mapping-guided ablation is recommended for ablation of VF/VT triggers in patients with storm or frequent shocks of ICD.	I	C-LD	293
CPVT: 3D mapping-guided ablation is recommended to eliminate VF/VT triggers since many trigger sources can be mapped.	I	C-EO	

extensive pericardial substrate has been proposed.[195] Berruezo et al proposes the identification of isthmus or scar-related channels of conduction, especially in pericardium. The ablation is facilitated by 3D mapping to make intra- or interscars lines of ablation to transect the isthmus, abolishing all the late potential or channels using dechanneling techniques. All of these ablation approaches are based in 3D mapping.[308,309]

In conclusion, the use of 3D mapping is necessary when planning an endocardial or epicardial ablation. Thus, the recommendations is Class I with level of evidence C.

13 | CHAPTER 13. VENTRICULAR FIBRILLATION: IDIOPATHIC, PURKINJE VF

Idiopathic VF is a syndrome characterized by VF episodes triggered by frequent PVCs falling into the vulnerable phase of the cardiac cycle in patients in whom structural disease or other known proarrhythmic syndrome has been excluded. The management of patients with IVF is challenging. IVF events are not typically related to predisposing factors such as stress or activity. Life-threatening ventricular arrhythmias may occur in clusters characterized by frequent PVCs and episodes of VF or polymorphic VT. There is a growing body of evidence that in the majority of IVF cases, the triggering focus originates from the Purkinje system that may play a crucial role in both the initiation and perpetuation of VF. In the rest of IVF cases the source of malignant arrhythmia can be found for example in the RVOT.

13.1 | Pathophysiology

The Purkinje system, a specialized conduction system of the heart, is localized in the endocardium and constitutes only a small portion of the myocardial mass. It consists of a single right and two left branches of specialized fibers insulated from the underlying myocardium until their peripheral extensive arborization into the myocardial muscle. The right branch ramifies in the anterior wall of the RV, whereas two left branches (fascicles) subdivide and interconnect over a great area of the LV. Animal studies have shown that the Purkinje network may generate or maintain arrhythmias by automaticity, reentry, or triggered activity in various conditions such as electrolyte imbalance, myocardial ischemia, catecholamines, or other drugs.[313–317] Other studies have also suggested the existence of reentry involving the Purkinje-myocardial junction.[318] A triggering PVC may originate from distal part of either the right or left Purkinje system and produce a characteristic 12-lead ECG pattern. PVCs originating in the right Purkinje system have a LBBB pattern with left superior axis, while PVCs originating in the left Purkinje system produce more variable ECG morphologies, reflecting the more complex Purkinje network. In the studies by Haissaguerre et al and Knecht et al,[319,320] PVCs were mapped to various locations in the Purkinje system, indicated by specific potentials preceding the local muscle activity. These Purkinje beats usually had short coupling intervals and characteristic morphologies similar to patterns encountered in the fascicular tachycardia if originated from the LV (RBBB morphology of QRS with either a superior or inferior axis) or LBBB patterns with left superior axis if arose from the RV. Leenhardt et al[321] were the first to describe a syndrome of idiopathic PVT associated with an extremely short-coupled PVCs (245 ± 28 milliseconds) in 14 patients without ischemic or structural heart disease and normal QT intervals. Why these triggers cause IVF in some individuals and not others remains unclear.

13.2 | EP study (EPS) and ablation

Ventricular activation during VF is chaotic and mapping is difficult not only from electrophysiological point of view, but also from patient's clinical status perspective. In order to overcome these limitations, EPS in patients with IVF focuses on the search of reliable triggers that initiate clinical episodes of VF. As mentioned previously, in the majority of IVF cases the triggering sources arise from the Purkinje/fascicular system. Such a triggering focus in the Purkinje

network can be mapped and ablated by identifying the earliest electrocardiogram relative to the onset of the initiating PVC. Purkinje potentials preceding ventricular activation by PVCs indicate their origin from the Purkinje fibers. In mapping of Purkinje beats the earliest site of activation should be targeted. Ventricular arrhythmia being focal in origin tends not to be initiated or entrained by pacing in either the atria or ventricles.

The involvement of the Purkinje conduction system in the initiation of life-threatening arrhythmias in patients with IVF was first demonstrated in 2002 by Haissaguerre and colleagues.[319] Of 27 patients resuscitated from IVF, electrophysiological mapping identified PVCs from the distal Purkinje conducting system in 23 patients (left ventricular septum in ten, anterior right ventricle in nine, both locations in four) and RVOT myocardium in four patients.[319] PVCs initiating VF showed an electrocardiographic morphology and coupling interval identical to the premature beats occurring immediately after resuscitation. The arrhythmic source was localized by the earliest electrogram relative to the onset of PVCs. A Purkinje potential preceding ventricular activation during PVCs indicated their origin in the Purkinje system, whereas its absence at the site of earliest activation indicated an origin in the ventricular muscle. During PVCs, the earliest Purkinje potential preceded the local muscle activation by a conduction interval of 38 ± 28 milliseconds, whereas during sinus rhythm only by 11 ± 5 milliseconds (distal Purkinje fibers). Differing conduction times at the same site, were associated with varying morphologies, suggesting either changes in the ventricular activation route or origin from another part of the Purkinje system.[319] PVCs emerging from RVOT and Purkinje fibers had not only distinct QRS morphologies, but also different QRS duration and coupling intervals (QRS duration and coupling intervals were shorter in PVCs arising from the Purkinje system). Ablation of Purkinje beats produced temporary exacerbation of ventricular arrhythmia followed by a disappearance of PVCs. There was no sudden death, syncope or recurrence of VF in 89% of patients during a mean follow-up of 24 ± 28 months.[319] In their paper, Haissaguerre et al showed for the first time that catheter ablation of short-coupled triggers originating from the Purkinje system may be feasible and effective.[319]

The long-term follow-up of patients after catheter ablation of idiopathic VF has been published in 2009 by Knecht et al.[320] In this multicenter study, 38 patients underwent catheter ablation for IVF initiated by short-coupled PVCs. The triggering ventricular beats originated from the right (n = 16), left (n = 14), or both (n = 3) Purkinje systems, while a myocardial origin was found in five patients. During a median follow-up of 63 months, only seven of 38 patients experienced VF recurrence at a median of 4 months; however, five of these seven patients underwent repeat ablation without further VF recurrence. In their study, Knecht et al showed a long-term freedom from IVF recurrence after ablation targeting short-coupled PVCs originating from the Purkinje system. However, a relatively high amount of RF current was required to abolish local potentials which is in line with some other studies showing that

Purkinje fibers are more resistant to ischemic and thermal damage in comparison with the rest of myocardium. Survival free of VF was predicted by transient bundle branch block in the originating ventricle during the EPS.[320]

As shown in these two relatively small studies[319,320] catheter ablation of the triggering ectopy appears to produce a desirable outcome and to have a high success rate; however, precise mapping is required. The success of VF ablation may improve when patients have the triggering ventricular ectopy present at the time of the procedure,[319] but the absence of frequent PVCs at the time of ablation did not predict an unfavorable outcome in the study by Knecht et al[320] During activation mapping of triggering PVCs, attention should be paid to the preceding Purkinje potentials. Mapping should be focused on determining the earliest potentials, which are the key to a successful ablation. However, if the earliest site cannot be determined or is located close to the His bundle, modification of the Purkinje network may also be performed. When clinical PVCs are infrequent or absent, localizing the Purkinje network remains the primary objective for procedural success.[320] In this setting, 12-lead ECG or Holter monitoring prior to the EPS may be necessary to identify a potential target for mapping and ablation. In the patients without the triggering ectopy during the EPS, the putative source of PVCs can be established based on pace-mapping. In some of these patients, multifocal PVCs may be present. In such cases the true triggering PVC has to be confirmed. Therefore, in certain clinical scenarios, it appears to be particularly useful to employ the 3D mapping system which allows for 3D reconstruction of the ventricular endocardial surface as well as tagging of potential points of interest such as the conduction system or the earliest activation sites.

In cases of successful mapping, the ablation site is usually contained within a small area in patients with IVF.[322] Due to the subendocardial location of Purkinje fibers, deep transmural lesion is not necessary and ablation at the critical sites allows very rapid stabilization of the patient's clinical status. In order to avoid unintended injury to the conduction system, catheter ablation should be performed from the apical toward basal parts of the ventricle until successful ablation is achieved. The main clinical end points during ablation are the absence of triggering PVCs and noninducibility of

TABLE 13-1 Consensus recommendations

Use of 3D mapping in idiopathic ventricular fibrillation			
Recommendation	Class	LOE	References
3D mapping-guided catheter ablation of PVCs triggering IVF is reasonable when performed by experienced operators.	IIa	B-NR	319–321,323
3D mapping-guided ablation is reasonable to ablate PVCs originating from Purkinje fibers and earliest site of activation should be targeted.	IIa	B-NR	319–321,323

malignant arrhythmias. Other end points may include the abolition of Purkinje potentials, slight delay in the local ventricular electrogram at the site of ablation or demonstration of diastolic Purkinje potentials. It is unknown whether additional substrate modification within the neighboring Purkinje network may further improve the clinical effect of the ablation, while it may increase the risk of complications especially at more basal ablation sites such as complete AVB or LBBB.

It is of note that short-coupled extrasystoles arising from the RVOT and leading to IVF may also be rarely encountered. Noda et al[323] described 16 patients with a malignant RVOT-related VF or polymorphic VT. The triggering PVCs originated mostly from a septal RVOT and catheter ablation at the initiating sites eliminated further episodes of syncope, VF, and cardiac arrest in all patients during the follow-up period of 54 ± 39 months.

VF is a lethal arrhythmia that may be present in patients without structural heart disease. The triggering sources in patients with IVF are located mainly in the Purkinje system. Catheter ablation of Purkinje or RVOT-related IVF is feasible and shows promising results. In patients with drug-refractory electrical storms, catheter ablation of the triggering PVCs from the Purkinje system should be used as an electrical bailout therapy. Further studies are necessary to evaluate pathophysiological mechanisms of this malignant arrhythmia and to improve current mapping and ablation techniques (Table 13-1).

14 | CHAPTER 14. A ZERO-FLUOROSCOPY APPROACH TO CATHETER ABLATION: ROLE OF 3D MAPPING SYSTEMS

The first available 3D mapping system that was introduced to clinical EP was hailed as a "nonfluoroscopic" 3D mapping system;[11,56] however, the transition from fluoroscopy-only to rely on the "virtual" 3D map was a quite challenging "leap of faith" for most EP operators in the late years of the last millennium, resulting in quite a lot of radiation exposure.[129,324] However, the key information of real-time depiction of the ablation catheter with colorful indicators at the tip

FIGURE 14-1 Examples of fluoro-less catheter manipulation. A, Depiction of the color of deflection of a bidirectional catheter (Navistar, Biosense Webster): the smaller curve on the handle deflects the catheter toward the red color of the tip, while the larger curve deflects toward blue. Rotation in clockwise or counterclockwise fashion allows due to a fairly stiff catheter (torque) to navigate completely nonfluoroscopically. B, Example of a nonfluoroscopic manual ablation of a midseptal accessory pathway using 3D EAM guidance (A). Please note the 3D depiction of the right atrial anatomy with tagging of the compact AV node (yellow tag) and depiction of two diagnostic catheters. The fluoroscopic system is not used at all (B) and all electrograms are displayed on the EP recording system (C). C, Example of 3D visualization of the vasculature after femoral venous access using the NavX system (courtesy of Dr L. Vitalli-Serdoz). Please note the renal and hepatic veins (in red). This allows to advance the mapping catheter nonfluoroscopically to the right atrium (in grey) which upon "arrival" will show an atrial signal. 3D, three-dimensional
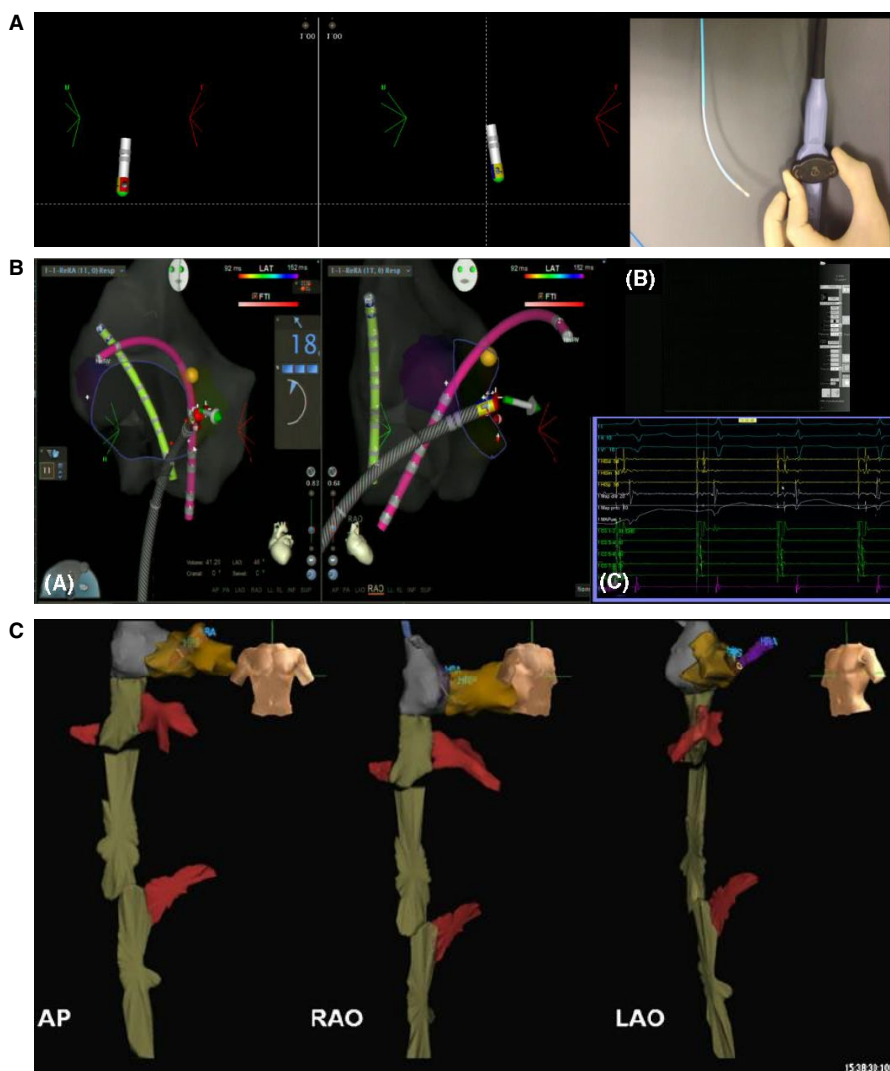
"color of deflection" (Figure 14-1) allowed a hand-eye-coordination to develop that was surpassing the information from the two-dimensional fluoroscopy screens, such that catheter 3D "navigation" became more and more fluoro-less.

The next important step to allow low or even ZERO fluoroscopy exposure was achieved when diagnostic catheters were visualized on the 3D mapping systems, allowing to navigate even nonsensor-equipped catheters with good precision (Figure 14-1B).[22] The first system of this kind was the LocaLisa system, which depicted all catheters albeit in a somewhat distorted 3D representation.[59] Besides aiding intracardiac navigation, this was extremely helpful when advancing the catheters from the femoral accesses toward the heart, a maneuver that otherwise exposed the "vulnerable" genital area when performed using fluoroscopic guidance (Figure 14-1C).[325] With the evolution of the 3D mapping systems over the last 20 years, especially with the improvement in the accuracy of the catheter position during the entire cardiac cycle with respiratory gating, the display of all (even nonsensored) catheters[22] and fast reconstructions of any given heart chamber has reduced total radiation exposure for nearly all procedures significantly.[79,326,327] Recommendations for 3D mapping of zero-fluoroscopy approch is described in Table 14-1.

14.1 | Importance of EP settings for fluoroscopy systems

More awareness has been raised to set the fluoroscopy systems to low exposure settings avoiding the use of the conventional "coronary" program as the metal in the catheters provide an excellent contrast such that the kV can be reduced drastically.[328–330] Also,

there are hardly any circumstances where contrast is injected using cine acquisitions which increases the radiation exposure massively. In EP, normal fluoroscopy is usually sufficient and cine acquisitions can usually be replaced by storage of the last fluoroscopy scene. Further steps such as interval screening, collimation, etc will allow to achieve an "as low as reasonably achievable" (ALARA) exposure.[327–329]

14.2 | Operator learning curves

Using a 3D mapping system is clearly a factor in this approach, but it is largely due to the individual training that LOW or even ZERO radiation can be achieved.[327,331,332] If all recommendations for settings of the imaging system including collimation, reduction in the frame rate, shielding, etc are applied correctly, then most of the radiation can be avoided but this requires dedicated adherence overcome a substantial learning curve.[327,328,331,332]

14.3 | Further tools that assist in further radiation exposure

Especially when 3D image integration was added, mapping the entire 3D chamber without missing important areas was much facilitated.[114,333,334] When using contrast CT imaging for 3D image integration, the patient is obviously exposed to substantial radiation; however, during the procedure the overall fluoroscopy time can be significantly reduced. Recently, noncontrast nonradiation cardiac magnetic resonance sequences have been introduced that allow the same quality of 3D reconstruction without adding any radiation burden.[334,335]
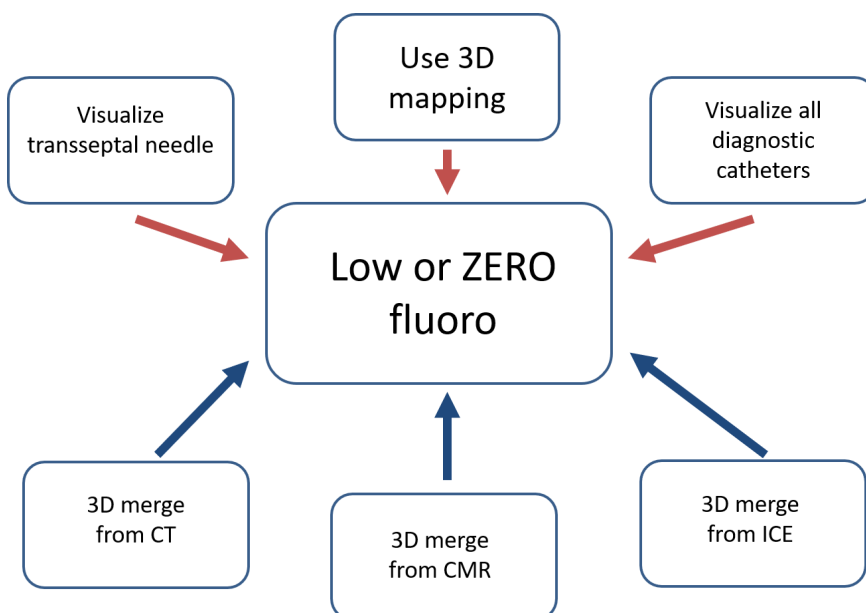
FIGURE 14-2 Schematic of options for reduction in fluoroscopy exposure. Concept of using all available information for 3D visualization of catheters and other tools (such as transseptal needle (upper panels, red), as well as all available anatomical information (lower panels, blue) from either 3D merge (computed tomographies (CT) or cardiac magnetic resonance (CMR) imaging) or intracardiac echocardiography (ICE). 3D: three-dimensional

14.4 | Further technical advances that may allow to reduce radiation burden

Whenever the target chamber is not directly accessible, a transseptal or transbaffle puncture is necessary to gain access. Visualization of the transseptal access can be achieved with real-time transesophageal echocardiography (TEE) or ICE, but require either an additional operator or additional vascular access.[336–338] Recently, a number of groups have reported on visualizing the tip of the transseptal needle on the 3D mapping system allowing thereby a totally ZERO radiation ablation approach in AF ablation procedures (Figure 14-2).[95,339]

14.5 | Patient groups requiring low or ZERO fluoroscopy exposure

14.5.1 | Young patients

Obvious group of patients who benefit most from low or ideally ZERO fluoroscopy procedures are children.[340] A larger number of centers have reported their experiences and the use of 3D mapping tools seems to allow a reproducible approach that does not increase the risk of complications (eg, for AV nodal conduction block in AVNRT ablation).[341,342] Remote magnetic navigation in young patients seems also result in lesser radiation exposure, a result that has been reported already as one the initial observations using the system in SVT ablation.[343,344]

14.5.2 | Pregnant patients

The unborn child of a pregnant women is obviously at highest risk which is why radiation exposure during pregnancy should be avoided as much as possible, but may be administered if absolutely necessary and not replaceable by a nonionizing technique.[345] A number of groups have reported of their experience using 3D mapping systems to allow completely ZERO radiation exposure during these procedures.[346–348] When transseptal access is necessary, then ICE or TEE guidance has been used mostly. However, data from larger cohorts are missing as these cases are rare and typically present as an emergency when all pharmacologic tools have failed.

14.6 | Professional radiation exposure

Reducing the amount of radiation exposure for the patient automatically reduces the professional risk for the operator which therefore should logically be one of the highest if not "selfish" interests for staff.[349] In order to protect against scattered radiation emitted from the patient's body, operators typically wear lead protection to avoid a significant professional radiation burden but seem to ignore the risk to their health.[329,330] Legislation about workers' radiation protection exist in virtually every country with monitoring of exposure mostly using passive dosimeters to estimate the risk. Correlation between professional exposure and developing malignancies has been reported as well as increased risk of malignancy for patients with high exposure rates.[350,351] Acting according to the "ALARA" principle seems paramount and further emphasis should be given to "train" even experienced operators to use as little radiation as possible (for their own and their patients' fate).

Taking advantage of all the features of a 3D mapping system allows the operator to substantially lower his or her own radiation exposure, with many procedures potentially being fluoro-less with currently available standard mapping systems. Both operators and patients should consider the use of these "radiation protection systems" especially when vulnerable patients such as young or pregnant patients are investigated.

15 | CHAPTER 15: SUMMARY AND FUTURE PERSPECTIVES

Three-dimensional mapping is an established method for tracking catheter movement and manipulation, using the capability to recognize the catheter as their primary visual modality, and to construct a 3D structure in real time.[352] To optimize the use of such systems, the anatomic shell thereby constructed is either integrated with the 3D anatomic dataset or generated by previous CT or MRI scans. This information might help in better planning procedural strategies, and reducing unexpected procedural complications in ablation, especially in congenital heart diseases that often have multiple anatomical variants.[353] Zero fluoroscopy ablation is possible for almost all types of arrhythmias to eliminate potential future complications for both the medical team and patients due to radiation and is highly recommended when catheter ablation becomes necessary in children and during pregnancy.[354]

15.1 | High definition in 3D mapping systems

There are several mapping systems, all of them offering similar type of anatomical and functional information. Comparative studies in a random and controlled way have not been possible due to rapid

TABLE 14-1 Consensus recommendation

Role of 3D mapping systems for fluoro-less approach to catheter ablation			
Recommendation	Class	LOE	References
3D mapping system is recommended to lower radiation exposure to enable "ALARA" principle or zero-fluoroscopy procedure for all patients, especially for children and during pregnancy.	I	C-LD	22,79,324,350

development and renewal in commercial platforms, but all of them offer catheter and software tools to improve high-density mapping leading to high definition maps. Currently, we have access to anatomical and functional approaches not available before. These tools may enable the 3D mapping of real-time activation and propagation patterns of the vast majority of typical arrhythmias. This information must be obtained and interpreted differently according to the arrhythmia, and there are still some concepts in order to define the correct interpretation mainly in complex arrhythmias.[41]

15.2 | Fractionation and voltage in AF

The mechanisms by which AF initiates, sustains, and terminates have been the subject of controversial theories and extensive investigation, most of them related to areas of low-voltage atrial electrograms and diverse fragmented frequencies that may arise from multiple factors, including atrial fibrosis, conduction delays, wave breaks, and anisotropy even in normal cardiac tissue conduction.[355] It should be recognized that although the techniques and end points of catheter ablation may differ significantly among centers, the resulting lesion set might be similar.[167,356,357] At the present time, 3D mapping systems offer the advantage to preselect the voltage thresholds and frequency filters according to ablation targets in each medical group. All mapping tools require precise validation and sensitivity analysis against optimal signal processing. We should standardize concepts about fractionation and low voltage, for a correct use of these important tools.

15.3 | Multielectrode tools for complex ventricular arrhythmias

High-resolution mapping with multielectrode mapping catheters provides enhanced capabilities for VT ablation in patients with structural heart disease, and permits identifying potentially arrhythmogenic regions of myocardium in sinus rhythm and during clinical VT. We can create the 3D anatomical substrate, and at the same time also appreciate their functional behavior, identify a complete reentrant circuit, and determine whether this circuit is actually passive and has no relevance to the tachycardia mechanism or is a true culprit circuit.[358] Technological improvement offers the use of catheters with smaller electrodes and closer interelectrode spacing. More recently, the introduction of microelectrodes embedded within the circumference of the distal electrode of the conventional ablation catheter enabled better differentiation of far-field from near-field electrograms to better characterize borders between scar and healthy tissue, and to map and ablate left ventricular summit arrhythmia.[359,360] All these new catheter developments provide an effective substrate approach in small zones and allow us to identify potentially arrhythmogenic regions even in sinus rhythm, avoiding arrhythmia induction. These tools improve our understanding of arrhythmias such as wobbling tachycardia, unmappable VT, ventricular fibrillation, and even channelopathies. Future studies

are needed to compare electrode diameter, interelectrode distance, and filter settings. Undoubtedly, with these new technologies we will be able to identify abnormal pathways, and even small islands of viable tissue surrounding dense scar. We need to reassign the parametric values in terms of voltage and frequency related to these heterogeneous tissues.

15.4 | Multimodal image in 3D mapping

The integration of several structural and functional imaging datasets will become routine in 3D mapping.[353] MRI has been the most used and helpful tool to provide structural and functional features of arrhythmias, but ICE is the only and most used current imaging modality in real time that we can integrate to a 3D model to reduce x-ray radiation. Hence, ICE must be part of electrophysiology training.[352,360] MRI compatible guidance platform for mapping and ablation has been incorporated to visualize 3D anatomy and 3D maps.[361,362] Although there is limited clinical evidence to date, these new technologies will make a strong impact on electrophysiology.

15.5 | Pixel signal intensity maps

Pixel signal intensity (PSI) mapping has emerged as a promising modality in substrate characterization of various arrhythmias. Late gadolinium enhancement MRI provides characterization of heterogeneous tissue and scar. This software depicts the tissue as PSI represented in color-coded PSI maps similar to 3D map voltage information with the advantage that they can be imported into 3D map to guide a substrate ablation.[363] This may be the ideal platform to characterize and validate our parametric values like voltage and frequency.

15.6 | Closing Remarks

The advent of 3D mapping has been a very useful development for the field of cardiac electrophysiology. Technological advances have made this technique increasingly useful for improving both the safety and efficacy of ablation therapy. It is increasingly accepted that 3D mapping is the first option in many arrhythmia substrates and we must improve our use of this technology to further understand the principles of cardiac electrophysiology. Through this, the mechanisms of arrhythmias and the strategies by which these can be treated may be enhanced.

ORCID

Yun Gi Kim https://orcid.org/0000-0003-2905-6609

REFERENCES

1. Asirvatham S, Narayan O. Advanced catheter mapping and navigation system. In: Huang S, Wood M, editors. Catheter ablation of cardiac arrhythmias. Philadelphia, PA: Saunders/Elsevier, 2006; p. 135–61.

2. Gurevitz OT, Glikson M, Asirvatham S, Kester TA, Grice SK, Munger TM, et al. Use of advanced mapping systems to guide ablation in complex cases: experience with noncontact mapping and electroanatomic mapping systems. Pacing Clin Electrophysiol. 2005;28:316–23.

3. Friedman PA. Novel mapping techniques for cardiac electrophysiology. Heart. 2002;87:575–82.

4. Corrado D, Basso C, Leoni L, Tokajuk B, Bauce B, Frigo G, et al. Three-dimensional electroanatomic voltage mapping increases accuracy of diagnosing arrhythmogenic right ventricular cardiomyopathy/dysplasia. Circulation. 2005;111:3042–50.

5. Nakagawa H, Shah N, Matsudaira K, Overholt E, Chandrasekaran K, Beckman KJ, et al. Characterization of reentrant circuit in macroreentrant right atrial tachycardia after surgical repair of congenital heart disease: isolated channels between scars allow "focal" ablation. Circulation. 2001;103:699–709.

6. Soejima K. How to troubleshoot the electroanatomic map. Heart Rhythm. 2010;7:999–1003.

7. de Groot NM, Schalij MJ, Zeppenfeld K, Blom NA, Van der Velde ET, Van der Wall EE. Voltage and activation mapping: how the recording technique affects the outcome of catheter ablation procedures in patients with congenital heart disease. Circulation. 2003;108:2099–106.

8. Lewis T, Meakins J, White PDX. The excitatory process in the dog's heart. Part I. The auricles. Phil Trans R Soc Lond B. 1914;205:375–420.

9. Cobb FR, Blumenschein SD, Sealy WC, Boineau JP, Wagner GS, Wallace AG. Successful surgical interruption of the bundle of Kent in a patient with Wolff-Parkinson-White syndrome. Circulation. 1968;38:1018–29.

10. Scherlag BJ, Lau SH, Helfant RH, Berkowitz WD, Stein E, Damato AN. Catheter technique for recording His bundle activity in man. Circulation. 1969;39:13–8.

11. Ben-Haim SA, Osadchy D, Schuster I, Gepstein L, Hayam G, Josephson ME. Nonfluoroscopic, in vivo navigation and mapping technology. Nat Med. 1996;2:1393–5.

12. Paul T, Moak JP, Morris C, Garson A Jr. Epicardial mapping: how to measure local activation? Pacing Clin Electrophysiol. 1990;13:285–92.

13. Iwai S, Markowitz SM, Stein KM, Mittal S, Slotwiner DJ, Das MK, et al. Response to adenosine differentiates focal from macroreentrant atrial tachycardia: validation using three-dimensional electroanatomic mapping. Circulation. 2002;106:2793–9.

14. Nademanee K, Kosar EM. A nonfluoroscopic catheter-based mapping technique to ablate focal ventricular tachycardia. Pacing Clin Electrophysiol. 1998;21:1442–7.

15. Shah DC, Jais P, Haissaguerre M, Chouairi S, Takahashi A, Hocini M, et al. Three-dimensional mapping of the common atrial flutter circuit in the right atrium. Circulation. 1997;96:3904–12.

16. Markowitz SM, Brodman RF, Stein KM, Mittal S, Slotwiner DJ, Iwai S, et al. Lesional tachycardias related to mitral valve surgery. J Am Coll Cardiol. 2002;39:1973–83.

17. Cantwell CD, Roney CH, Ng FS, Siggers JH, Sherwin SJ, Peters NS. Techniques for automated local activation time annotation and conduction velocity estimation in cardiac mapping. Comput Biol Med. 2015;65:229–42.

18. Nakagawa H, Ikeda A, Sharma T, Lazzara R, Jackman WM. Rapid high resolution electroanatomical mapping: evaluation of a new system in a canine atrial linear lesion model. Circ Arrhythm Electrophysiol. 2012;5:417–24.

19. Schaeffer B, Hoffmann BA, Meyer C, Akbulak RO, Moser J, Jularic M, et al. Characterization, mapping, and ablation of complex atrial tachycardia: initial experience with a novel method of ultra high-density 3D mapping. J Cardiovasc Electrophysiol. 2016;27:1139–50.

20. El Haddad M, Houben R, Stroobandt R, Van Heuverswyn F, Tavernier R, Duytschaever M. Novel algorithmic methods in mapping of atrial and ventricular tachycardia. Circ Arrhythm Electrophysiol. 2014;7:463–72.

21. Luther V, Sikkel M, Bennett N, Guerrero F, Leong K, Qureshi N, et al. Visualizing localized reentry with ultra-high density mapping in iatrogenic atrial tachycardia: beware pseudo-reentry. Circ Arrhythm Electrophysiol. 2017;10(4). https://doi.org/10.1161/CIRCEP.116.004724

22. Scaglione M, Biasco L, Caponi D, Anselmino M, Negro A, Di Donna P, et al. Visualization of multiple catheters with electroanatomical mapping reduces X-ray exposure during atrial fibrillation ablation. Europace. 2011;13:955–62.

23. Kuck KH, Reddy VY, Schmidt B, Natale A, Neuzil P, Saoudi N, et al. A novel radiofrequency ablation catheter using contact force sensing: Toccata study. Heart Rhythm. 2012;9:18–23.

24. Natale A, Reddy VY, Monir G, Wilber DJ, Lindsay BD, McElderry HT, et al. Paroxysmal AF catheter ablation with a contact force sensing catheter: results of the prospective, multicenter SMART-AF trial. J Am Coll Cardiol. 2014;64:647–56.

25. Dickfeld T, Tian J, Ahmad G, Jimenez A, Turgeman A, Kuk R, et al. MRI-Guided ventricular tachycardia ablation: integration of late gadolinium-enhanced 3D scar in patients with implantable cardioverter-defibrillators. Circ Arrhythm Electrophysiol. 2011;4:172–84.

26. Hutchinson MD, Gerstenfeld EP, Desjardins B, Bala R, Riley MP, Garcia FC, et al. Endocardial unipolar voltage mapping to detect epicardial ventricular tachycardia substrate in patients with nonischemic left ventricular cardiomyopathy. Circ Arrhythm Electrophysiol. 2011;4:49–55.

27. Sosa E, Scanavacca M, d'Avila A, Pilleggi F. A new technique to perform epicardial mapping in the electrophysiology laboratory. J Cardiovasc Electrophysiol. 1996;7:531–6.

28. AbdelWahab A, Stevenson W, Thompson K, Parkash R, Gray C, Gardner M, et al. Intramural ventricular recording and pacing in patients with refractory ventricular tachycardia: initial findings and feasibility with a retractable needle catheter. Circ Arrhythm Electrophysiol. 2015;8:1181–8.

29. Wang L, Gharbia OA, Horacek BM, Sapp JL. Noninvasive epicardial and endocardial electrocardiographic imaging of scar-related ventricular tachycardia. J Electrocardiol. 2016;49:887–93.

30. Takigawa M, Derval N, Frontera A, Martin R, Yamashita S, Cheniti G, et al. Revisiting anatomic macroreentrant tachycardia after atrial fibrillation ablation using ultrahigh-resolution mapping: implications for ablation. Heart Rhythm. 2018;15(3):326–33.

31. Soejima K, Stevenson WG, Delacretaz E, Brunckhorst CB, Maisel WH, Friedman PL. Identification of left atrial origin of ectopic tachycardia during right atrial mapping: analysis of double potentials at the posteromedial right atrium. J Cardiovasc Electrophysiol. 2000;11:975–80.

32. Markowitz SM, Lerman BB. How to interpret electroanatomic maps. Heart Rhythm. 2006;3:240–6.

33. Santangeli P, Dixit S. Role of entrainment in the era of high-density activation mapping for characterizing the reentrant circuit. Heart Rhythm. 2017;14:1550–1.

34. Soejima K, Stevenson WG, Maisel WH, Sapp JL, Epstein LM. Electrically unexcitable scar mapping based on pacing threshold for identification of the reentry circuit isthmus: feasibility for guiding ventricular tachycardia ablation. Circulation. 2002;106:1678–83.

35. Irie T, Yu R, Bradfield JS, Vaseghi M, Buch EF, Ajijola O, et al. Relationship between sinus rhythm late activation zones and critical sites for scar-related ventricular tachycardia: systematic analysis of isochronal late activation mapping. Circ Arrhythm Electrophysiol. 2015;8:390–9.

36. Stevenson WG, Khan H, Sager P, Saxon LA, Middlekauff HR, Natterson PD, et al. Identification of reentry circuit sites during catheter mapping and radiofrequency ablation of ventricular tachycardia late after myocardial infarction. Circulation. 1993;88:1647–70.

37. Delacretaz E, Ganz LI, Soejima K, Friedman PL, Walsh EP, Triedman JK, et al. Multi atrial maco-re-entry circuits in adults with repaired congenital heart disease: entrainment mapping combined with three-dimensional electroanatomic mapping. J Am Coll Cardiol. 2001;37:1665–76.

38. Miyazaki H, Stevenson WG, Stephenson K, Soejima K, Epstein LM. Entrainment mapping for rapid distinction of left and right atrial tachycardias. Heart Rhythm. 2006;3:516–23.

39. Verma A, Jiang CY, Betts TR, Chen J, Deisenhofer I, Mantovan R, et al. Approaches to catheter ablation for persistent atrial fibrillation. N Engl J Med. 2015;372:1812–22.

40. Nademanee K, Lockwood E, Oketani N, Gidney B. Catheter ablation of atrial fibrillation guided by complex fractionated atrial electrogram mapping of atrial fibrillation substrate. J Cardiol. 2010;55:1–12.

41. Calkins H, Hindricks G, Cappato R, Kim YH, Saad EB, Aguinaga L, et al. 2017 HRS/EHRA/ECAS/APHRS/SOLAECE expert consensus statement on catheter and surgical ablation of atrial fibrillation. Heart Rhythm. 2017;14:e275–e444.

42. Tsai WC, Lin YJ, Tsao HM, Chang SL, Lo LW, Hu YF, et al. The optimal automatic algorithm for the mapping of complex fractionated atrial electrograms in patients with atrial fibrillation. J Cardiovasc Electrophysiol. 2010;21:21–6.

43. Bencsik G, Martinek M, Hassanein S, Aichinger J, Nesser HJ, Purerfellner H. Acute effects of complex fractionated atrial electrogram ablation on dominant frequency and regulatory index for the fibrillatory process. Europace. 2009;11:1011–7.

44. Jais P, Maury P, Khairy P, Sacher F, Nault I, Komatsu Y, et al. Elimination of local abnormal ventricular activities: a new end point for substrate modification in patients with scar-related ventricular tachycardia. Circulation. 2012;125:2184–96.

45. Marchlinski FE, Callans DJ, Gottlieb CD, Zado E. Linear ablation lesions for control of unmappable ventricular tachycardia in patients with ischemic and nonischemic cardiomyopathy. Circulation. 2000;101:1288–96.

46. Arenal A, del Castillo S, Gonzalez-Torrecilla E, Atienza F, Ortiz M, Jimenez J, et al. Tachycardia-related channel in the scar tissue in patients with sustained monomorphic ventricular tachycardias: influence of the voltage scar definition. Circulation. 2004;110:2568–74.

47. Tung R, Mathuria NS, Nagel R, Mandapati R, Buch EF, Bradfield JS, et al. Impact of local ablation on interconnected channels within ventricular scar: mechanistic implications for substrate modification. Circ Arrhythm Electrophysiol. 2013;6:1131–8.

48. Berruezo A, Fernandez-Armenta J, Andreu D, Penela D, Herczku C, Evertz R, et al. Scar dechanneling: new method for scar-related left ventricular tachycardia substrate ablation. Circ Arrhythm Electrophysiol. 2015;8:326–36.

49. Tzou WS, Frankel DS, Hegeman T, Supple GE, Garcia FC, Santangeli P, et al. Core isolation of critical arrhythmia elements for treatment of multiple scar-based ventricular tachycardias. Circ Arrhythm Electrophysiol. 2015;8:353–61.

50. de Chillou C, Groben L, Magnin-Poull I, Andronache M, MagdiAbbas M, Zhang N, et al. Localizing the critical isthmus of postinfarct ventricular tachycardia: the value of pace-mapping during sinus rhythm. Heart Rhythm. 2014;11:175–81.

51. Luther V, Linton NWF, Jamil-Copley S, Koa-Wing M, Lim PB, Qureshi N, et al. A prospective study of ripple mapping the post-infarct ventricular scar to guide substrate ablation for ventricular tachycardia. Circ Arrhythm Electrophysiol. 2016;9(6). https://doi.org/10.1161/CIRCEP.116.004072

52. Jamil-Copley S, Vergara P, Carbucicchio C, Linton N, Koa-Wing M, Luther V, et al. Application of ripple mapping to visualize slow conduction channels within the infarct-related left ventricular scar. Circ Arrhythm Electrophysiol. 2015;8:76–86.

53. Moak JP, Sumihara K, Swink J, Hanumanthaiah S, Berul CI. Ablation of the vanishing PVC, facilitated by quantitative morphology-matching software. Pacing Clin Electrophysiol. 2017;40:1227–33.

54. Sapp JL, Gardner MJ, Parkash R, Basta M, Warren JW, Horacek BM. Body-surface potential mapping to aid ablation of scar-related ventricular tachycardia. J Electrocardiol. 2006;39:S87–95.

55. Bhakta D, Miller JM. Principles of electroanatomic mapping. Indian Pacing Electrophysiol J. 2008;8:32–50.

56. Gepstein L, Hayam G, Ben-Haim SA. A novel method for non-fluoroscopic catheter-based electroanatomical mapping of the heart. In vitro and in vivo accuracy results. Circulation. 1997;95:1611–22.

57. Jiang Y, Farina D, Bar-Tal M, Dossel O. An impedance-based catheter positioning system for cardiac mapping and navigation. IEEE Trans Biomed Eng. 2009;56:1963–70.

58. Koutalas E, Rolf S, Dinov B, Richter S, Arya A, Bollmann A, et al. Contemporary mapping techniques of complex cardiac arrhythmias—identifying and modifying the arrhythmogenic substrate. Arrhythm Electrophysiol Rev. 2015;4:19–27.

59. Wittkampf FHM, Wever EFD, Derksen R, Wilde AAM, Ramanna H, Hauer RNW, et al. LocaLisa: new technique for real-time 3-dimensional localization of regular intracardiac electrodes. Circulation. 1999;99:1312–7.

60. Eitel C, Hindricks G, Dagres N, Sommer P, Piorkowski C. EnSite Velocity cardiac mapping system: a new platform for 3D mapping of cardiac arrhythmias. Expert Rev Med Devices. 2010;7:185–92.

61. Anter E, Tschabrunn CM, Contreras-Valdes FM, Li J, Josephson ME. Pulmonary vein isolation using the Rhythmia mapping system: verification of intracardiac signals using the Orion mini-basket catheter. Heart Rhythm. 2015;12:1927–34.

62. Anter E, McElderry TH, Contreras-Valdes FM, Li J, Tung P, Leshem E, et al. Evaluation of a novel high-resolution mapping technology for ablation of recurrent scar-related atrial tachycardias. Heart Rhythm. 2016;13:2048–55.

63. Ptaszek LM, Chalhoub F, Perna F, Beinart R, Barrett CD, Danik SB, et al. Rapid acquisition of high-resolution electroanatomical maps using a novel multielectrode mapping system. Journal of Interventional Cardiac Electrophysiology. 2013;36:233–42.

64. Del Carpio MF, Buescher T, Asirvatham SJ. Teaching points with 3-dimensional mapping of cardiac arrhythmias: taking points: activation mapping. Circ Arrhythm Electrophysiol. 2011;4:e22–e25.

65. Haissaguerre M, Shah AJ, Cochet H, Hocini M, Dubois R, Efimov I, et al. Intermittent drivers anchoring to structural heterogeneities as a major pathophysiological mechanism of human persistent atrial fibrillation. J Physiol. 2016;594:2387–98.

66. Cuculich PS, Schill MR, Kashani R, Mutic S, Lang A, Cooper D, et al. Noninvasive cardiac radiation for ablation of ventricular tachycardia. N Engl J Med. 2017;377:2325–36.

67. Callans DJ, Ren JF, Michele J, Marchlinski FE, Dillon SM. Electroanatomic left ventricular mapping in the porcine model of healed anterior myocardial infarction. Correlation with intracardiac echocardiography and pathological analysis. Circulation. 1999;100:1744–50.

68. Patel AM, d'Avila A, Neuzil P, Kim SJ, Mela T, Singh JP, et al. Atrial tachycardia after ablation of persistent atrial fibrillation:

identification of the critical isthmus with a combination of multielectrode activation mapping and targeted entrainment mapping. Circ Arrhythm Electrophysiol. 2008;1:14–22.

69. Tung R, Nakahara S, Ramirez R, Gui D, Magyar C, Lai C, et al. Accuracy of combined endocardial and epicardial electroanatomic mapping of a reperfused porcine infarct model: a comparison of electrofield and magnetic systems with histopathologic correlation. Heart Rhythm. 2011;8:439–47.

70. Narayan SM, Krummen DE, Shivkumar K, Clopton P, Rappel WJ, Miller JM. Treatment of atrial fibrillation by the ablation of localized sources: CONFIRM (Conventional Ablation for Atrial Fibrillation With or Without Focal Impulse and Rotor Modulation) trial. J Am Coll Cardiol. 2012;60:628–36.

71. Anter E, Josephson ME. Substrate mapping for ventricular tachycardia. JACC Clin Electrophysiol. 2015;1:341–52.

72. Tschabrunn CM, Roujol S, Dorman NC, Nezafat R, Josephson ME, Anter E. High-resolution mapping of ventricular scar. Circ Arrhythm Electrophysiol. 2016;9(6): https://doi.org/10.1161/CIRCEP.115.003841

73. Berte B, Relan J, Sacher F, Pillois X, Appetiti A, Yamashita S, et al. Impact of electrode type on mapping of scar-related VT. J Cardiovasc Electrophysiol. 2015;26(11):1213–23.

74. Tung R, Kim S, Yagishita D, Vaseghi M, Ennis DB, Ouadah S, et al. Scar voltage threshold determination using ex vivo magnetic resonance imaging integration in a porcine infarct model: influence of interelectrode distances and three-dimensional spatial effects of scar. Heart Rhythm. 2016;13:1993–2002.

75. Liang JJ, Elafros MA, Muser D, Pathak RK, Santangeli P, Supple GE, et al. Comparison of left atrial bipolar voltage and scar using multielectrode fast automated mapping versus point-by-point contact electroanatomic mapping in patients with atrial fibrillation undergoing repeat ablation. J Cardiovasc Electrophysiol. 2017;28:280–8.

76. Page RL, Joglar JA, Caldwell MA, Calkins H, Conti JB, Deal BJ, et al. 2015 ACC/AHA/HRS guideline for the management of adult patients with supraventricular tachycardia: a report of the American College of Cardiology/American Heart Association Task Force on Clinical Practice Guidelines and the Heart Rhythm Society. Circulation. 2016;133:e506–e574.

77. Kuck KH, Böcker D, Chun J, Deneke T, Hindricks G, Hoffmann E, et al. Qualitätskriterien zur Durchführung der Katheterablation von Vorhofflimmern. Der Kardiologe. 2017;11:161–82.

78. Ma Y, Qiu J, Yang Y, Tang A. Catheter ablation of right-sided accessory pathways in adults using the three-dimensional mapping system: a randomized comparison to the conventional approach. PLoS ONE. 2015;10:e0128760.

79. Sporton SC, Earley MJ, Nathan AW, Schilling RJ. Electroanatomic versus fluoroscopic mapping for catheter ablation procedures: a prospective randomized study. J Cardiovasc Electrophysiol. 2004;15:310–5.

80. Kesek M, Wallenius N, Ronn F, Hoglund N, Jensen S. Reduction of fluoroscopy duration in radiofrequency ablation obtained by the use of a non-fluoroscopic catheter navigation system. Europace. 2006;8:1027–30.

81. Earley MJ, Showkathali R, Alzetani M, Kistler PM, Gupta D, Abrams DJ, et al. Radiofrequency ablation of arrhythmias guided by non-fluoroscopic catheter location: a prospective randomized trial. Eur Heart J. 2006;27:1223–9.

82. Einstein AJ. Medical imaging: the radiation issue. Nat Rev Cardiol. 2009;6:436.

83. Perisinakis K, Damilakis J, Theocharopoulos N, Manios E, Vardas P, Gourtsoyiannis N. Accurate assessment of patient effective radiation dose and associated detriment risk from radiofrequency catheter ablation procedures. Circulation. 2001;104:58–62.

84. Kozluk E, Piatkowska A, Kiliszek M, Lodzinski P, Malkowska S, Balsam P, et al. Catheter ablation of cardiac arrhythmias in

pregnancy without fluoroscopy: a case control retrospective study. Adv Clin Exp Med. 2017;26:129–34.

85. Khoury DS, Taccardi B, Lux RL, Ershler PR, Rudy Y. Reconstruction of endocardial potentials and activation sequences from intracavitary probe measurements. Localization of pacing sites and effects of myocardial structure. Circulation. 1995;91:845–63.

86. Dalal AS, Nguyen HH, Bowman T, Van Hare GF, Avari Silva JN. Force-sensing catheters during pediatric radiofrequency ablation: the FEDERATION study. J Am Heart Assoc. 2017;6(5). https://doi.org/10.1161/JAHA.117.005772

87. Gulletta S, Tsiachris D, Della BP. Catheter ablation of an anteroseptal accessory pathway guided by contact force monitoring technology and precise electroanatomical mapping. Europace. 2014;16:825.

88. Ueda A, Suman-Horduna I, Mantziari L, Gujic M, Marchese P, Ho SY, et al. Contemporary outcomes of supraventricular tachycardia ablation in congenital heart disease: a single-center experience in 116 patients. Circ Arrhythm Electrophysiol. 2013;6:606–13.

89. Smith G, Clark JM. Elimination of fluoroscopy use in a pediatric electrophysiology laboratory utilizing three-dimensional mapping. Pacing Clin Electrophysiol. 2007;30:510–8.

90. Tuzcu V. A nonfluoroscopic approach for electrophysiology and catheter ablation procedures using a three-dimensional navigation system. Pacing Clin Electrophysiol. 2007;30:519–25.

91. Nagaraju L, Menon D, Aziz PF. Use of 3D electroanatomical navigation (CARTO-3) to minimize or eliminate fluoroscopy use in the ablation of pediatric supraventricular tachyarrhythmias. Pacing Clin Electrophysiol. 2016;39:574–80.

92. Casella M, Pelargonio G, Dello Russo A, Riva S, Bartoletti S, Santangeli P, et al. "Near-zero" fluoroscopic exposure in supraventricular arrhythmia ablation using the EnSite NavX mapping system: personal experience and review of the literature. J Interv Card Electrophysiol. 2011;31:109–18.

93. Álvarez M, Tercedor L, Almansa I, Ros N, Galdeano RS, Burillo F, et al. Safety and feasibility of catheter ablation for atrioventricular nodal re-entrant tachycardia without fluoroscopic guidance. Heart Rhythm. 2009;6:1714–20.

94. Fernández-Gómez JM, Moriña-Vázquez P, Morales EDR, Venegas-Gamero J, Barba-Pichardo R, Carranza MH. Exclusion of fluoroscopy use in catheter ablation procedures: six years of experience at a single center. J Cardiovasc Electrophysiol. 2014;25:638–44.

95. Giaccardi M, Del Rosso A, Guarnaccia V, Ballo P, Mascia G, Chiodi L, et al. Near-zero x-ray in arrhythmia ablation using a 3-dimensional electroanatomic mapping system: a multicenter experience. Heart Rhythm. 2016;13:150–6.

96. Papagiannis J, Tsoutsinos A, Kirvassilis G, Sofianidou I, Koussi T, Laskari C, et al. Nonfluoroscopic catheter navigation for radiofrequency catheter ablation of supraventricular tachycardia in children. Pacing Clin Electrophysiol. 2006;29:971–8.

97. Drago F, Silvetti MS, Di Pino A, Grutter G, Bevilacqua M, Leibovich S. Exclusion of fluoroscopy during ablation treatment of right accessory pathway in children. J Cardiovasc Electrophysiol. 2002;13:778–82.

98. Avila P, Oliver JM, Gallego P, Gonzalez-Garcia A, Rodriguez-Puras MJ, Cambronero E, et al. Natural history and clinical predictors of atrial tachycardia in adults with congenital heart disease. Circ Arrhythm Electrophysiol. 2017;10.

99. Labombarda F, Hamilton R, Shohoudi A, Aboulhosn J, Broberg CS, Chaix MA, et al. Increasing prevalence of atrial fibrillation and permanent atrial arrhythmias in congenital heart disease. J Am Coll Cardiol. 2017;70:857–65.

100. Khairy P, Van Hare GF, Balaji S, Berul CI, Cecchin F, Cohen MI, et al. Expert consensus statement on the recognition and management of arrhythmias in adult congenital heart disease: developed in partnership between the Pediatric and Congenital Electrophysiology Society (PACES) and the Heart Rhythm Society (HRS). Endorsed

by the governing bodies of PACES, HRS, the American College of Cardiology (ACC), the American Heart Association (AHA), the European Heart Rhythm Association (EHRA), the Canadian Heart Rhythm Society (CHRS), and the International Society for Adult Congenital Heart Disease (ISACHD). Heart Rhythm. 2014;11:e102–e165.

101. Wasmer K, Eckardt L. Management of supraventricular arrhythmias in adults with congenital heart disease. Heart. 2016;102:1614–9.

102. Triedman JK. Arrhythmias in adults with congenital heart disease. Heart. 2002;87:383–9.

103. Sherwin ED, Triedman JK, Walsh EP. Update on interventional electrophysiology in congenital heart disease: evolving solutions for complex hearts. Circ Arrhythm Electrophysiol. 2013;6:1032–40.

104. Walsh EP. Interventional electrophysiology in patients with congenital heart disease. Circulation. 2007;115:3224–34.

105. Ernst S, Yen Ho S, McCarthy K. Arrhythmia in adults with congenital heart defects: atrial tachycardia. Herzschrittmacherther Elektrophysiol. 2016;27:122–30.

106. Masuda K, Ishizu T, Niwa K, Takechi F, Tateno S, Horigome H, et al. Increased risk of thromboembolic events in adult congenital heart disease patients with atrial tachyarrhythmias. Int J Cardiol. 2017;234:69–75.

107. Teuwen CP, Ramdjan TT, Gotte M, Brundel BJ, Evertz R, Vriend JW, et al. Time course of atrial fibrillation in patients with congenital heart defects. Circ Arrhythm Electrophysiol. 2015;8:1065–72.

108. Mantziari L, Babu-Narayan SV, Suman-Horduna I, Rigby ML, Ernst S. Atrial arrhythmia after Fontan surgery leads to giant thrombus: opening Pandora's box. Int J Cardiol. 2013;166:e23–e24.

109. Triedman JK, Alexander ME, Berul CI, Bevilacqua LM, Walsh EP. Electroanatomic mapping of entrained and exit zones in patients with repaired congenital heart disease and intra-atrial reentrant tachycardia. Circulation. 2001;103:2060–5.

110. Yap SC, Harris L, Silversides CK, Downar E, Chauhan VS. Outcome of intra-atrial re-entrant tachycardia catheter ablation in adults with congenital heart disease: negative impact of age and complex atrial surgery. J Am Coll Cardiol. 2010;56:1589–96.

111. Laţcu DG, Bun S-S, Viera F, Delassi T, El Jamili M, Al Amoura A, et al. Selection of critical isthmus in scar-related atrial tachycardia using a new automated ultrahigh resolution mapping system. Circ Arrhythm Electrophysiol. 2017;10(1). https://doi.org/10.1161/CIRCEP.116.004510

112. Ernst S, Saenen J, Rydman R, Gomez F, Roy K, Mantziari L, et al. Utility of noninvasive arrhythmia mapping in patients with adult congenital heart disease. Card Electrophysiol Clin. 2015;7:117–23.

113. Reddy VY, Malchano ZJ, Holmvang G, Schmidt EJ, d'Avila A, Houghtaling C, et al. Integration of cardiac magnetic resonance imaging with three-dimensional electroanatomic mapping to guide left ventricular catheter manipulation: feasibility in a porcine model of healed myocardial infarction. J Am Coll Cardiol. 2004;44:2202–13.

114. Brooks AG, Wilson L, Kuklik P, Stiles MK, John B, Shashidhar, et al. Image integration using NavX Fusion: initial experience and validation. Heart Rhythm. 2008;5:526–35.

115. Ernst S, Babu-Narayan SV, Keegan J, Horduna I, Lyne J, Till J, et al. Remote-controlled magnetic navigation and ablation with 3D image integration as an alternative approach in patients with intra-atrial baffle anatomy. Circ Arrhythm Electrophysiol. 2012;5:131–9.

116. Kean AC, Gelehrter SK, Shetty I, Dick M 2nd, Bradley DJ. Experience with CartoSound for arrhythmia ablation in pediatric and congenital heart disease patients. J Interv Card Electrophysiol. 2010;29:139–45.

117. Wu J, Pflaumer A, Deisenhofer I, Hoppmann P, Hess J, Hessling G. Mapping of atrial tachycardia by remote magnetic navigation in postoperative patients with congenital heart disease. J Cardiovasc Electrophysiol. 2010;21:751–9.

118. Akca F, Bauernfeind T, Witsenburg M, Dabiri Abkenari L, Cuypers JA, Roos-Hesselink JW, et al. Acute and long-term outcomes of catheter ablation using remote magnetic navigation in patients with congenital heart disease. Am J Cardiol. 2012;110:409–14.

119. Refaat MM, Ballout J, Mansour M. Ablation of atrial fibrillation in patients with congenital heart disease. Arrhythm Electrophysiol Rev. 2017;6:191–4.

120. Nie JG, Dong JZ, Salim M, Li SN, Wu XY, Chen YW, et al. Catheter ablation of atrial fibrillation in patients with atrial septal defect: long-term follow-up results. J Interv Card Electrophysiol. 2015;42:43–9.

121. Acena M, Anguera I, Dallaglio PD, Rodriguez M, Sabate X. Atrial fibrillation ablation in adults with repaired congenital heart disease. J Atr Fibrillation. 2016;8:1363.

122. Zeppenfeld K, Schalij MJ, Bartelings MM, Tedrow UB, Koplan BA, Soejima K, et al. Catheter ablation of ventricular tachycardia after repair of congenital heart disease: electroanatomic identification of the critical right ventricular isthmus. Circulation. 2007;116:2241–52.

123. Haissaguerre M, Jais P, Shah DC, Takahashi A, Hocini M, Quiniou G, et al. Spontaneous initiation of atrial fibrillation by ectopic beats originating in the pulmonary veins. N Engl J Med. 1998;339:659–66.

124. Chen SA, Hsieh MH, Tai CT, Tsai CF, Prakash VS, Yu WC, et al. Initiation of atrial fibrillation by ectopic beats originating from the pulmonary veins: electrophysiological characteristics, pharmacological responses, and effects of radiofrequency ablation. Circulation. 1999;100:1879–86.

125. Calkins H, Hindricks G, Cappato R, Kim YH, Saad EB, Aguinaga L, et al. 2017 HRS/EHRA/ECAS/APHRS/SOLAECE expert consensus statement on catheter and surgical ablation of atrial fibrillation: Executive summary. Europace. 2018;20:157–208.

126. Hassink RJ, Aretz HT, Ruskin J, Keane D. Morphology of atrial myocardium in human pulmonary veins: a postmortem analysis in patients with and without atrial fibrillation. J Am Coll Cardiol. 2003;42:1108–14.

127. Khan R. Identifying and understanding the role of pulmonary vein activity in atrial fibrillation. Cardiovasc Res. 2004;64:387–94.

128. Tagawa M, Higuchi K, Chinushi M, Washizuka T, Ushiki T, Ishihara N, et al. Myocardium extending from the left atrium onto the pulmonary veins: a comparison between subjects with and without atrial fibrillation. Pacing Clin Electrophysiol. 2001;24:1459–63.

129. Pappone C, Oreto G, Lamberti F, Vicedomini G, Loricchio ML, Shpun S, et al. Catheter ablation of paroxysmal atrial fibrillation using a 3D mapping system. Circulation. 1999;100:1203–8.

130. Pappone C, Rosanio S, Oreto G, Tocchi M, Gugliotta F, Vicedomini G, et al. Circumferential radiofrequency ablation of pulmonary vein ostia: A new anatomic approach for curing atrial fibrillation. Circulation. 2000;102:2619–28.

131. Tamborero D, Mont L, Nava S, de Caralt TM, Molina I, Scalise A, et al. Incidence of pulmonary vein stenosis in patients submitted to atrial fibrillation ablation: a comparison of the selective segmental ostial ablation vs the circumferential pulmonary veins ablation. J Interv Card Electrophysiol. 2005;14:21–5.

132. Masuda M, Fujita M, Iida O, Okamoto S, Ishihara T, Nanto K, et al. The identification of conduction gaps after pulmonary vein isolation using a new electroanatomic mapping system. Heart Rhythm. 2017;14:1606–14.

133. Lin CY, Te ALD, Lin YJ, Chang SL, Lo LW, Hu YF, et al. High-resolution mapping of pulmonary vein potentials improved the successful pulmonary vein isolation using small electrodes and inter-electrode spacing catheter. Int J Cardiol. 2018;272:90–6.

134. Hori Y, Nakahara S, Fukuda R, Taguchi I. Utility of the ultra-high-resolution 3-dimensional mapping catheter for isolated pulmonary vein reentrant tachycardia. Heart Rhythm. 2018;15:308–9.

135. Kistler PM, Rajappan K, Jahngir M, Earley MJ, Harris S, Abrams D, et al. The impact of CT image integration into an electroanatomic mapping system on clinical outcomes of catheter ablation of atrial fibrillation. J Cardiovasc Electrophysiol. 2006;17:1093–101.

136. Kimura M, Sasaki S, Owada S, Horiuchi D, Sasaki K, Itoh T, et al. Validation of accuracy of three-dimensional left atrial CartoSound and CT image integration: influence of respiratory phase and cardiac cycle. J Cardiovasc Electrophysiol. 2013;24:1002–7.

137. Ikeda A, Nakagawa H, Lambert H, Shah DC, Fonck E, Yulzari A, et al. Relationship between catheter contact force and radiofrequency lesion size and incidence of steam pop in the beating canine heart: electrogram amplitude, impedance, and electrode temperature are poor predictors of electrode-tissue contact force and lesion size. Circ Arrhythm Electrophysiol. 2014;7:1174–80.

138. Shurrab M, Di Biase L, Briceno DF, Kaoutskaia A, Haj-Yahia S, Newman D, et al. Impact of contact force technology on atrial fibrillation ablation: a meta-analysis. J Am Heart Assoc. 2015;4:e002476.

139. Neuzil P, Reddy VY, Kautzner J, Petru J, Wichterle D, Shah D, et al. Electrical reconnection after pulmonary vein isolation is contingent on contact force during initial treatment: results from the EFFICAS I study. Circ Arrhythm Electrophysiol. 2013;6:327–33.

140. Kautzner J, Neuzil P, Lambert H, Peichl P, Petru J, Cihak R, et al. EFFICAS II: optimization of catheter contact force improves outcome of pulmonary vein isolation for paroxysmal atrial fibrillation. Europace. 2015;17:1229–35.

141. Reddy VY, Dukkipati SR, Neuzil P, Natale A, Albenque JP, Kautzner J, et al. Randomized, controlled trial of the safety and effectiveness of a contact force-sensing irrigated catheter for ablation of paroxysmal atrial fibrillation: results of the tacticath contact force ablation catheter study for atrial fibrillation (TOCCASTAR) study. Circulation. 2015;132:907–15.

142. Zucchelli G, Sirico G, Rebellato L, Marini M, Stabile G, Del Greco M, et al. Contiguity between ablation lesions and strict catheter stability settings assessed by VISITAG(TM) module improve clinical outcomes of paroxysmal atrial fibrillation ablation—results from the VISITALY study. Circ J. 2018;82:974–82.

143. Tanaka N, Inoue K, Tanaka K, Toyoshima Y, Oka T, Okada M, et al. Automated ablation annotation algorithm reduces re-conduction of isolated pulmonary vein and improves outcome after catheter ablation for atrial fibrillation. Circ J. 2017;81:1596–602.

144. Brooks AG, Stiles MK, Laborderie J, Lau DH, Kuklik P, Shipp NJ, et al. Outcomes of long-standing persistent atrial fibrillation ablation: a systematic review. Heart Rhythm. 2010;7:835–46.

145. Parkash R, Verma A, Tang AS. Persistent atrial fibrillation: current approach and controversies. Curr Opin Cardiol. 2010;25:1–7.

146. Lin YJ, Lo MT, Chang SL, Lo LW, Hu YF, Chao TF, et al. Benefits of atrial substrate modification guided by electrogram similarity and phase mapping techniques to eliminate rotors and focal sources versus conventional defragmentation in persistent atrial fibrillation. JACC Clin Electrophysiol. 2016;2:667–78.

147. Willems S, Klemm H, Rostock T, Brandstrup B, Ventura R, Steven D, et al. Substrate modification combined with pulmonary vein isolation improves outcome of catheter ablation in patients with persistent atrial fibrillation: a prospective randomized comparison. Eur Heart J. 2006;27:2871–8.

148. January CT, Wann LS, Alpert JS, Calkins H, Cigarroa JE, Cleveland JC Jr, et al. 2014 AHA/ACC/HRS guideline for the management of patients with atrial fibrillation: executive summary: a report of the American College of Cardiology/American Heart Association Task Force on practice guidelines and the Heart Rhythm Society. Circulation. 2014;130:2071–104.

149. Narayan SM, Wright M, Derval N, Jadidi A, Forclaz A, Nault I, et al. Classifying fractionated electrograms in human atrial fibrillation using monophasic action potentials and activation mapping: evidence for localized drivers, rate acceleration, and nonlocal signal etiologies. Heart Rhythm. 2011;8:244–53.

150. Narayan SM, Baykaner T, Clopton P, Schricker A, Lalani GG, Krummen DE, et al. Ablation of rotor and focal sources reduces late recurrence of atrial fibrillation compared with trigger ablation alone: extended follow-up of the CONFIRM trial (Conventional Ablation for Atrial Fibrillation With or Without Focal Impulse and Rotor Modulation). J Am Coll Cardiol. 2014;63:1761–8.

151. Marrouche NF, Wilber D, Hindricks G, Jais P, Akoum N, Marchlinski F, et al. Association of atrial tissue fibrosis identified by delayed enhancement MRI and atrial fibrillation catheter ablation: the DECAAF study. JAMA. 2014;311:498–506.

152. Wang XH, Li Z, Mao JL, He B. A novel individualized substrate modification approach for the treatment of long-standing persistent atrial fibrillation: preliminary results. Int J Cardiol. 2014;175:162–8.

153. Miyazaki S, Taniguchi H, Komatsu Y, Uchiyama T, Kusa S, Nakamura H, et al. Sequential biatrial linear defragmentation approach for persistent atrial fibrillation. Heart Rhythm. 2013;10:338–46.

154. Miyazaki S, Taniguchi H, Kusa S, Uchiyama T, Nakamura H, Hachiya H, et al. Impact of atrial fibrillation termination site and termination mode in catheter ablation on arrhythmia recurrence. Circ J. 2014;78:78–84.

155. Pak HN, Oh YS, Lim HE, Kim YH, Hwang C. Comparison of voltage map-guided left atrial anterior wall ablation versus left lateral mitral isthmus ablation in patients with persistent atrial fibrillation. Heart Rhythm. 2011;8:199–206.

156. Hu X, Jiang J, Ma Y, Tang A. Is there still a role for additional linear ablation in addition to pulmonary vein isolation in patients with paroxysmal atrial fibrillation? An updated meta-analysis of randomized controlled trials. Int J Cardiol. 2016;209:266–74.

157. Chae S, Oral H, Good E, Dey S, Wimmer A, Crawford T, et al. Atrial tachycardia after circumferential pulmonary vein ablation of atrial fibrillation: mechanistic insights, results of catheter ablation, and risk factors for recurrence. J Am Coll Cardiol. 2007;50:1781–7.

158. Lo LW, Lin YJ, Chang SL, Hu YF, Chao TF, Chung FP, et al. Predictors and characteristics of multiple (more than 2) catheter ablation procedures for atrial fibrillation. J Cardiovasc Electrophysiol. 2015;26:1048–56.

159. Fink T, Schlüter M, Heeger C-H, Lemes C, Maurer T, Reissmann B, et al. Stand-alone pulmonary vein isolation versus pulmonary vein isolation with additional substrate modification as index ablation procedures in patients with persistent and long-standing persistent atrial fibrillation. Circ Arrhythm Electrophysiol. 2017;10(7). https://doi.org/10.1161/CIRCEP.117.005114

160. Lin WS, Tai CT, Hsieh MH, Tsai CF, Lin YK, Tsao HM, et al. Catheter ablation of paroxysmal atrial fibrillation initiated by non-pulmonary vein ectopy. Circulation. 2003;107:3176–83.

161. Higa S, Tai CT, Chen SA. Catheter ablation of atrial fibrillation originating from extrapulmonary vein areas: Taipei approach. Heart Rhythm. 2006;3:1386–90.

162. Chen SA, Tai CT, Yu WC, Chen YJ, Tsai CF, Hsieh MH, et al. Right atrial focal atrial fibrillation: electrophysiologic characteristics and radiofrequency catheter ablation. J Cardiovasc Electrophysiol. 1999;10:328–35.

163. Tai CT, Hsieh MH, Tsai CF, Lin YK, Yu WC, Lee SH, et al. Differentiating the ligament of Marshall from the pulmonary vein musculature potentials in patients with paroxysmal atrial fibrillation: electrophysiological characteristics and results of radiofrequency ablation. Pacing Clin Electrophysiol. 2000;23:1493–501.

164. Js A, Hocini M, Pascale P, Roten L, Komatsu Y, Daly M, et al. Surface electrocardiographic mapping for non-invasive identification of arrhythmic sources. Arrhythm Electrophysiol Rev. 2013;2:16–22.

165. Lim HS, Hocini M, Dubois R, Denis A, Derval N, Zellerhoff S, et al. Complexity and distribution of drivers in relation to duration of persistent atrial fibrillation. J Am Coll Cardiol. 2017;69:1257–69.

166. Matsunaga-Lee Y, Takano Y. A novel mapping technique to detect non-pulmonary vein triggers: a case report of self-reference mapping technique. HeartRhythm Case Rep. 2018;4:26–8.

167. Haissaguerre M, Hocini M, Denis A, Shah AJ, Komatsu Y, Yamashita S, et al. Driver domains in persistent atrial fibrillation. Circulation. 2014;130:530–8.

168. Atienza F, Almendral J, Ormaetxe JM, Moya A, Martinez-Alday JD, Hernandez-Madrid A, et al. Comparison of radiofrequency catheter ablation of drivers and circumferential pulmonary vein isolation in atrial fibrillation: a noninferiority randomized multicenter RADAR-AF trial. J Am Coll Cardiol. 2014;64:2455–67.

169. Jadidi AS, Lehrmann H, Keyl C, Sorrel J, Markstein V, Minners J, et al. Ablation of persistent atrial fibrillation targeting low-voltage areas with selective activation characteristics. Circ Arrhythm Electrophysiol. 2016;9.

170. Seitz J, Bars C, Theodore G, Beurtheret S, Lellouche N, Bremondy M, et al. AF ablation guided by spatiotemporal electrogram dispersion without pulmonary vein isolation: a wholly patient-tailored approach. J Am Coll Cardiol. 2017;69:303–21.

171. Ramirez FD, Birnie DH, Nair GM, Szczotka A, Redpath CJ, Sadek MM, et al. Efficacy and safety of driver-guided catheter ablation for atrial fibrillation: a systematic review and meta-analysis. J Cardiovasc Electrophysiol. 2017;28:1371–8.

172. Chrispin J, Ipek EG, Habibi M, Yang E, Spragg D, Marine JE, et al. Clinical predictors of cardiac magnetic resonance late gadolinium enhancement in patients with atrial fibrillation. Europace. 2017;19:371–7.

173. Dewire J, Khurram IM, Pashakhanloo F, Spragg D, Marine JE, Berger RD, et al. The association of pre-existing left atrial fibrosis with clinical variables in patients referred for catheter ablation of atrial fibrillation. Clin Med Insights Cardiol. 2014;8:25–30.

174. Khurram IM, Habibi M, Gucuk Ipek E, Chrispin J, Yang E, Fukumoto K, et al. Left atrial LGE and arrhythmia recurrence following pulmonary vein isolation for paroxysmal and persistent AF. JACC Cardiovasc Imaging. 2016;9:142–8.

175. Karim R, Housden RJ, Balasubramaniam M, Chen Z, Perry D, Uddin A, et al. Evaluation of current algorithms for segmentation of scar tissue from late gadolinium enhancement cardiovascular magnetic resonance of the left atrium: an open-access grand challenge. J Cardiovasc Magn Reson. 2013;15:105.

176. Reddy VY, Wrobleski D, Houghtaling C, Josephson ME, Ruskin JN. Combined epicardial and endocardial electroanatomic mapping in a porcine model of healed myocardial infarction. Circulation. 2003;107:3236–42.

177. Casella M, Perna F, Dello Russo A, Pelargonio G, Bartoletti S, Ricco A, et al. Right ventricular substrate mapping using the Ensite Navx system: accuracy of high-density voltage map obtained by automatic point acquisition during geometry reconstruction. Heart Rhythm. 2009;6:1598–605.

178. Tanaka Y, Genet M, Chuan Lee L, Martin AJ, Sievers R, Gerstenfeld EP. Utility of high-resolution electroanatomic mapping of the left ventricle using a multispline basket catheter in a swine model of chronic myocardial infarction. Heart Rhythm. 2015;12:144–54.

179. Tschabrunn CM, Roujol S, Nezafat R, Faulkner-Jones B, Buxton AE, Josephson ME, et al. A swine model of infarct-related reentrant ventricular tachycardia: electroanatomic, magnetic resonance, and histopathological characterization. Heart Rhythm. 2016;13:262–73.

180. Guiraudon G, Fontaine G, Frank R, Escande G, Etievent P, Cabrol C. Encircling endocardial ventriculotomy: a new surgical treatment for life-threatening ventricular tachycardias resistant to medical treatment following myocardial infarction. Ann Thorac Surg. 1978;26:438–44.

181. Hsia HH, Lin D, Sauer WH, Callans DJ, Marchlinski FE. Anatomic characterization of endocardial substrate for hemodynamically stable reentrant ventricular tachycardia: identification of endocardial conducting channels. Heart Rhythm. 2006;3:503–12.

182. Reddy VY, Reynolds MR, Neuzil P, Richardson AW, Taborsky M, Jongnarangsin K, et al. Prophylactic catheter ablation for the prevention of defibrillator therapy. N Engl J Med. 2007;357:2657–65.

183. Tanner H, Hindricks G, Volkmer M, Furniss S, Kühlkamp V, Lacroix D, et al. Catheter ablation of recurrent scar-related ventricular tachycardia using electroanatomical mapping and irrigated ablation technology: results of the prospective multicenter Euro-VT-study. J Cardiovasc Electrophysiol. 2010;21:47–53.

184. Di Biase L, Burkhardt JD, Lakkireddy D, Carbucicchio C, Mohanty S, Mohanty P, et al. Ablation of stable VTs versus substrate ablation in ischemic cardiomyopathy: the VISTA randomized multicenter trial. J Am Coll Cardiol. 2015;66:2872–82.

185. Di Biase L, Santangeli P, Burkhardt DJ, Bai R, Mohanty P, Carbucicchio C, et al. Endo-epicardial homogenization of the scar versus limited substrate ablation for the treatment of electrical storms in patients with ischemic cardiomyopathy. J Am Coll Cardiol. 2012;60:132–41.

186. Gokoglan Y, Mohanty S, Gianni C, Santangeli P, Trivedi C, Gunes MF, et al. Scar homogenization versus limited-substrate ablation in patients with nonischemic cardiomyopathy and ventricular tachycardia. J Am Coll Cardiol. 2016;68:1990–8.

187. Tung R, Josephson ME, Bradfield JS, Shivkumar K. Directional influences of ventricular activation on myocardial scar characterization: voltage mapping with multiple wavefronts during ventricular tachycardia ablation. Circ Arrhythm Electrophysiol. 2016;9(8): https://doi.org/10.1161/CIRCEP.116.004155

188. Sosa E, Scanavacca M, d'Avila A, Oliveira F, Ramires JA. Nonsurgical transthoracic epicardial catheter ablation to treat recurrent ventricular tachycardia occurring late after myocardial infarction. J Am Coll Cardiol. 2000;35:1442–9.

189. Sosa E, Scanavacca M, D'Avila A, Piccioni J, Sanchez O, Velarde JL, et al. Endocardial and epicardial ablation guided by nonsurgical transthoracic epicardial mapping to treat recurrent ventricular tachycardia. J Cardiovasc Electrophysiol. 1998;9:229–39.

190. Tung R, Nakahara S, Ramirez R, Lai C, Fishbein MC, Shivkumar K. Distinguishing epicardial fat from scar: analysis of electrograms using high-density electroanatomic mapping in a novel porcine infarct model. Heart Rhythm. 2010;7:389–95.

191. Soejima K, Stevenson WG, Sapp JL, Selwyn AP, Couper G, Epstein LM. Endocardial and epicardial radiofrequency ablation of ventricular tachycardia associated with dilated cardiomyopathy: the importance of low-voltage scars. J Am Coll Cardiol. 2004;43:1834–42.

192. Garcia FC, Bazan V, Zado ES, Ren JF, Marchlinski FE. Epicardial substrate and outcome with epicardial ablation of ventricular tachycardia in arrhythmogenic right ventricular cardiomyopathy/dysplasia. Circulation. 2009;120:366–75.

193. Cano O, Hutchinson M, Lin D, Garcia F, Zado E, Bala R, et al. Electroanatomic substrate and ablation outcome for suspected epicardial ventricular tachycardia in left ventricular nonischemic cardiomyopathy. J Am Coll Cardiol. 2009;54:799–808.

194. Tung R, Vaseghi M, Frankel DS, Vergara P, Di Biase L, Nagashima K, et al. Freedom from recurrent ventricular tachycardia after catheter ablation is associated with improved survival in patients with structural heart disease: an international

VT ablation center collaborative group study. Heart Rhythm. 2015;12:1997–2007.

195. Polin GM, Haqqani H, Tzou W, Hutchinson MD, Garcia FC, Callans DJ, et al. Endocardial unipolar voltage mapping to identify epicardial substrate in arrhythmogenic right ventricular cardiomyopathy/dysplasia. Heart Rhythm. 2011;8:76–83.

196. Bogun F, Good E, Reich S, Elmouchi D, Igic P, Lemola K, et al. Isolated potentials during sinus rhythm and pace-mapping within scars as guides for ablation of post-infarction ventricular tachycardia. J Am Coll Cardiol. 2006;47:2013–9.

197. Vergara P, Trevisi N, Ricco A, Petracca F, Baratto F, Cireddu M, et al. Late potentials abolition as an additional technique for reduction of arrhythmia recurrence in scar related ventricular tachycardia ablation. J Cardiovasc Electrophysiol. 2012;23:621–7.

198. Berruezo A, Fernandez-Armenta J, Mont L, Zeljko H, Andreu D, Herczku C, et al. Combined endocardial and epicardial catheter ablation in arrhythmogenic right ventricular dysplasia incorporating scar dechanneling technique. Circ Arrhythm Electrophysiol. 2012;5:111–21.

199. Jamil-Copley S, Vergara P, Carbucicchio C, Linton N, Koa-Wing M, Luther V, et al. Application of ripple mapping to visualise slow conduction channels within the infarct-related left ventricular scar. Circ Arrhythm Electrophysiol. 2015;8:76–86.

200. Stevenson WG, Weiss JN, Wiener I, Rivitz SM, Nademanee K, Klitzner T, et al. Fractionated endocardial electrograms are associated with slow conduction in humans: evidence from pace-mapping. J Am Coll Cardiol. 1989;13:369–76.

201. Tung R, Mathuria N, Michowitz Y, Yu R, Buch E, Bradfield J, et al. Functional pace-mapping responses for identification of targets for catheter ablation of scar-mediated ventricular tachycardia. Circ Arrhythm Electrophysiol. 2012;5:264–72.

202. Hsia HH, Callans DJ, Marchlinski FE. Characterization of endocardial electrophysiological substrate in patients with nonischemic cardiomyopathy and monomorphic ventricular tachycardia. Circulation. 2003;108:704–10.

203. de Chillou C, Lacroix D, Klug D, Magnin-Poull I, Marquie C, Messier M, et al. Isthmus characteristics of reentrant ventricular tachycardia after myocardial infarction. Circulation. 2002;105:726–31.

204. Carbucicchio C, Ahmad Raja N, Di Biase L, Volpe V, Dello Russo A, Trivedi C, et al. High-density substrate-guided ventricular tachycardia ablation: role of activation mapping in an attempt to improve procedural effectiveness. Heart Rhythm. 2013;10:1850–8.

205. Anter E, Tschabrunn CM, Buxton AE, Josephson ME. High-Resolution mapping of postinfarction reentrant ventricular tachycardia: electrophysiological characterization of the circuit. Circulation. 2016;134:314–27.

206. Viswanathan K, Mantziari L, Butcher C, Hodkinson E, Lim E, Khan H, et al. Evaluation of a novel high-resolution mapping system for catheter ablation of ventricular arrhythmias. Heart Rhythm. 2017;14(2):176–83.

207. Della Bella P, Baratto F, Tsiachris D, Trevisi N, Vergara P, Bisceglia C, et al. Management of ventricular tachycardia in the setting of a dedicated unit for the treatment of complex ventricular arrhythmias: long-term outcome after ablation. Circulation. 2013;127:1359–68.

208. Soejima K, Suzuki M, Maisel WH, Brunckhorst CB, Delacretaz E, Blier L, et al. Catheter ablation in patients with multiple and unstable ventricular tachycardias after myocardial infarction: short ablation lines guided by reentry circuit isthmuses and sinus rhythm mapping. Circulation. 2001;104:664–9.

209. Tung R, Michowitz Y, Yu R, Mathuria N, Vaseghi M, Buch E, et al. Epicardial ablation of ventricular tachycardia: an institutional experience of safety and efficacy. Heart Rhythm. 2013;10:490–8.

210. Sacher F, Roberts-Thomson K, Maury P, Tedrow U, Nault I, Steven D, et al. Epicardial ventricular tachycardia ablation a multicenter safety study. J Am Coll Cardiol. 2010;55:2366–72.

211. Tung R, Nakahara S, Maccabelli G, Buch E, Wiener I, Boyle NG, et al. Ultra high-density multipolar mapping with double ventricular access: a novel technique for ablation of ventricular tachycardia. J Cardiovasc Electrophysiol. 2011;22:49–56.

212. Yamashita S, Cochet H, Sacher F, Mahida S, Berte B, Hooks D, et al. Impact of new technologies and approaches for post-myocardial infarction ventricular tachycardia ablation during long-term follow-up. Circ Arrhythm Electrophysiol. 2016;9(7). https://doi.org/10.1161/CIRCEP.116.003901

213. Acosta J, Penela D, Andreu D, Cabrera M, Carlosena A, Vassanelli F, et al. Multielectrode vs. point-by-point mapping for ventricular tachycardia substrate ablation: a randomized study. Europace. 2018;20:512–9.

214. Nogami A. Idiopathic left ventricular tachycardia: assessment and treatment. Cardiac Electrophysiol Rev. 2002;6:448–57.

215. Talib AK, Nogami A, Nishiuchi S, Kowase S, Kurosaki K, Matsui Y, et al. Verapamil-sensitive upper septal idiopathic left ventricular tachycardia: prevalence, mechanism, and electrophysiological characteristics. JACC Clin Electrophysiol. 2015;1:369–80.

216. Komatsu Y, Nogami A, Kurosaki K, Morishima I, Masuda K, Ozawa T, et al. Fascicular ventricular tachycardia originating from papillary muscles: Purkinje network involvement in the reentrant circuit. Circ Arrhythm Electrophysiol. 2017;10:e004549.

217. Zipes DP, Foster PR, Troup PJ, Pedersen DH. Atrial induction of ventricular tachycardia: reentry versus triggered automaticity. Am J Cardiol. 1979;44:1–8.

218. Belhassen B, Rotmensch HH, Laniado S. Response of recurrent sustained ventricular tachycardia to verapamil. Heart. 1981;46:679–82.

219. Ohe T, Shimomura K, Aihara N, Kamakura S, Matsuhisa M, Sato I, et al. Idiopathic sustained left ventricular tachycardia: clinical and electrophysiologic characteristics. Circulation. 1988;77:560–8.

220. Nishiuchi S, Nogami A, Naito S. A case with occurrence of antidromic tachycardia after ablation of idiopathic left fascicular tachycardia: mechanism of left upper septal ventricular tachycardia. J Cardiovasc Electrophysiol. 2013;24:825–7.

221. Gallagher JJ, Selle JG, Svenson RH, Fedor JM, Zimmern SH, Sealy WC, et al. Surgical treatment of arrhythmias. Am J Cardiol. 1988;61:27a–44a.

222. Suwa M, Yoneda Y, Nagao H, Sakai Y, Nakayama Y, Hirota Y, et al. Surgical correction of idiopathic paroxysmal ventricular tachycardia possibly related to left ventricular false tendon. Am J Cardiol. 1989;64:1217–20.

223. Thakur RK, Klein GJ, Sivaram CA, Zardini M, Schleinkofer DE, Nakagawa H, et al. Anatomic substrate for idiopathic left ventricular tachycardia. Circulation. 1996;93:497–501.

224. Maruyama M, Tadera T, Miyamoto S, Ino T. Demonstration of the reentrant circuit of verapamil-sensitive idiopathic left ventricular tachycardia: direct evidence for macroreentry as the underlying mechanism. J Cardiovasc Electrophysiol. 2001;12:968–72.

225. Nogami A, Naito S, Tada H, Oshima S, Taniguchi K, Aonuma K, et al. Verapamil-sensitive left anterior fascicular ventricular tachycardia: results of radiofrequency ablation in six patients. J Cardiovasc Electrophysiol. 1998;9:1269–78.

226. Lin D, Hsia HH, Gerstenfeld EP, Dixit S, Callans DJ, Nayak H, et al. Idiopathic fascicular left ventricular tachycardia: linear ablation lesion strategy for noninducible or nonsustained tachycardia. Heart Rhythm. 2005;2:934–9.

227. Hayashi M, Kobayashi Y, Iwasaki Y-K, Morita N, Miyauchi Y, Kato T, et al. Novel mechanism of postinfarction ventricular tachycardia originating in surviving left posterior Purkinje fibers. Heart rhythm. 2006;3:908–18.

228. Bogun F, Good E, Reich S, Elmouchi D, Igic P, Tschopp D, et al. Role of Purkinje fibers in post-infarction ventricular tachycardia. J Am Coll Cardiol. 2006;48:2500–7.

229. Morishima I, Nogami A, Tsuboi H, Sone T. Verapamil-sensitive left anterior fascicular ventricular tachycardia associated with a healed myocardial infarction: changes in the delayed Purkinje potential during sinus rhythm. J Interv Cardiac Electrophysiol. 2008;22:233.

230. Keita M, Akihiko N, Kenji K, Miyako I, Yuki K, Shinya K, et al. Conversion to Purkinje-related monomorphic ventricular tachycardia after ablation of ventricular fibrillation in ischemic heart disease. Circ Arrhythm Electrophysiol. 2016;9.

231. Talib AK, Nogami A, Morishima I, Oginosawa Y, Kurosaki K, Kowase S, et al. Non-reentrant fascicular tachycardia: clinical and electrophysiological characteristics of a distinct type of idiopathic ventricular tachycardia. Circ Arrhythm Electrophysiol. 2016;9:e004177.

232. Lerman BB, Stein KM, Markowitz SM. Mechanisms of idiopathic left ventricular tachycardia. J Cardiovasc Electrophysiol. 1997;8:571–83.

233. Lopera G, Stevenson WG, Soejima K, Maisel WH, Koplan B, Sapp JL, et al. Identification and ablation of three types of ventricular tachycardia involving the His-Purkinje system in patients with heart disease. J Cardiovasc Electrophysiol. 2004;15:52–8.

234. Gonzalez RP, Scheinman MM, Lesh MD, Helmy I, Torres V, Van Hare GF. Clinical and electrophysiologic spectrum of fascicular tachycardias. Am Heart J. 1994;128:147–56.

235. Rodriguez LM, Smeets JL, Timmermans C, Trappe HJ, Wellens HJ. Radiofrequency catheter ablation of idiopathic ventricular tachycardia originating in the anterior fascicle of the left bundle branch. J Cardiovasc Electrophysiol. 1996;7:1211–6.

236. Caceres J, Jazayeri M, McKinnie J, Avitall B, Denker ST, Tchou P, et al. Sustained bundle branch reentry as a mechanism of clinical tachycardia. Circulation. 1989;79:256–70.

237. Delacretaz E, Stevenson WG, Ellison KE, Maisel WH, Friedman PL. Mapping and radiofrequency catheter ablation of the three types of sustained monomorphic ventricular tachycardia in nonischemic heart disease. J Cardiovasc Electrophysiol. 2000;11:11–7.

238. Cantillon DJ, Bianco C, Wazni OM, Kanj M, Smedira NG, Wilkoff BL, et al. Electrophysiologic characteristics and catheter ablation of ventricular tachyarrhythmias among patients with heart failure on ventricular assist device support. Heart Rhythm. 2012;9:859–64.

239. Tchou P, Mehdirad AA. Bundle branch reentry ventricular tachycardia. Pacing Clin Electrophysiol. 1995;18:1427–37.

240. Machino T, Tada H, Sekiguchi Y, Aonuma K. Three-dimensional visualization of the entire reentrant circuit of bundle branch reentrant tachycardia. Heart rhythm. 2013;10:459–60.

241. Cohen TJ, Chien WW, Lurie KG, Young C, Goldberg HR, Wang Y-S, et al. Radiofrequency catheter ablation for treatment of bundle branch reentrant ventricular tachycardia: results and long-term follow-up. J Am Coll Cardiol. 1991;18:1767–73.

242. Schmidt B, Tang M, Chun KJ, Antz M, Tilz RR, Metzner A, et al. Left bundle branch–Purkinje system in patients with bundle branch reentrant tachycardia: lessons from catheter ablation and electroanatomic mapping. Heart Rhythm. 2009;6:51–8.

243. Lerman BB. Outflow tract ventricular arrhythmias: an update. Trends Cardiovasc Med. 2015;25:550–8.

244. Heeger CH, Hayashi K, Kuck KH, Ouyang F. Catheter ablation of idiopathic ventricular arrhythmias arising from the cardiac outflow tracts- recent insights and techniques for the successful treatment of common and challenging cases. Circ J. 2016;80:1073–86.

245. Dixit S, Gerstenfeld EP, Callans DJ, Marchlinski FE. Electrocardiographic patterns of superior right ventricular outflow tract tachycardias: distinguishing septal and free-wall sites of origin. J Cardiovasc Electrophysiol. 2003;14:1–7.

246. Park KM, Kim YH, Marchlinski FE. Using the surface electrocardiogram to localize the origin of idiopathic ventricular tachycardia. Pacing Clin Electrophysiol. 2012;35:1516–27.

247. Ho SY. Anatomic insights for catheter ablation of ventricular tachycardia. Heart Rhythm. 2009;6:S77–80.

248. Tanawuttiwat T, Nazarian S, Calkins H. The role of catheter ablation in the management of ventricular tachycardia. Eur Heart J. 2016;37:594–609.

249. Priori SG, Blomstrom-Lundqvist C, Mazzanti A, Blom N, Borggrefe M, Camm J, et al. 2015 ESC Guidelines for the management of patients with ventricular arrhythmias and the prevention of sudden cardiac death: The Task Force for the Management of Patients with Ventricular Arrhythmias and the Prevention of Sudden Cardiac Death of the European Society of Cardiology (ESC). Endorsed by: Association for European Paediatric and Congenital Cardiology (AEPC). Eur Heart J. 2015;36:2793–867.

250. Zhong L, Lee YH, Huang XM, Asirvatham SJ, Shen WK, Friedman PA, et al. Relative efficacy of catheter ablation vs antiarrhythmic drugs in treating premature ventricular contractions: a single-center retrospective study. Heart Rhythm. 2014;11:187–93.

251. Lamberti F, Di Clemente F, Remoli R, Bellini C, De Santis A, Mercurio M, et al. Catheter ablation of idiopathic ventricular tachycardia without the use of fluoroscopy. Int J Cardiol. 2015;190:338–43.

252. Acosta J, Penela D, Herczku C, Macias Y, Andreu D, Fernandez-Armenta J, et al. Impact of earliest activation site location in the septal right ventricular outflow tract for identification of left vs right outflow tract origin of idiopathic ventricular arrhythmias. Heart Rhythm. 2015;12:726–34.

253. Zhang J, Tang C, Zhang Y, Su X. Pulmonary sinus cusp mapping and ablation: a new concept and approach for idiopathic right ventricular outflow tract arrhythmias. Heart Rhythm. 2018;15:38–45.

254. Azegami K, Wilber DJ, Arruda M, Lin AC, Denman RA. Spatial resolution of pacemapping and activation mapping in patients with idiopathic right ventricular outflow tract tachycardia. J Cardiovasc Electrophysiol. 2005;16:823–9.

255. Baser K, Bas HD, Yokokawa M, Latchamsetty R, Morady F, Bogun F. Infrequent intraprocedural premature ventricular complexes: implications for ablation outcome. J Cardiovasc Electrophysiol. 2014;25:1088–92.

256. Jularic M, Akbulak RO, Schaffer B, Moser J, Nuehrich J, Meyer C, et al. Image integration into 3-dimensional-electro-anatomical mapping system facilitates safe ablation of ventricular arrhythmias originating from the aortic root and its vicinity. Europace. 2018;20:520–7.

257. Tovia-Brodie O, Belhassen B, Glick A, Shmilovich H, Aviram G, Rosso R, et al. Use of new imaging CARTO(R) segmentation module software to facilitate ablation of ventricular arrhythmias. J Cardiovasc Electrophysiol. 2017;28:240–8.

258. Yamada T, Yoshida N, Doppalapudi H, Litovsky SH, McElderry HT, Kay GN. Efficacy of an anatomical approach in radiofrequency catheter ablation of idiopathic ventricular arrhythmias originating from the left ventricular outflow tract. Circ Arrhythm Electrophysiol. 2017;10:e004959.

259. Chen YH, Lin JF. Catheter ablation of idiopathic epicardial ventricular arrhythmias originating from the vicinity of the coronary sinus system. J Cardiovasc Electrophysiol. 2015;26:1160–7.

260. Pavlovic N, Knecht S, Kuhne M, Sticherling C. Changing exits in ventricular outflow tract tachycardia. Heart Rhythm. 2014;11:1495–6.

261. Doppalapudi H, Yamada T, McElderry T, Plumb VJ, Epstein AE, Kay GN. Ventricular tachycardia originating from the posterior papillary muscle in the left ventricle. Circ Arrhythm Electrophysiol. 2008;1:23–9.

262. Naksuk N, Kapa S, Asirvatham SJ. Spectrum of ventricular arrhythmias arising from papillary muscle in the structurally normal heart. Cardiac Electrophysiol Clin. 2016;8:555–65.

263. Yamada T, Doppalapudi H, McElderry HT, Okada T, Murakami Y, Inden Y, et al. Electrocardiographic and electrophysiological

characteristics in idiopathic ventricular arrhythmias originating from the papillary muscles in the left ventricle: relevance for catheter ablation. Circ Arrhythm Electrophysiol. 2010;3:324–31.

264. Enriquez A, Supple GE, Marchlinski FE, Garcia FC. How to map and ablate papillary muscle ventricular arrhythmias. Heart rhythm. 2017;14:1721–8.

265. Fulton BL, Liang JJ, Enriquez A, Garcia FC, Supple GE, Riley MP, et al. Imaging characteristics of papillary muscle site of origin of ventricular arrhythmias in patients with mitral valve prolapse. J Cardiovasc Electrophysiol. 2018;29:146–53.

266. Van Herendael H, Zado ES, Haqqani H, Tschabrunn CM, Callans DJ, Frankel DS, et al. Catheter ablation of ventricular fibrillation: importance of left ventricular outflow tract and papillary muscle triggers. Heart Rhythm. 2014;11:566–73.

267. Santoro F, Biase LD, Hranitzky P, Sanchez JE, Santangeli P, Perini AP, et al. Ventricular fibrillation triggered by PVCs from papillary muscles: clinical features and ablation. J Cardiovasc Electrophysiol. 2014;25:1158–64.

268. Loukas M, Klaassen Z, Tubbs RS, Derderian T, Paling D, Chow D, et al. Anatomical observations of the moderator band. Clin Anat. 2010;23:443–50.

269. Bogun F, Desjardins B, Crawford T, Good E, Jongnarangsin K, Oral H, et al. Post-infarction ventricular arrhythmias originating in papillary muscles. J Am Coll Cardiol. 2008;51:1794–802.

270. Santoro F, Di Biase L, Hranitzky P, Sanchez JE, Santangeli P, Perini AP, et al. Ventricular tachycardia originating from the septal papillary muscle of the right ventricle: electrocardiographic and electrophysiological characteristics. J Cardiovasc Electrophysiol. 2015;26:145–50.

271. Yamada T, Doppalapudi H, McElderry HT, Okada T, Murakami Y, Inden Y, et al. Idiopathic ventricular arrhythmias originating from the papillary muscles in the left ventricle: prevalence, electrocardiographic and electrophysiological characteristics, and results of the radiofrequency catheter ablation. J Cardiovasc Electrophysiol. 2010;21:62–9.

272. Sadek MM, Benhayon D, Sureddi R, Chik W, Santangeli P, Supple GE, et al. Idiopathic ventricular arrhythmias originating from the moderator band: electrocardiographic characteristics and treatment by catheter ablation. Heart Rhythm. 2015;12:67–75.

273. Enriquez A, Pathak RK, Santangeli P, Liang JJ, Al Rawahi M, Hayashi T, et al. Inferior lead discordance in ventricular arrhythmias: a specific marker for certain arrhythmia locations. J Cardiovasc Electrophysiol. 2017;28:1179–86.

274. Good E, Desjardins B, Jongnarangsin K, Oral H, Chugh A, Ebinger M, et al. Ventricular arrhythmias originating from a papillary muscle in patients without prior infarction: a comparison with fascicular arrhythmias. Heart Rhythm. 2008;5:1530–7.

275. Al'Aref SJ, Ip JE, Markowitz SM, Liu CF, Thomas G, Frenkel D, et al. Differentiation of papillary muscle from fascicular and mitral annular ventricular arrhythmias in patients with and without structural heart disease. Circ Arrhythm Electrophysiol. 2015;8:616–24.

276. Crawford T, Mueller G, Good E, Jongnarangsin K, Chugh A, Pelosi F Jr, et al. Ventricular arrhythmias originating from papillary muscles in the right ventricle. Heart Rhythm. 2010;7:725–30.

277. Proietti R, Rivera S, Dussault C, Essebag V, Bernier ML, Ayala-Paredes F, et al. Intracardiac echo-facilitated 3D electroanatomical mapping of ventricular arrhythmias from the papillary muscles: assessing the 'fourth dimension' during ablation. Ep Europace. 2017;19:21–8.

278. Rivera S, Ricapito MdlP, Tomas L, Parodi J, Bardera Molina G, Banega R, et al. Results of cryoenergy and radiofrequency-based catheter ablation for treating ventricular arrhythmias arising from the papillary muscles of the left ventricle, guided by intracardiac echocardiography and image integration. Circ Arrhythm Electrophysiol. 2016;9:e003874.

279. Ban J-E, Lee H-S, Lee D-I, Park H-C, Park J-S, Nagamoto Y, et al. Electrophysiological characteristics related to outcome after catheter ablation of idiopathic ventricular arrhythmia originating from the papillary muscle in the left ventricle. Korean Circ J. 2013;43:811–8.

280. Berte B, Derval N, Sacher F, Yamashita S, Haissaguerre M, Jais P. A case of incessant VT from an intramural septal focus: ethanol or bipolar ablation? HeartRhythm Case Rep. 2015;1:89–94.

281. Sauer WH, Steckman DA, Zipse MM, Tzou WS, Aleong RG. High-power bipolar ablation for incessant ventricular tachycardia utilizing a deep midmyocardial septal circuit. HeartRhythm Case Rep. 2015;1:397–400.

282. Wo H-T, Liao F-C, Chang P-C, Chou C-C, Wen M-S, Wang C-C, et al. Circumferential ablation at the base of the left ventricular papillary muscles: a highly effective approach for ventricular arrhythmias originating from the papillary muscles. Int J Cardiol. 2016;220:876–82.

283. Priori SG, Wilde AA, Horie M, Cho Y, Behr ER, Berul C, et al. HRS/EHRA/APHRS expert consensus statement on the diagnosis and management of patients with inherited primary arrhythmia syndromes. J Arrhythm. 2014;30:1–28.

284. Hocini M, Pison L, Proclemer A, Larsen TB, Madrid A, Blomstrom-Lundqvist C, et al. Diagnosis and management of patients with inherited arrhythmia syndromes in Europe: results of the European Heart Rhythm Association Survey. Europace. 2014;16:600–3.

285. Sanchez-Munoz JJ, Garcuia-Alberola A, Martinez-Sanchez J, Garcia-Molina E, Valdes-Chavarri M. Ablation of premature ventricular complexes triggering ventricular fibrillation in a patient with long QT syndrome. Indian Pacing Electrophysiol J. 2011;11:81–3.

286. Srivathsan K, Gami AS, Ackerman MJ, Asirvatham SJ. Treatment of ventricular fibrillation in a patient with prior diagnosis of long QT syndrome: importance of precise electrophysiologic diagnosis to successfully ablate the trigger. Heart Rhythm. 2007;4:1090–3.

287. Cheng Z, Gao P, Cheng K, Chen T, Deng H, Chang B, et al. Elimination of fatal arrhythmias through ablation of triggering premature ventricular contraction in type 3 long QT syndrome. Ann Noninvasive Electrocardiol. 2012;17:394–7.

288. Yap J, Tan VH, Hsu LF, Liew R. Catheter ablation of ventricular fibrillation storm in a long QT syndrome genotype carrier with normal QT interval. Singapore Med J. 2013;54:e1–4.

289. Kaneshiro T, Naruse Y, Nogami A, Tada H, Yoshida K, Sekiguchi Y, et al. Successful catheter ablation of bidirectional ventricular premature contractions triggering ventricular fibrillation in catecholaminergic polymorphic ventricular tachycardia with RyR2 mutation. Circ Arrhythm Electrophysiol. 2012;5:e14–e17.

290. Shirai Y, Goya M, Ohno S, Horie M, Doi S, Isobe M, et al. Elimination of ventricular arrhythmia in catecholaminergic polymorphic ventricular tachycardia by targeting "catecholamine-sensitive area": a dominant-subordinate relationship between origin sites of bidirectional ventricular premature contractions. Pacing Clin Electrophysiol. 2017;40:600–4.

291. Darmon JP, Bettouche S, Deswardt P, Tiger F, Ricard P, Bernasconi F, et al. Radiofrequency ablation of ventricular fibrillation and multiple right and left atrial tachycardia in a patient with Brugada syndrome. J Interv Card Electrophysiol. 2004;11:205–9.

292. Nakagawa E, Takagi M, Tatsumi H, Yoshiyama M. Successful radiofrequency catheter ablation for electrical storm of ventricular fibrillation in a patient with Brugada syndrome. Circ J. 2008;72:1025–9.

293. Haissaguerre M, Extramiana F, Hocini M, Cauchemez B, Jais P, Cabrera JA, et al. Mapping and ablation of ventricular fibrillation associated with long-QT and Brugada syndromes. Circulation. 2003;108:925–8.

294. Nademanee K, Veerakul G, Chandanamattha P, Chaothawee L, Ariyachaipanich A, Jirasirirojanakorn K, et al. Prevention of

ventricular fibrillation episodes in Brugada syndrome by catheter ablation over the anterior right ventricular outflow tract epicardium. Circulation. 2011;123:1270–9.

295. Sunsaneewitayakul B, Yao Y, Thamaree S, Zhang S. Endocardial mapping and catheter ablation for ventricular fibrillation prevention in Brugada syndrome. J Cardiovasc Electrophysiol. 2012;23(Suppl 1):S10–S16.

296. Brugada J, Pappone C, Berruezo A, Vicedomini G, Manguso F, Ciconte G, et al. Brugada syndrome phenotype elimination by epicardial substrate ablation. Circ Arrhythm Electrophysiol. 2015;8:1373–81.

297. Pappone C, Brugada J, Vicedomini G, Ciconte G, Manguso F, Saviano M, et al. Electrical substrate elimination in 135 consecutive patients with brugada syndrome. Circ Arrhythm Electrophysiol. 2017;10:e005053.

298. Philips B, Madhavan S, James C, Tichnell C, Murray B, Dalal D, et al. Outcomes of catheter ablation of ventricular tachycardia in arrhythmogenic right ventricular dysplasia/cardiomyopathy. Circ Arrhythm Electrophysiol. 2012;5:499–505.

299. Ellison K, Friedman P, Ganz L, Stevenson W. Entrainment mapping and radiofrequency catheter ablation of ventricular tachycardia in right ventricular dysplasia. J Am Coll Cardiol. 1998;32:724–8.

300. Nogami A, Sugiyasu A, Tada H, Kurosaki K, Sakamaki M, Kowase S, et al. Changes in the isolated delayed component as an endpoint of catheter ablation in arrhythmogenic right ventricular cardiomyopathy: predictor for long-term success. J Cardiovasc Electrophysiol. 2008;19:681–8.

301. Dalal D, Jain R, Tandri H, Dong J, Eid SM, Prakasa K, et al. Long-term efficacy of catheter ablation of ventricular tachycardia in patients with arrhythmogenic right ventricular dysplasia/cardiomyopathy. J Am Coll Cardiol. 2007;50:432–40.

302. Bai R, Di Biase L, Shivkumar K, Mohanty P, Tung R, Santangeli P, et al. Ablation of ventricular arrhythmias in arrhythmogenic right ventricular dysplasia/cardiomyopathy: arrhythmia-free survival after endo-epicardial substrate based mapping and ablation. Circ Arrhythm Electrophysiol. 2011;4:478–85.

303. Philips B, te Riele ASJM, Sawant A, Kareddy V, James CA, Murray B, et al. Outcomes and ventricular tachycardia recurrence characteristics after epicardial ablation of ventricular tachycardia in arrhythmogenic right ventricular dysplasia/cardiomyopathy. Heart Rhythm. 2015;12:716–25.

304. Santangeli P, Zado ES, Supple GE, Haqqani HM, Garcia FC, Tschabrunn CM, et al. Long-term outcome with catheter ablation of ventricular tachycardia in patients with arrhythmogenic right ventricular cardiomyopathy. Circ Arrhythm Electrophysiol. 2015;8:1413–21.

305. Müssigbrodt A, Efimova E, Knopp H, Bertagnolli L, Dagres N, Richter S, et al. Should all patients with arrhythmogenic right ventricular dysplasia/cardiomyopathy undergo epicardial catheter ablation? J Interv Cardiac Electrophysiol. 2017;48:193–9.

306. Marchlinski FE, Zado E, Dixit S, Gerstenfeld E, Callans DJ, Hsia H, et al. Electroanatomic substrate and outcome of catheter ablative therapy for ventricular tachycardia in setting of right ventricular cardiomyopathy. Circulation. 2004;110:2293–8.

307. Verma A, Kilicaslan F, Schweikert RA, Tomassoni G, Rossillo A, Marrouche NF, et al. Short-and long-term success of substrate-based mapping and ablation of ventricular tachycardia in arrhythmogenic right ventricular dysplasia. Circulation. 2005;111:3209–16.

308. Berruezo A, Acosta J, Fernández-Armenta J, Pedrote A, Barrera A, Arana-Rueda E, et al. Safety, long-term outcomes and predictors of recurrence after first-line combined endoepicardial ventricular tachycardia substrate ablation in arrhythmogenic cardiomyopathy. Impact of arrhythmic substrate distribution pattern. A prospective multicentre study. Europace. 2016;19:607–16.

309. Berruezo A, Fernández-Armenta J, Mont L, Zeljko H, Andreu D, Herczku C, et al. Combined endocardial and epicardial catheter ablation in arrhythmogenic right ventricular dysplasia incorporating scar dechanneling techniqueclinical perspective. Circ Arrhythm Electrophysiol. 2012;5:111–21.

310. Haïssaguerre M, Extramiana F, Hocini Mélèze, Cauchemez B, Jaïs P, Cabrera JA, et al. Mapping and ablation of ventricular fibrillation associated with long-QT and Brugada syndromes. Circulation. 2003;108:925–8.

311. Shirai Y, Goya M, Ohno S, Horie M, Doi S, Isobe M, et al. Elimination of ventricular arrhythmia in catecholaminergic polymorphic ventricular tachycardia by targeting "catecholamine-sensitive area": a dominant-subordinate relationship between origin sites of bidirectional ventricular premature contractions. Pacing Clin Electrophysiol. 2017;40:600–4.

312. Darmon J-P, Bettouche S, Deswardt P, Tiger F, Ricard P, Bernasconi F, et al. Radiofrequency ablation of ventricular fibrillation and multiple right and left atrial tachycardia in a patient with Brugada syndrome. J Interv Cardiac Electrophysiol. 2004;11:205–9.

313. Sasyniuk BI, Mendez C. A mechanism for reentry in canine ventricualar tissue. Circ Res. 1971;28:3–15.

314. Friedman PL, Stewart JR, Wit AL. Spontaneous and induced cardiac arrhythmias in subendocardial Purkinje fibers surviving extensive myocardial infarction in dogs. Circ Res. 1973;33:612–26.

315. Tabereaux PB, Walcott GP, Rogers JM, Kim J, Dosdall DJ, Robertson PG, et al. Activation patterns of Purkinje fibers during long-duration ventricular fibrillation in an isolated canine heart model. Circulation. 2007;116:1113–9.

316. Dosdall DJ, Tabereaux PB, Kim JJ, Walcott GP, Rogers JM, Killingsworth CR, et al. Chemical ablation of the Purkinje system causes early termination and activation rate slowing of long-duration ventricular fibrillation in dogs. Am J Physiol Heart Circ Physiol. 2008;295:H883–H889.

317. Moise NS, Gilmour RF Jr, Riccio ML. An animal model of spontaneous arrhythmic death. J Cardiovasc Electrophysiol. 1997;8:98–103.

318. Berenfeld O, Jalife J. Purkinje-muscle reentry as a mechanism of polymorphic ventricular arrhythmias in a 3-dimensional model of the ventricles. Circ Res. 1998;82:1063–77.

319. Haissaguerre M, Shah DC, Jais P, Shoda M, Kautzner J, Arentz T, et al. Role of Purkinje conducting system in triggering of idiopathic ventricular fibrillation. Lancet. 2002;359:677–8.

320. Knecht S, Sacher F, Wright M, Hocini M, Nogami A, Arentz T, et al. Long-term follow-up of idiopathic ventricular fibrillation ablation: a multicenter study. J Am Coll Cardiol. 2009;54:522–8.

321. Leenhardt A, Glaser E, Burguera M, Nurnberg M, Maison-Blanche P, Coumel P. Short-coupled variant of torsade de pointes. A new electrocardiographic entity in the spectrum of idiopathic ventricular tachyarrhythmias. Circulation. 1994;89:206–15.

322. Kautzner J, Peichl P. Catheter ablation of polymorphic ventricular tachycardia and ventricular fibrillation. Arrhythm Electrophysiol Rev. 2013;2:135–40.

323. Noda T, Shimizu W, Taguchi A, Aiba T, Satomi K, Suyama K, et al. Malignant entity of idiopathic ventricular fibrillation and polymorphic ventricular tachycardia initiated by premature extrasystoles originating from the right ventricular outflow tract. J Am Coll Cardiol. 2005;46:1288–94.

324. Kuck KH, Ernst S, Cappato R, Braun E, Lang M, Ben-Haim SA, et al. Nonfluoroscopic endocardial catheter mapping of atrial fibrillation. J Cardiovasc Electrophysiol. 1998;9:S57–62.

325. Papez AL, Al-Ahdab M, Dick M 2nd, Fischbach PS. Impact of a computer assisted navigation system on radiation exposure during pediatric ablation procedures. J Interv Card Electrophysiol. 2007;19:121–7.

326. Bulava A, Hanis J, Eisenberger M. Catheter ablation of atrial fibrillation using zero-fluoroscopy technique: a randomized trial. Pacing Clin Electrophysiol. 2015;38:797–806.

327. Thibault B, Macle L, Mondesert B, Dubuc M, Shohoudi A, Dyrda K, et al. Reducing radiation exposure during procedures performed in the electrophysiology laboratory. J Cardiovasc Electrophysiol. 2018;29:308–15.

328. Estner HL, Grazia Bongiorni M, Chen J, Dagres N, Hernandez-Madrid A, Blomström-Lundqvist C, et al. Use of fluoroscopy in clinical electrophysiology in Europe: results of the European Heart Rhythm Association Survey. Europace. 2015;17:1149–52.

329. Picano E, Vano E, Rehani MM, Cuocolo A, Mont L, Bodi V, et al. The appropriate and justified use of medical radiation in cardiovascular imaging: a position document of the ESC associations of cardiovascular imaging, percutaneous cardiovascular interventions and electrophysiology. Eur Heart J. 2014;35:665–72.

330. Heidbuchel H, Wittkampf FH, Vano E, Ernst S, Schilling R, Picano E, et al. Practical ways to reduce radiation dose for patients and staff during device implantations and electrophysiological procedures. Europace. 2014;16:946–64.

331. Sommer P, Bertagnolli L, Kircher S, Arya A, Bollmann A, Richter S, et al. Safety profile of near-zero fluoroscopy atrial fibrillation ablation with non-fluoroscopic catheter visualization: experience from 1000 consecutive procedures. Europace. 2018;20(12):1952–8.

332. Wannagat S, Loehr L, Lask S, Volk K, Karakose T, Ozcelik C, et al. Implementation of a near-zero fluoroscopy approach in interventional electrophysiology: impact of operator experience. J Interv Card Electrophysiol. 2018;51(3):215–20.

333. Brooks AG, Wilson L, Chia NH, Lau DH, Alasady M, Leong DP, et al. Accuracy and clinical outcomes of CT image integration with Carto-Sound compared to electro-anatomical mapping for atrial fibrillation ablation: a randomized controlled study. Int J Cardiol. 2013;168:2774–82.

334. Caponi D, Corleto A, Scaglione M, Blandino A, Biasco L, Cristoforetti Y, et al. Ablation of atrial fibrillation: does the addition of three-dimensional magnetic resonance imaging of the left atrium to electroanatomic mapping improve the clinical outcome?: a randomized comparison of Carto-Merge vs. Carto-XP three-dimensional mapping ablation in patients with paroxysmal and persistent atrial fibrillation. Europace. 2010;12:1098–104.

335. Keegan J, Jhooti P, Babu-Narayan SV, Drivas P, Ernst S, Firmin DN. Improved respiratory efficiency of 3D late gadolinium enhancement imaging using the continuously adaptive windowing strategy (CLAWS). Magn Reson Med. 2014;71:1064–74.

336. Jan M, Zizek D, Rupar K, Mazic U, Kuhelj D, Lakic N, et al. Fluoroless catheter ablation of various right and left sided supra-ventricular tachycardias in children and adolescents. Int J Cardiovasc Imaging. 2016;32:1609–16.

337. Mah DY, Miyake CY, Sherwin ED, Walsh A, Anderson MJ, Western K, et al. The use of an integrated electroanatomic mapping system and intracardiac echocardiography to reduce radiation exposure in children and young adults undergoing ablation of supraventricular tachycardia. Europace. 2014;16:277–83.

338. Raju H, Whitaker J, Taylor C, Wright M. Electroanatomic mapping and transoesophageal echocardiography for near zero fluoroscopy during complex left atrial ablation. Heart Lung Circ. 2016;25:652–60.

339. Mansour M, Afzal MR, Gunda S, Pillarisetti J, Heist K, Acha MR, et al. Feasibility of transseptal puncture using a nonfluoroscopic catheter tracking system. Pacing Clin Electrophysiol. 2015;38:791–6.

340. Strauss KJ, Kaste SC. ALARA in pediatric interventional and fluoroscopic imaging: striving to keep radiation doses as low as possible during fluoroscopy of pediatric patients–a white paper executive summary. J Am Coll Radiol. 2006;3:686–8.

341. Pass RH, Gates GG, Gellis LA, Nappo L, Ceresnak SR. Reducing patient radiation exposure during paediatric SVT ablations: use of CARTO(R) 3 in concert with "ALARA" principles profoundly lowers total dose. Cardiol Young. 2015;25:963–8.

342. Clark BC, Sumihara K, McCarter R, Berul CI, Moak JP. Getting to zero: impact of electroanatomical mapping on fluoroscopy use in pediatric catheter ablation. J Interv Card Electrophysiol. 2016;46:183–9.

343. Roudijk RW, Gujic M, Suman-Horduna I, Marchese P, Ernst S. Catheter ablation in children and young adults: is there an additional benefit from remote magnetic navigation? Neth Heart J. 2013;21:296–303.

344. Ernst S, Ouyang F, Linder C, Hertting K, Stahl F, Chun J, et al. Initial experience with remote catheter ablation using a novel magnetic navigation system: magnetic remote catheter ablation. Circulation. 2004;109:1472–5.

345. American College of Obstetricians and Gynecologists' Committee on Obstetric Practice. Committee opinion no. 656 summary: guidelines for diagnostic imaging during pregnancy and lactation. Obstet Gynecol. 2016;127:418.

346. Wu H, Ling LH, Lee G, Kistler PM. Successful catheter ablation of incessant atrial tachycardia in pregnancy using three-dimensional electroanatomical mapping with minimal radiation. Intern Med J. 2012;42:709–12.

347. Casella M, Bartoletti S, Dello Russo A, Tondo C. 9 pregnant women with drug-refractory supraventricular tachyarrhythmias. Catheter ablation during pregnancy. J Cardiovasc Electrophysiol. 2010;21:E80; author reply E81.

348. Berruezo A, Diez GR, Berne P, Esteban M, Mont L, Brugada J. Low exposure radiation with conventional guided radiofrequency catheter ablation in pregnant women. Pacing Clin Electrophysiol. 2007;30:1299–302.

349. Sarkozy A, De Potter T, Heidbuchel H, Ernst S, Kosiuk J, Vano E, et al.; Group ESCSD. Occupational radiation exposure in the electrophysiology laboratory with a focus on personnel with reproductive potential and during pregnancy: a European Heart Rhythm Association (EHRA) consensus document endorsed by the Heart Rhythm Society (HRS). Europace. 2017;19:1909–22.

350. Picano E, Vano E. Radiation exposure as an occupational hazard. EuroIntervention. 2012;8:649–53.

351. Cohen S, Liu A, Gurvitz M, Guo L, Therrien J, Laprise C, et al. Exposure to low-dose ionizing radiation from cardiac procedures and malignancy risk in adults with congenital heart disease. Circulation. 2018;137(13):1334–45.

352. Lerman BB, Markowitz SM, Liu CF, Thomas G, Ip JE, Cheung JW. Fluoroless catheter ablation of atrial fibrillation. Heart Rhythm. 2017;14:928–34.

353. Njeim M, Desjardins B, Bogun F. Multimodality imaging for guiding EP ablation procedures. JACC Cardiovasc Imaging. 2016;9:873–86.

354. Ernst S. Catheter ablation: general principles and advances. Card Electrophysiol Clin. 2017;9:311–7.

355. van der Does LJ, de Groot NM. Inhomogeneity and complexity in defining fractionated electrograms. Heart Rhythm. 2017;14:616–24.

356. Pachon MJ, Pachon ME, Pachon MJ, Lobo TJ, Pachon MZ, Vargas RN, et al. A new treatment for atrial fibrillation based on spectral analysis to guide the catheter RF-ablation. Europace. 2004;6:590–601.

357. Jalife J. Mechanisms of persistent atrial fibrillation. Curr Opin Cardiol. 2014;29:20–7.

358. Santangeli P, Marchlinski FE. Substrate mapping for unstable ventricular tachycardia. Heart Rhythm. 2016;13:569–83.

359. Leshem E, Tschabrunn CM, Jang J, Whitaker J, Zilberman I, Beeckler C, et al. High-resolution mapping of ventricular scar: evaluation of a novel integrated multielectrode mapping and ablation catheter. JACC Clin Electrophysiol. 2017;3:220–31.

360. Enriquez A, Malavassi F, Saenz LC, Supple G, Santangeli P, Marchlinski FE, et al. How to map and ablate left ventricular summit arrhythmias. Heart Rhythm. 2017;14:141–8.

361. Anter E. Cardiac magnetic resonance imaging to guide ventricular tachycardia ablation: are we there? Heart Rhythm. 2017;14:1494–5.

362. Chubb H, Harrison JL, Weiss S, Krueger S, Koken P, Bloch LO, et al. Development, preclinical validation, and clinical translation of a cardiac magnetic resonance – electrophysiology system with active catheter tracking for ablation of cardiac arrhythmia. JACC Clin Electrophysiol. 2017;3:89–103.

363. Andreu D, Penela D, Acosta J, Fernandez-Armenta J, Perea RJ, Soto-Iglesias D, et al. Cardiac magnetic resonance-aided scar dechanneling: Influence on acute and long-term outcomes. Heart Rhythm. 2017;14:1121–8.

SUPPORTING INFORMATION

Additional supporting information may be found online in the Supporting Information section.